

Aim and Scope

The objective of the *Journal of Residuals Science & Technology* is to provide a forum for technical research on the management and disposal of residuals from pollution control activities. The Journal publishes papers that examine the characteristics, effects, and management principles of various residuals from such sources as wastewater treatment, water treatment, air pollution control, hazardous waste treatment, solid waste, industrial waste treatment, and other pollution control activities. Papers on health and the environmental effects of residuals production, management, and disposal and are also welcome.

Editor-in-Chief

P. Brent Duncan
Department of Biology
University of North Texas
Denton, TX, USA
pduncan@unt.edu

Editorial Advisory Board

Muhammad Abu-Orf
U.S.Filter
Vineland, NJ, USA
Abu-OrfM@USFilter.com

Yoram Avnimelech
Technion, Israel
agyoram@tx.technion.ac.il

Steve Dentel
University of Delaware
Newark, DE, USA
dentel@udel.edu

Richard Dick
Cornell University
Ithaca NY, USA
rid1@cornell.edu

Robert Hale
Virginia Institute of Marine Science
USA
hale@vims.edu

Blanca E. Jimenez
Inst. de Ingenieria, UNAM
Mexico City, D. F., Mexico
bjc@mumas.iingen.unam.mx

Julia Kopp
Technische Universitat Braunschweig
D-38106 Braunschwig, Germany
j.kopp@tu-bs.de

Uta Krogmann
Rutgers University
New Brunswick, NJ, USA
krogmann@aesop.rutgers.edu

D. J. Lee
National Taiwan University
Taipei, Taiwan
djlee@ccms.ntu.edu.tw

Giuseppe Mininni
Via Reno 1
00198 Rome, Italy
mininni@irsa.rm.cnr.it

John Novak
Virginia Tech
Blacksburg, VA, USA
jtnov@vt.edu

Rod O'Connor
Chemical Consulting Services
College Station, TX, USA
docroc34@hotmail.com

Nagaharu Okuno
The University of Shiga Prefecture
Hatssaka, Kitone, Shiga, Japan
okuno@ses.usp.ac.jp

Jan Oleszkiewicz
University of Manitoba
Winnipeg, Manitoba, Canada
oleszkie@ms.umanitoba.ca

Banu Örmeci
Carleton University
Ottawa, Canada
banu_ormeci@carleton.ca

Ian L. Pepper
University of Arizona
Tucson, AZ, USA
ipepper@ag.arizona.edu

Ioana G. Petrisor
Co-Editor-in-Chief
Environmental Forensics Journal, USA
Environmental.Forensics@gmail.com

Bob Reimers
Tulane University
New Orleans, LA, USA
rreimers@tulane.edu

Dilek Sanin
Middle East Technical University
Ankara, Turkey
dsanin@metu.edu.tr

Mike Switzenbaum
Marquette University
Milwaukee, WI, USA
michael.switzenbaum@marquette.edu

Heidi Snyman
Golder Associates Africa (Pty) Ltd.
Halfway House, South Africa
hsnyman@golder.co.za

Ludovico Spinosa
CNR-IRSA
Bari, Italy
spinosa@area.ba.cnr.it


P. Aarne Vesilind
Bucknell University
Lewisburg, PA, USA
Vesilind@bucknell.edu

Doug Williams
California Polytechnic State University
San Luis Obispo, CA, USA
dwwillia@calpoly.edu

JOURNAL OF RESIDUALS SCIENCE & TECHNOLOGY—Published quarterly—January, April, July and October by DEStech Publications, Inc., 439 North Duke Street, Lancaster, PA 17602.

Indexed by Chemical Abstracts Service. Indexed/abstracted in Science Citation Index Expanded. Abstracted in Current Contents/Engineering, Computing & Technology. Listed in ISI Master Journal.

Subscriptions: Annual \$199 per year. Single copy price \$50. Foreign subscriptions add \$40 per year for postage. (ISSN 1544-8053)

 DEStech Publications, Inc.
439 North Duke Street, Lancaster, PA 17602, U.S.A.

©Copyright by DEStech Publications, Inc. 2010—All Rights Reserved

C O N T E N T S

Research

- Evaluation of Odors Associated with Land Application of Biosolids** 73
EDWIN F. BARTH, ROBERT FORBES, PATRICK CLARK, ERIC FOOTE and LAURA L. MCCONNELL
- Comparison of *Salmonella enterica* subsp. *enterica* Survival in Agricultural Soil Amended with Vermicompost and Class A Biosolids** 81
NOHELIA CASTRO-DEL CAMPO, ELIZABETH ESPINOZA, JOSÉ B. VALDEZ-TORRES, CHARLES P. GERBA and CRISTÓBAL CHAIDEZ
- The Relationship Between Particle Size and Turbidity Fluctuations in Coagulation Process** 87
WEN PO CHENG, WEI YI CHEN, RUEY FANG YU and YING JU HSIEH
- Landfill Disposal of Alum Water Treatment Residues: Some Pertinent Geoenvironmental Properties** 95
BRENDAN C. O'KELLY
- Neuropsychiatric Effects of Lead and Arsenic: Were these associated with “A Touch of Evil”?** 115
ROD O'CONNOR, THOMAS G. BURNS and P. “BRENT” DUNCAN
- Elemental Concentrations of Atmospheric Aerosols and the Soil Samples on the Selected Playgrounds in Istanbul.** 123
GOKSEL DEMIR, SELDA YIGIT, HUSEYIN OZDEMIR, GULSUM BORUCU and ARSLAN SARAL

Evaluation of Odors Associated with Land Application of Biosolids

EDWIN F. BARTH^{1,*}, ROBERT FORBES², PATRICK CLARK¹, ERIC FOOTE³ and LAURA L. McCONNELL⁴

¹National Risk Management Research Laboratory, Office of Research and Development, Cincinnati, OH

²CH₂M HILL, Charlotte, NC

³Battelle, Columbus, OH

⁴US Department of Agriculture, Agricultural Research Services, Henry A. Wallace Beltsville Agricultural Research Center, Beltsville, MD

ABSTRACT: An odor study was performed at a biosolids application demonstration site using several different gas collection devices and analytical methods to determine changes in air concentration of several organic and inorganic compounds associated with biosolids application over various time periods. Various organic and inorganic odorants were detected at 1.5 m above the ground surface within the biosolids application zone area immediately after application. They then decreased to non-detectable levels within 196 h after application, consistent with other biosolids application studies. Air samples collected from flux chambers installed within the application zone contained detectable concentrations of various organic odorants immediately after biosolids application. The concentrations of these odorants may have been influenced by the increased temperature within the flux chambers, and the change in concentration of these odorants over time was affected by the various sample analysis method. Airborne concentrations of ammonia and hydrogen sulfide rapidly decreased within 4 h after biosolids application, and they further decreased to non-detectable levels within 196 h after application. The highest measurements for both ammonia and hydrogen sulfide did not approach any health criterion or guidance levels for these compounds. The effects of the specific biosolids process and management variables on odor generation were not studied.

INTRODUCTION

NUISANCE odors are one of the chief complaints associated with human and animal waste (fecal) management activities. Specific compound classes associated with these odors may include sulfur compounds (hydrogen sulfide, mercaptans (or thiols), and other organic sulfur compounds), nitrogen compounds (ammonia, amines) and volatile fatty acids (USEPA, 2000). These odors may be a nuisance or elicit health complaints that are poorly understood (WERF, 2004; Schiffman et al. 2000). Misperception of the risk from odors may change a person's sensory perception of odor levels and their feeling of well being (WERF, 2004; Dalton et al. 2002; Dalton, 1999).

A number of variables in wastewater treatment operations and biosolids management processes, as well as chemical additives such as metal salts, polymers or lime

may affect the production of odors during any part of the wastewater or biosolids management chain (Gabriel et al. 2006). Dimethyl disulfide, trimethylamine, and ammonia were detected in the headspace of laboratory scale flux chambers containing biosolids, dewatered with the aid of polymers; whereas dimethyl sulfide, acetone, and methyl ethyl ketone were detected below the detection limit (Rosenfeld et al. 2001). Biosolids may also contain a wide variety of natural and man-made compounds including industrial-based wastes, endocrine disrupting compounds (EDCs), and flame retardant polybrominated diphenyl ethers (PBDE), if those compounds are present in the wastewater being treated. Measured Henry's law constants, particle/water partition coefficients, and particle/air partitioning coefficients are all strongly temperature dependent, and high temperatures (such as attained during quicklime reactions) favor partitioning into the vapor phase in three phase systems (Sediak et al. 1991).

Several site-specific factors may affect the degree of odor generated at a biosolids application site such as

* Author to whom correspondence should be addressed.
E-mail: barth.ed@epa.gov

wind velocity, atmospheric stability, temperature, humidity, the amount of material being applied, and the particular application method. Temperature and pH are usually the most important factors that influence the amount of ammonia release from sewage sludge treated with quicklime (Weissinger and Girovich, 1994). After sludge application, fluxes of ammonia follow a diurnal pattern, with maximum exposure occurring at mid-day, decreasing exponentially with time (Beauchamp et al. 1978). In another field application study, odors were strongly dependent upon the meteorological conditions. Weak to moderate odors were observed to last from one day to more than one week, with the odors dissipating more rapidly when the biosolids were incorporated into the field (Hamel, et al., 2004). Fluxes can be used in statistical models to predict air concentrations of odors during and after land application of biosolids (Gabriel et al. 2005; WERF, 2004).

The National Risk Management Research Laboratory (NRMRL) of the United States Environmental Protection Agency (USEPA) and the Environmental Microbial Safety Laboratory (EMSL) of the United States Department of Agriculture (USDA), along with several other organizations performed a field study of a biosolids land application process. One of the primary objectives for this task was to determine the presence and concentrations of a selected group of organic and inorganic compounds and odorants in emissions from samples collected within and downwind of the application area of the biosolids land application test site.

MATERIALS AND METHODS

The biosolids were delivered to the application site at a pH of 7.4 and a solids content of 28%. The biosolids were treated at a conventional municipal wastewater treatment plant with a biosolids processing scheme that included anaerobic digestion, centrifugation with a high dosage of polymer, followed by low-dosage lime treatment, but the exact dosages of polymer and lime were not known. The biosolids could be described as a gel-like, cohesive material, that may not have been readily dispersed into fine particulates during land application as other wastewater biosolids. The effect of these physical properties on subsequent odor measurements were not determined.

Air measurements for a select group of inorganic, organic, and other odorous compounds were performed on biosolids samples collected: (1) within the air space of the truck delivering the biosolids from the treatment

plant to the field location, (2) from a temporary biosolids stockpile, (3) from exhaust air from constructed flux chambers that covered a small portion of the land area, and (4) from the biosolids application area during the application trial date (day 0), and post-application days (days 1–4). The sampling locations for all measurements for this study are shown in Figure 1. A control trial was performed for comparison purposes the day before the application trial (day -1), that involved the movement of the biosolids application machinery over the application area without the application of biosolids.

Headspace Analysis of Biosolids

The headspace emissions of biosolids samples that were progressively collected from the on-site stockpile at the time of land application 0 h, 24 h, and 48 h after application to the field were determined with the use of specially fabricated glass containers. Each of these three samples was collected in triplicate, with each of the triplicate samples comprising a composite sample of seven sample locations within a limited area of the biosolids stockpile. The containers were air-tight and equipped with a sealing cap and a septum sealed sampling port and refrigerated at 4°C. Prior to analysis, each sample was allowed to equilibrate to laboratory temperature (20°C) for 5 h. 2.0 cm³ of air was withdrawn from each 100 g (normalized) sample placed into the sealed container. Each headspace sample was analyzed for targeted organic compounds (such as carbon disulfide, dimethyl sulfide, and dimethyl disulfide) following a modification of USEPA Method TO-15 analysis by GC/MS (USEPA, 1996). The modified procedure analyzed for a partial list of hazardous air pollutants, but the analysis did not include mercaptan compounds. An estimated emission factor for the targeted organic compounds for each of three sampling periods was determined using Equation (1):

$$\text{Emission factor (ng g}^{-1}\text{)} = \frac{\text{concentration (ng L}^{-1}\text{)} \times \text{volume (L)}}{\text{mass of sample (g)}} \quad (1)$$

Flux Chambers Measurements

Four flux chambers (A, C, D, and E) were randomly placed within the biosolids application area, as shown in Figure 1. A fifth flux chamber (B) was placed in the same quadrant (northwest) as flux chamber A to serve as a duplicate chamber. The stainless steel flux cham-

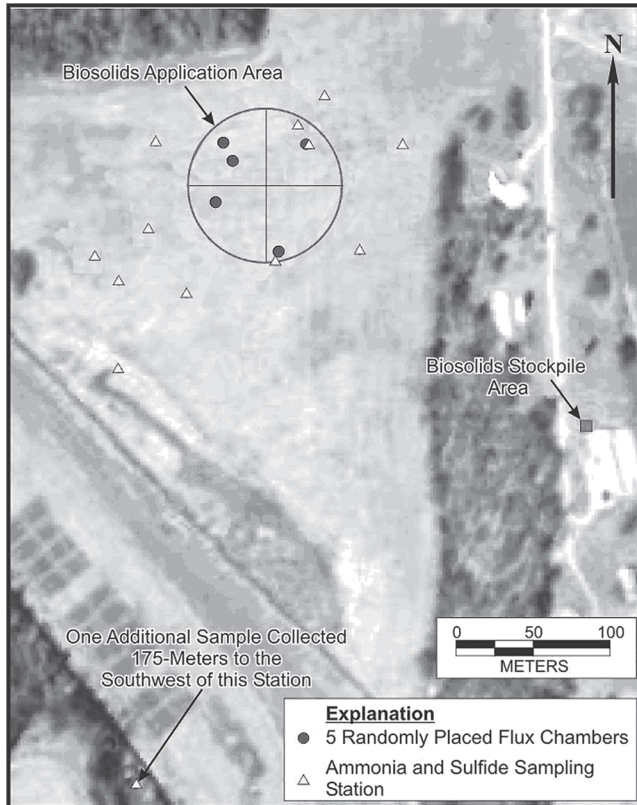


Figure 1. Aerial view of test site and sampling stations.

bers were used to estimate the rate of volatile emissions from the ground surface relative to a known ground surface area. The flux chambers were constructed with a cylindrical bottom, 120 cm width, and 60 cm high, funneling upward to an opening of 7.6 cm for collection of exhaust that was covered with aluminum foil to prevent downdrafts. Ultra-high purity air was evenly introduced into the bottom for makeup air (sweep air) to generate enough sample volume. Air samples were pulled into a 5.0 L SUMMA canister by vacuum and analyzed following USEPA Method TO-15 (USEPA, 1996).

Flux chamber off-gas was also collected in Tedlar® bags within each flux chamber and subsequently analyzed using a solid phase micro-extraction (SPME) absorption technique. The coated fused silica fibers (75 μm carboxen-polydimethylsiloxane fiber) were exposed to the inside of the Tedlar® collection bags for one hour for sample equilibrium, then stored on dry ice before being analyzed by GC/MS. The SPME was injected directly into the GC/MS port and the contaminants were released from the coating in the hot GC/MS port. Specific analytes included trimethylamine, carbon disulfide, dimethyl sulfide, dimethyl disulfide, ethyl mercaptan, propyl mercaptan, and butyl mercaptan. Methyl mercaptan was too volatile and re-

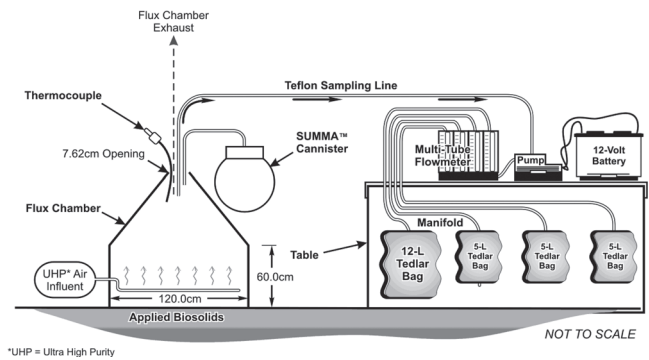


Figure 2. Illustration of flux chamber.

active, and was not able to be calibrated with the SPME method of analysis. The analyte response for SPME analysis was calibrated using gas standards generated from certified permeation devices (VICI Metronics, Poughbo, WA) containing the pure compound.

Figure 2 illustrates the flux chamber design and Figure 3 shows a flux chamber that was installed on the test site. The estimated flux rate for each of the flux chambers was determined using Equation (2):

$$\text{Flux rate } (\mu\text{g m}^{-2} \text{ h}^{-1}) = \frac{\text{amount of contaminant collected in SUMMA canister } (\mu\text{g}) \times \text{ground surface area of chamber } (\text{m}^{-2}) \times \text{collection time } (\text{h}^{-1})}{\text{collection time } (\text{h}^{-1})} \quad (2)$$

Odor Threshold Analysis

On-site odor measurements were determined at various locations at the biosolids application site using hand-held olfactometers (Nasal Rangers®, St. Croix Sensory, Lake Elmo, MN). In addition, air samples were collected from two of the flux chambers by being pulled into a 12.0 L Tedlar® air sample bag via an air



Figure 3. Flux chamber unit installed at field study site.

pump for odor threshold analysis at an off-site location. A certified odor panel was used to conduct the odor analysis following ASTM method E 679-91 (ASTM, 1991). The sample's dilution level (with air) at which an odor is barely detected from three sources (two are odor-free) by a human panelist is termed the detection threshold. Dilutions-to-threshold (D/T) measurements are used to measure detectability.

Direct Gas Measurements (Ammonia, Hydrogen Sulfide)

Field measurements of ammonia were performed using chemical sensory Drager tubes (Model No. 6733231) coupled with a hand-operated vacuum pump, with a detection limit of 0.100 ppmv. In addition, a direct reading instrument was used for hydrogen sulfide. This gas was measured with a Jerome™ gold-film analyzer (Arizona Instruments, Chandler, AZ) with a detection limit of 0.001 ppmv.

RESULTS AND DISCUSSION

Headspace Analysis of Biosolids

Detectable levels of acetone, 2-butanone, methylene chloride, toluene, dimethyl sulfide, and dimethyl disulfide were associated with the biosolids that were collected from the stockpile. As shown in Figure 4, the estimated emission factor was highest for dimethyl sulfide among the organic odorants, with the mean values of the triplicate samples decreasing from 607.1 ng g⁻¹ to 338.5 ng g⁻¹ to 240.9 ng g⁻¹ over the three sampling periods (0 h, 24 h, and 48 h). The estimated emission fac-

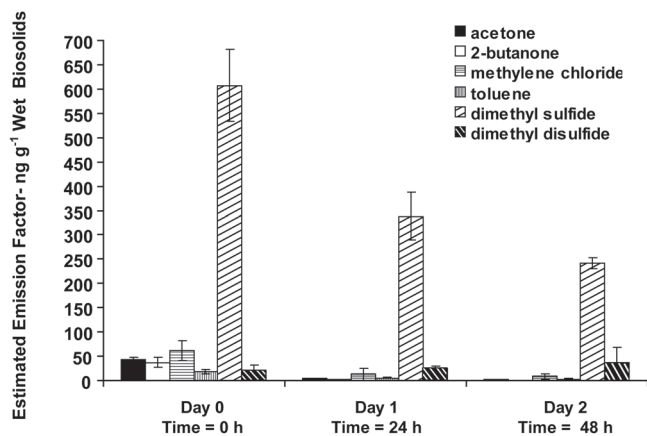


Figure 4. Estimated emission factor of stockpiled biosolids over time.

tor for all of the compounds detected decreased for each of the following two days, except for dimethyl disulfide, which remained relatively constant or showed a slight increase over time. While methylene chloride was suspected as a laboratory contaminant, the fact that the concentrations appeared to decrease over time suggests that it also could have been a volatile emission from the biosolids. The other detected compounds, including acetone, are likely organic byproducts of the degradation process.

Flux Chambers

The calculated flux rates for all of the flux chambers (collected in the SUMMA canisters and analyzed by GC/MS) for acetone, trimethylamine, dimethyl sulfide, and dimethyl disulfide for several of the post application sampling times ($t = 0$ h, $t = 3$ h, $t = 4$ h), and the sampling termination period ($t = 20$ h) are shown in Figure 5. The compounds selected for presentation in Figure 5 exceeded an arbitrarily selected flux rate of 1.0 $\mu\text{g m}^{-2} \text{h}^{-1}$, a value that has no engineering or health significance, but was selected for presentation purposes only.

For all of the flux chambers, acetone was barely detected during the control trial and was present immediately after biosolids placement ($t = 0$ h). It then declined with time after biosolids placement (up to $t = 20$ h). Trimethylamine was not detected immediately after placement ($t = 0$ h) for chambers A, D, and E, increased from $t = 3$ h to 4 h, then was not detected at $t = 20$ h. Trimethylamine odor has been reported to be influenced by the type of polymer used in the biosolids processing (Chang et al. 2005; Kim, et al. 2003).

The estimated flux rates for dimethyl sulfide and dimethyl disulfide showed an initial decrease immediately after application, then increased between the $t = 3$ h and $t = 4$ h time period, then decreased through $t = 20$ h. These flux rates may have been enhanced by an incubator effect in the flux chambers, as temperature reached 42°C within the flux chambers, exceeding the ambient temperature. The magnitude of the flux rates was larger for chamber B, which was located near flux chamber A and was considered a duplicate.

Other measured organic odorants such isopropyl alcohol, 2-butanone, carbon disulfide, methyl isobutyl ketone, toluene, 2-hexanone, styrene, 1,2,4-trimethylbenzene, and 1,4 dichlorobenzene were detected at trace levels (2.4 to 3.8 $\mu\text{g m}^{-3}$), but never exceeded the arbitrary flux rate above 1.0 $\mu\text{g m}^{-2} \text{h}^{-1}$ for any post-application time (therefore are not shown on

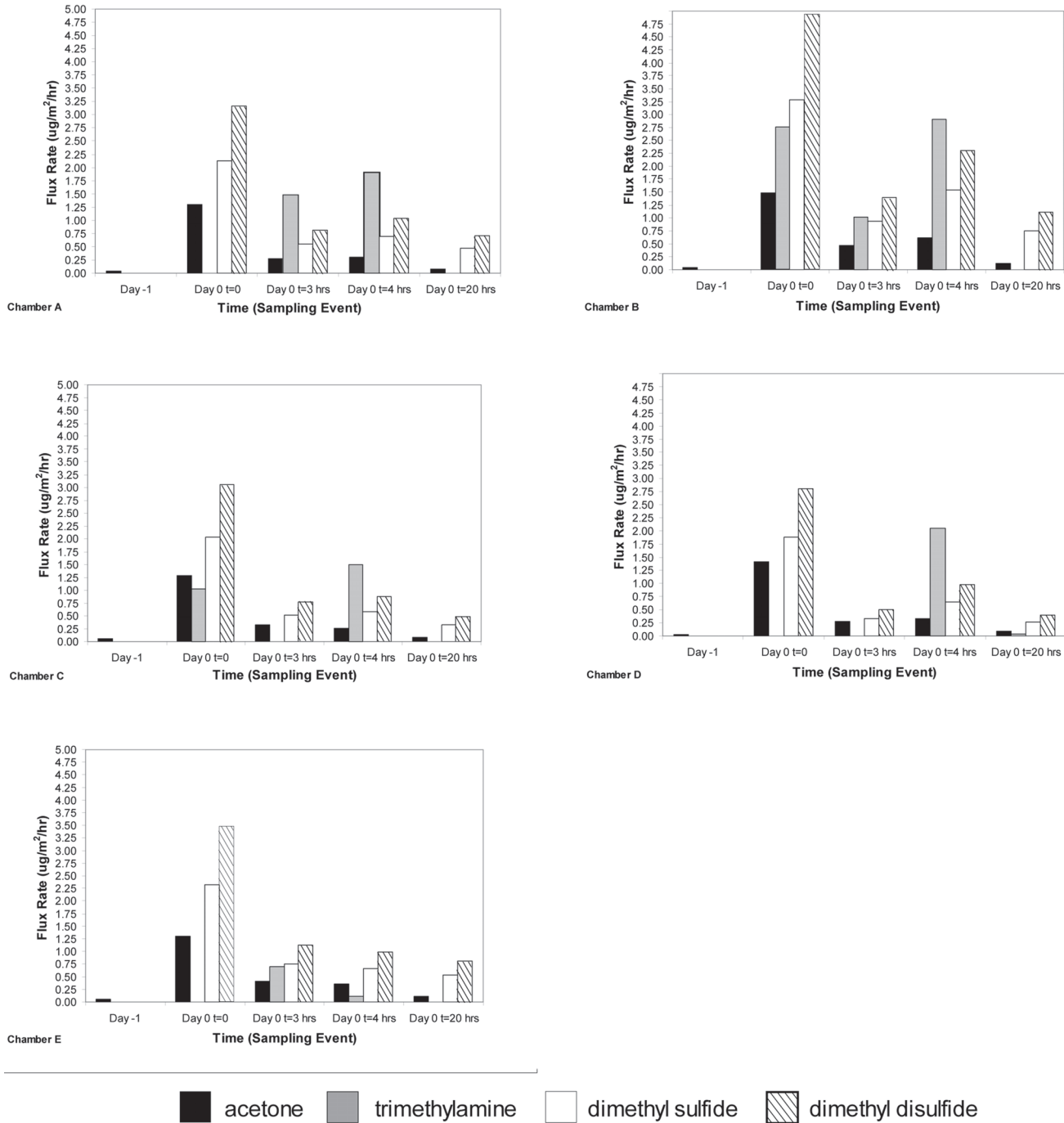


Figure 5. Calculated flux rates for acetone, trimethylamine, dimethylsulfide, and dimethyldisulfide in flux chambers for up to 20 hr after biosolids application.

these figures). The flux rates were negligible for all compounds during the control trial.

The flux chamber air concentrations using SPME for the most frequently detected compounds (dimethyl disulfide, carbon disulfide, dimethyl sulfide, and trimethylamine) for the five flux chambers, are shown in Figure 6. The results presented here are derived from SPMEs that were exposed to Tedlar® bags in the field

and analyzed via a calibrated GC/MS in the laboratory after the field event was completed, as time did not permit the on-site calibration of the GC/MS unit in the field. The SPME data were therefore considered semi-qualitative and direct, temporal comparisons to other air sample results may not be valid. In addition, there may have been potential compound losses during extended holding times and trip blanks were not avail-

able to confirm the extent of these potential losses. Dimethyl disulfide was not detected immediately after application (at $t = 0$ h) and $t = 4$ h, but was detected at $t = 20$ h (range 0.07–0.15 ppmv). Carbon disulfide was detected at low levels in all flux chamber samples but was also present in the baseline sampling, indicating possible interference within the Tedlar® bag. Dimethyl sulfide was detected in all but two samples and the levels remained approximately the same ranging from 0.012 to 0.11 ppmv through $t = 20$ h. Trimethylamine concentrations (range 0.01–0.04 ppmv) were highest at $t = 0$ h, decreased at $t = 3$ h, increased at $t = 4$ h, then decreased at $t = 20$ h. Most of these levels are above the human detection threshold. Ethyl mercaptan, propyl mercaptan, and butyl mercaptan were not detected. The increase in levels of certain compounds over time (up to $t = 20$ h) is different from the previously presented flux chamber results, but may not be valid given the analytical limitations described above.

Although the use of chambers seemed to be an effective approach for measuring flux emissions, the elevated temperatures (greater than 40°C) and humidity inside the chambers due to an incubator effect most likely increased the volatility of the organic compounds measured and may have facilitated microbial activity on the ground. Also, in retrospect, a more focused sam-

pling schedule with better resolution between 4 and 20 h after biosolids application, combined with other weather effects data, would have provided a better understanding of the extent of volatile emissions.

Odor Threshold Analysis

Only ambient trace odor levels were detected at 1.5 m above the surface within the biosolids application area with the Nasal Ranger® instruments prior to biosolids application. Immediately after biosolids application, the DTs levels were 2–7 D/T at 25 m upwind of the application area, 15 to 30 D/T approximately 25 m downwind of the application site, and not detected at distances greater than 75 m from the application area. Slightly less than 24 h after biosolids application, odor levels were approximately 15 D/T in the application area and were undetected above background levels elsewhere in the project area. After 48 h, odors were barely detected downwind of the site, and after 196 h, no odors were detected above background in any location, consistent with other biosolids application studies (Krach et al. 2008; Hamel et al. 2004). As expected, the odor measurements decreased vertically above ground surface and horizontally at increased distances from the application area. The downwind values may have been

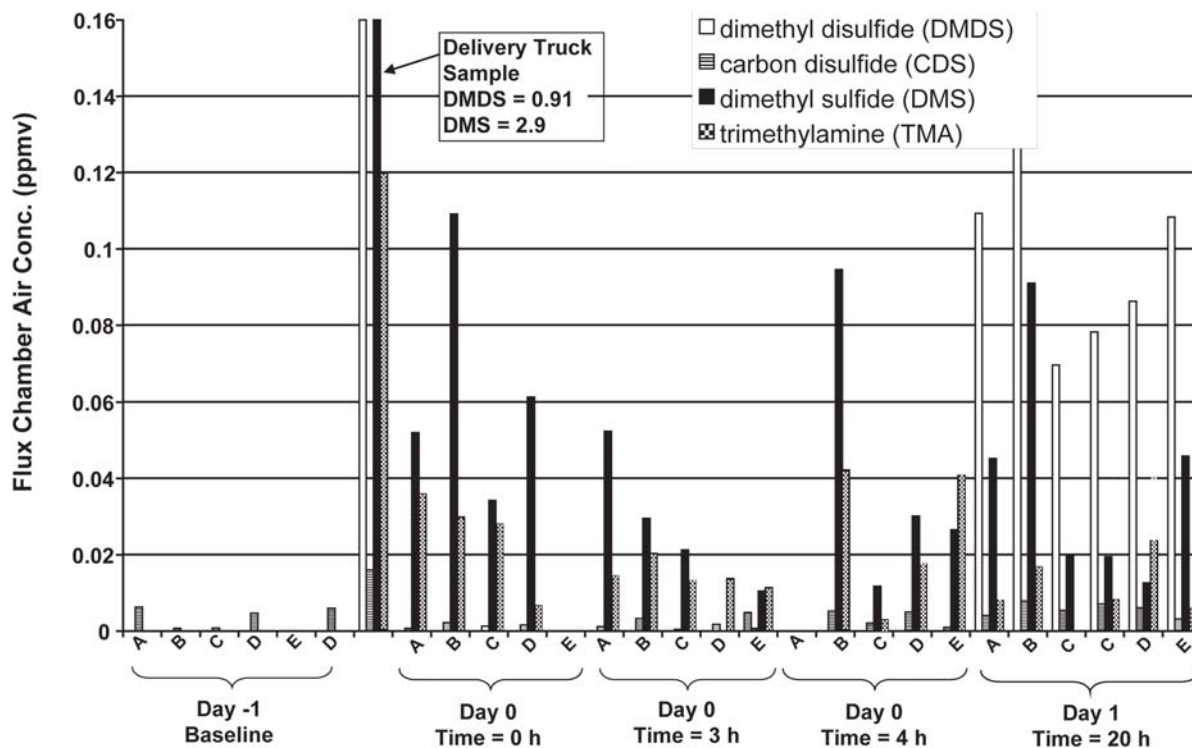


Figure 6. Concentration (SPMEs exposed) to air samples collected within flux chambers over time.

enhanced if a larger amount of biosolids were applied, as the scale of this demonstration was smaller than typical biosolids application sites.

The odor results for two of the flux chambers (B and D) revealed that the detection threshold increased from the control trial readings of 70–90 D/T to the application trial readings of 330–500 D/T immediately after biosolids application ($t = 0$ h). An increase in intensity was observed after the application trial (up to $t = 22$ h) of 2500–6100 D/T, suggesting that either further biological degradation occurred after the biosolids were applied or the incubator effect mentioned previously. Some of these data are consistent with the SPME flux chamber measurements, which showed an increase in concentrations up to $t = 20$ h, but contradictory to both the flux chamber—flux rate results (collected in the SUMMA canisters and analyzed by GC/MS), which showed a decrease after $t = 4$ h, and the field odor threshold results, which showed a decrease in odor with time.

Direct Gas Measurements (Ammonia, Hydrogen sulfide)

Ammonia was not detected 1.5 m above the ground surface during the control trial within the application zone area. Immediately after the application trial, ammonia was detected within the range of 0.10–0.90 ppmv within 200 m of the center of the application area, and from a flux chamber exhaust sample at 15 ppmv. The concentration of ammonia was below detection limits 400 m downwind of the application area during the application trial. Ammonia levels may have been higher had the pH been higher than measured (pH of 7.4) and had the ambient temperature been higher than 25°C.

Hydrogen sulfide was detected at levels near the recognition threshold at concentrations from 0.002 to 0.050 ppmv during the control trial within the application zone area, and at levels of 0.007–0.021 ppmv directly behind the moving biosolids application equipment. Background levels from nearby farming operations as well as the exhaust from the biosolids applicator machinery may have been responsible for some of the hydrogen sulfide measured. Immediately after the application trial ($t = 0$ h), hydrogen sulfide was detected at concentrations within 200 m of the center of the application area slightly lower than the control trial, within the range of 0.001 to 0.007 ppmv for near-ground air samples and from a flux chamber exhaust sample at 0.160 ppmv. The highest measurements

for each of the gases never approached any health criterion nor guidance level. The concentration of hydrogen sulfide was below detection limits 400 m downwind of the application area during the application trial.

The concentrations of both gases decreased to the detection limit the day after application, as expected because of their high vapor pressures, and were below detection limits within 196 h. These data suggest that the volatile odors associated with degradation products may increase for a limited time period after application. Airborne concentrations for both ammonia and hydrogen sulfide were observed to decrease vertically away from the surface and horizontally away from the application area.

Environmental Conditions

In addition to the effects of the physical and chemical properties of the biosolids on odor generation, environmental conditions differed between the control trial and the biosolids application trial which may have also influenced the volatilization of odorants. For the control trial, the empty biosolids application machinery that did not contain any biosolids, was driven over the application field (no biosolids applied to field) at approximately 2:00 P.M. day (–1), with the ambient temperature at 25°C, relative humidity of 50%, and a solar index for the period of 644 w m(–2). For the application trial (day 0), the biosolids application was started at 9:30 A.M., temperature of 19.8°C, relative humidity of 86% (with a visible light fog), and solar index of 404 w m(–2).

CONCLUSIONS

Consistent with previously reported studies, the odorants associated with these particular biosolids, as well as potential polymer degradation products, contained volatile sulfur containing compounds and volatile amine compounds, and dissipated in distance away from the application area and with time. In addition, inorganic gases such as ammonia and hydrogen sulfide were detected within the application area immediately after biosolids application, then decreased both with time and distance away from the application area. The highest measurements for each of the inorganic gases never approached any health criterion nor guidance level. The results of this particular study may not have application to other biosolids applications sites since the biosolids were in a physical form that was less friable than typical biosolids, and the experimental ap-

plication plot of the two acres was somewhat smaller than most agricultural biosolids application sites.

REFERENCES

- ASTM. 1991. Standard Practice for Determination of Odor and Taste Thresholds by a Forced-Choice Series Method of Limits. Method E679-91. Vol. 15.08. American Standard for Testing and Materials. W. Conshocken, PA.
- Beauchamp, E., G. Kidd, and G. Thurtell. 1978. Ammonia Volatilization from Sewage Sludge Applied in the Field. *Journal of Environmental Quality*, 7(1), 141–146.
- Chang, J., M. Abu-Orf, and S. Dentel. 2005. Alkylamine Odors from Degradation of Flocculant Polymers in Sludges. *Water Research*, 39, 3369–3375.
- Dalton, P., N. Doolittle, and P. Breslin. 2002. Gender-specific Induction of Enhanced Sensitivity to Odors. *Nature Neuroscience*, 5, 199–200.
- Dalton, P. 1999. Cognitive Influences on Health Symptoms from Acute Chemical Exposure. *Health Psychology*, 18(6), 579–590.
- Gabriel, S., S. Vilalai, S., C. Peot, and M. Ramirez. 2006. Statistical Modeling to Forecast Odor Levels of Biosolids Applied to Reuse Sites. *Journal of Environmental Engineering*, 132(5), 479–488.
- Gabriel, S., S. Vilalai, S. Arispe, H. Kim, L. McConnell, A. Torrents, C. Peot, and M. Ramirez. 2005. Prediction of Dimethyl Disulfide Levels from Biosolids Using Statistical Modeling. *Journal of Environmental Science and Health, Part A*, 40(11), 2009–2025.
- Hamel, K., L. Walters, C. Sulerud, M. McGinley. 2004. Land Application Odor Control Case Study. Water Environmental Federation Residuals and Biosolids Management Conference, Salt Lake City, Utah.
- Kim, H., S. Murthy, L. McConnell, C. Peot, M. Ramirez, and M. Strawn. 2003. Examination of Mechanisms for Odor Compound Generation During Lime Stabilization. *Water Environmental Research*, 75(2), 121–125.
- Krach, K., B. Burns, B. Li, A. Shuler, C. Colee, and Y. Xie. 2008. Odor Control for Land Application of Lime Stabilized Biosolids. *Water Air & Soil Pollution: Focus* 8(3–4), 368–378.
- Rosenfeld, P., C. Henry, and D. Bennett. 2001. Wastewater Dewatering Polymer Affect on Biosolids Odor Emissions and Microbial Activity. *Water Environmental Research*, 73(3), 363–367.
- Schiffman, S., J. Walker, P. Dalton, T. Lorig, J. Raymer, D. Shusterman, and C. Williams. 2000. Potential Health Effects of Odor from Animal Operations, Wastewater Treatment, and Recycling of Byproducts. *Journal of Agromedicine*, 7(1), 7–81.
- Sediak, D., K. Dean, D. Armstrong, and A. Andren. 1991. Interaction of Quicklime with Polychlorobiphenyl-Contaminated Soils. *Environmental Science and Technology*, 25(11), 1936–1940.
- USEPA. 2000. Guide to Field Storage of Biosolids. Office of Wastewater Management. Report No. EPA 832-B-00-007.
- USEPA. 1996. EPA Method TO-15. The Determination of Volatile Organic Compounds in Air Collected in Summa Canisters and Analyzed by Gas Chromatography/Mass Spectrometry (GC/MS).
- Water Environmental Research Foundation (WERF). 2004. Health Effect of Biosolids Odors: A Literature Review and Analysis. WERF Project No. 00-HHE-5C, Alexandria, VA.
- Weissinger, T. and M. Girovich. 1994. Evaluation of a Chemical Stabilization Process. *Remediation Journal*, 5(1), 77–99.

Comparison of *Salmonella enterica* subsp. *enterica* Survival in Agricultural Soil Amended with Vermicompost and Class A Biosolids

NOHELIA CASTRO-DEL CAMPO¹, ELIZABETH ESPINOZA¹, JOSÉ B. VALDEZ-TORRES¹, CHARLES P. GERBA² and CRISTÓBAL CHAIDEZ^{1,*}

¹Centro de Investigación en Alimentación y Desarrollo A.C., Culiacán, Sinaloa 80110

²The University of Arizona, Department of Soil, Water, and Environmental Science, Tucson, Arizona 85721

ABSTRACT: Organic fertilizers use has been recently questioned because of the potential for *Salmonella* regrowth if animal manure is used as the starting organic waste. The aim of this study was to determine the potential for *Salmonella enteric* subsp. *enterica* regrowth in a vermicompost and compare it to a Class A biosolids, soil, and amended soil. Different initial *Salmonella* inocula were added to the mixtures with 30% moisture content and incubated for 20 days. *Salmonella* first declined to undetectable levels in the biosolids, followed by vermicompost, and persisted the longest in soil and amended soil. No *Salmonella* regrowth was observed in any of the treatments tested.

INTRODUCTION

MÉXICO generates an estimated 16 1/2 million tons/year of organic wastes [15]. Organic wastes are derived from plant or animal residues such as manure, food, crops and biosolids [5]. Agricultural re-use of organic waste is considered an important approach for reducing inadequate waste disposal and increasing recycling [7]. Vermicompost produced from cattle manure residues by the earthworm, *Eisenia foetida*, along with biosolids from wastewater treatment are being utilized as organic fertilizers in the Americas. These are rich in organic matter and nutrients and have improved texture and water holding capacity that make them adequate for crop production [3].

Vermicompost and biosolids may contain microbial pathogens including *Salmonella*, a pathogenic bacteria commonly present in wastewater and animal manures. Biosolids generally contain 10² to 10³ *Salmonella* colony forming units (CFU)/g of dry weight [16]. In England, animal manure has been reported to contain from 10² to 10⁷ *Salmonella* CFU/g [11].

Composting, alkaline stabilization, heat drying, solar drying beds and vermicomposting are treatments commonly used to reduce the levels of pathogens before

they are applied to land. Nevertheless studies have documented the survival of *Salmonella* at low initial concentrations during the composting process. *Salmonella* has also been demonstrated to regrow under favorable environmental conditions [14,1]. In addition, other studies have shown that recontamination of the final product might occur by external sources (birds and other animals) [21]. *Salmonella* survival and regrowth are determined by factors such as temperature, soil type, pH, organic matter, moisture content, nutrients and the antagonistic effects of indigenous microbiota such as bacteria and fungi [4].

The objective of the present study was to determine the potential of *Salmonella enterica* subsp. *enterica* to survive/grow in vermicompost, and compare it to Class A biosolids and after their addition to soil at rates normally applied to agricultural land.

MATERIAL AND METHODS

Soil and Amendments

Soil was collected from the Instituto Nacional de Investigaciones Forestales, Agrícolas y Pecuarias (INIFAP) located at Culiacán-Eldorado km 17.5 México. Vermicompost and biosolids were obtained from the Humi-Bac Company (Culiacan, Sinaloa, Mexico) and Milorganite® (Class A pellets, Milwaukee,

* Author to whom correspondence should be addressed.
E-mail: chaqui@ciad.edu.mx

WI), respectively. Both vermicompost and Class A biosolids were tested for the presence of *Salmonella* before proceeding with the study. Table 1 lists some physical-chemical characteristics of the vermicompost, biosolids and agricultural soil used in this study. The rate of application recommended by fertilizer companies for vermicompost and biosolids is equivalent to 2 t/ha. For those experiments this was approximated by adding the amendments at a level of 0.1% (800 mg per 800 g soil).

Preparation of Inoculum

Salmonella enterica subsp. *enterica* (ATCC 23564) was obtained from the American Type Culture Collection (Manassas, VA). The inoculum was prepared by adding a loop of *Salmonella* to 75 mL of Trypticase Soy Broth (TSB) (Bioxon, México). After overnight incubation at 37°C in a shaking water bath, the culture of *Salmonella* was centrifuged for 10 min at 13,800 × g at 4°C. The pellet was then washed two times and re-suspended in 100 mL of sterile 0.1 M monophosphate buffer. The concentration of the inoculum was determined by spread plate assay onto Hektoen agar (Difco Co., Detroit, MI).

Inoculation of *Salmonella enterica* subsp. *enterica*

Vermicompost, biosolids, soil or amended soil were placed in separate sterile plastic containers and inoculated by addition of suspensions of 10¹, 10⁴, and 10⁶ CFU/mL to produce a final moisture content of 30% (field capacity). Next, 25 g of each mixture was placed in sterile 50 mL polypropylene conical centrifuge tubes with screw caps, held at 28°C, and sacrificed at intervals of 0, 1, 3, 5, 10, 15 and 20 days. Two replicates per day were assayed.

Salmonella enterica subsp. *enterica* Assay

Salmonella concentrations were determined by removing 10 g of sample from each conical tube and placing them in a flask containing 95 mL of sodium novobiocin (40 µg/mL) buffered peptone water (Difco Co., Detroit, MI), and placement on a shaker for 15 min. Serial dilutions were made in sterile monophosphate buffer and 0.1 mL was spread onto Hektoen agar (Difco Co., Detroit, MI). Plates were incubated at 37°C for 24 h and then *Salmonella* colonies were enumerated (Yeager and Ward, 1981). Randomly selected colonies of *Salmonella* from the Hektoen plates were confirmed by polymerase chain reaction (PCR) using the kit PCR Core System I (Promega, Madison, WI).

Heterotrophic Plate Count

Samples of 10 g from each treatment were collected and placed into 95 mL of Trypticase Soy Broth (TSB), and agitated for 15 min. Heterotrophic plate count bacteria (HPC) were assayed on R2A agar (Difco Co., Detroit, MI) and incubated at 28°C for 5 days [21].

Data Analysis

Data registered consisted of CFU/g, transformed to base 10 logarithms. No detections were recorded as 0 (log(1)). A three factor completely randomized design, with two replicates, was implemented using MINITAB 14.0 (Minitab Inc). Treatment effects were determined by analysis of variance and significant differences by the Tukey test ($P \geq 0.05$).

RESULTS

Analysis of variance (ANOVA) showed that all treat-

Table 1. Physical and Chemical Characteristics of Substrates.

Parameter/substrate	Vermicompost (Mean ± std. dev)	Milorganite®	Agricultural Soil sand 25%, silt 18%, clay 57%
N	0.84 ± 0.05%	6%	43.2 mg/kg
P ₂ O ₅	1.33 ± 1.05%	2%	16 mg/kg
Ca	4.98 ± 4.86%	1.2%	2050 mg/kg
Cl	–	1%	–
Fe	2975.9 ± 214.3 mg/kg	4%	3.3 mg/kg
Zn	87.76 ± 30.35 mg/kg	500 mg/kg	0.9 mg/kg
Cu	9.54 ± 6.39 mg/kg	240 mg/kg	3.2 mg/kg
Organic matter	13.65 ± 3.39%	–	1.33%
pH	7.4 ± 0.59	–	7.6

Sources: CIAD for vermicompost; milorganite.com; INIFAP for soil.

Table 2. ANOVA for Log Transformed Counts of *Salmonella enterica subsp. enterica* in the Different Treatments.

Source	DF	Seq SS	Adj MS	F	P
Mixture*	4	100.515	25.219	375.05	0.000
Concentration	2	568.674	284.337	4243.83	0.000
Mixture & Concentration	8	36.666	4.583	68.40	0.000
Time	6	164.237	27.372	408.55	0.000
Mixture & Time	24	36.705	1.529	22.82	0.000
Concentration & Time	12	66.480	5.538	82.65	0.000
Mixture & Concentration & Time	48	43.586	0.908	13.55	0.000
Error	105	6.053	0.067		
Total	209				

*Soil (S), Vermicompost (V), Biosolids (B), soil+vermicompost (S+V), soil+biosolids (S+B).

ments were significantly different in terms of die-off of *Salmonella* ($P \leq 0.00$) (Table 2). *Salmonella* inoculated at a concentration of 1×10^1 CFU/g was not detected after one day in soil or any other mixture [Figure 1(a)]. *Salmonella* inoculated at a concentration of 1×10^4 CFU/g declined rapidly in the biosolids, followed by vermicompost [Figure 1(b)] and was not detectable after 5 and 10 days, respectively. In soil and soil amended with both organic fertilizers, *Salmonella* survived over the entire 20 days, declining by only one log. A similar trend was observed at the inoculated concentration of 1×10^6 CFU/g [Figure 1(c)], where *Salmonella* declined to non-detectable levels in the biosolids within 10 days and vermicompost within 15 days, but not in amended soil.

No significant differences between treatments (in terms of die-off) were observed at the initial inoculated concentration of 1×10^1 CFU/g. *Salmonella* inoculated at 1×10^4 CFU/g in soil amended with biosolids was detectable longer, only being reduced by one log after 20 days. In the agricultural soil and soil amended with vermicompost, *Salmonella* declined only at day 10, whereas in vermicompost, a 3-log reduction occurred by day 5 and *Salmonella* was not detected after 10 days. *Salmonella* decreased by 2 logs at 3 days and did not survive for more than 5 days in the Class A biosolids. *Salmonella* inoculated at a concentration of 1×10^6 CFU/g were recoverable for 20 days in soil, but only 10 and 15 days when inoculated in biosolids and vermicompost, respectively. *Salmonella* was reduced at a similar rate regardless of initial concentration.

Similar *Salmonella* behavior was observed at the treatments with initial inoculated concentrations of 1×10^4 and 1×10^6 CFU/g. More specifically, the same was observed when *Salmonella* was added to agricultural soil and soil amended with biosolids and vermicompost. In contrast, survival in both vermicompost and biosolids class A alone were statisti-

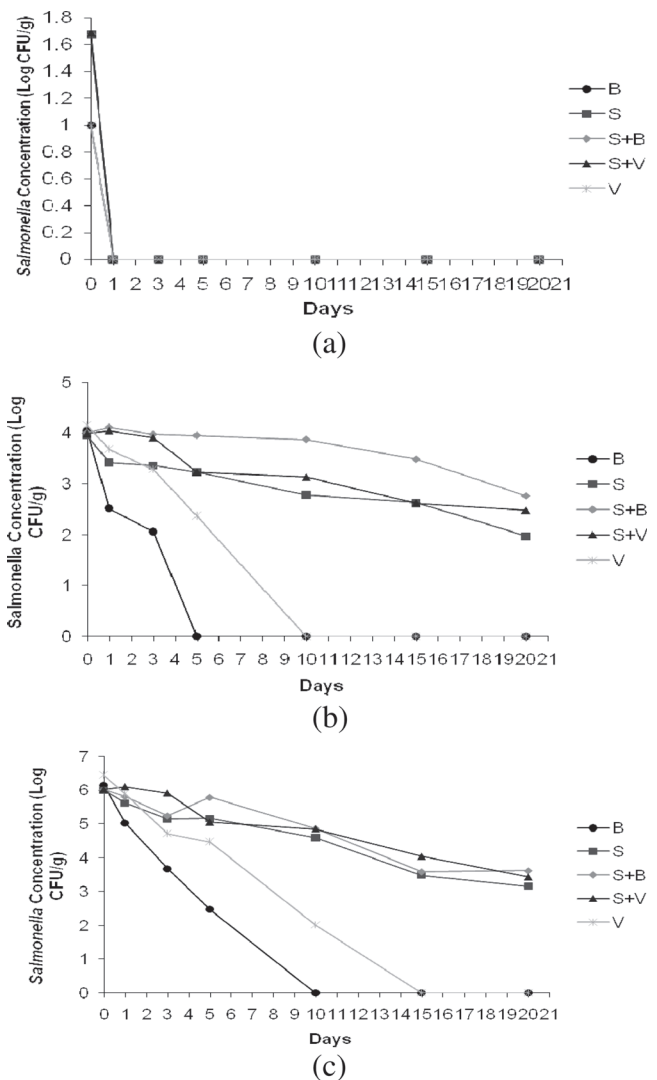


Figure 1. *Salmonella* recovery in the different mixtures when inoculated at the three initial inoculums, (a) 1×10^1 CFU/g, (b) 1×10^4 CFU/g, (c) 1×10^6 CFU/g.

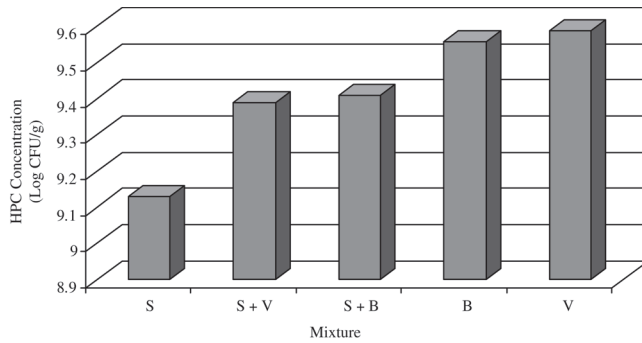


Figure 1. HPC values during the 20 day-experiment for each one of the different mixtures.

cally different ($P = 0$) decreasing rapidly and not detected after 10 to 15 days. In agricultural soil, *Salmonella* was able to survive during the 20 days of the experiment and the addition of the organic fertilizers reduced the rate of *Salmonella* decline; however, there were no statistical differences in *Salmonella* survival.

High concentrations of HPC (> 9 log/dry g) were detected in both organic fertilizers, in soil amended with both fertilizers, and in the soil alone (Figure 2). The concentrations of HPC remained stable throughout the experiment.

DISCUSSION

The rate of *Salmonella* decline was greatest in vermicompost and Class A biosolids, followed by soil, and then the mixtures of soil + amendments. It was observed that *Salmonella* was not detectable after 10 days in the Class A biosolids and vermicompost, compared to soil and the mixtures of soil + vermicompost or biosolid, in which *Salmonella* decreased an average of 2.0 log₁₀ by day 20. Nevertheless, there was no significant difference between these reductions. It has been observed that *Salmonella* survives longer in clay-type soils than in sand-type soils [9]. Bacterial pathogens such as *Salmonella*, *Escherichia coli* O157:H7 and *Listeria* survive longer in manure amended with clay loam grassland soil than in sandy arable soil. Comparing our results to those obtained previously [2] using a sandy loam soil, we observed that clay loam provided a better environment for *Salmonella*, enabling it to survive longer. Soil particles are believed to function as micro-ecological niches rich in nutrients in which species of *Salmonella* can survive, replicate, and be protected from predation [19]. Pepper et al. [12] observed that soil with fine texture provided greater protection to enteric bacteria and thus their longer persistence in the environment.

Salmonella was detected for longer periods in mixtures containing fertilizers and soil. This corresponds with the results obtained by Paluszac et al. [10] in which the survival of *E. coli*, *Streptococcus* and *Salmonella* in soil increased with the addition of animal manure. This effect is due to the higher availability of nutrients following the addition of the manure. Zaleski et al. [21] performed a field study to determine the regrowth of *Salmonella* in aerobically and anaerobically digested Class B biosolids following rainfall events. They concluded that *Salmonella* regrowth occurred only after rainfall episodes and the reintroduction of *Salmonella* from external sources.

In the current study, we observed that neither Class A biosolids nor vermicompost by themselves support *Salmonella* regrowth and that the initial *Salmonella* concentration decreased following inoculation. These results are similar to those of a previous study [2] in which *Salmonella* concentrations declined at a higher rate in biosolids after inoculation at 20% moisture content. Hussong et al. [6] evaluated *Salmonella* growth in 30 composted samples inoculated with *Salmonella* at a concentration of 1×10^7 CFU/g. *Salmonella* did not survive more than 7 days in 50% of the samples. Several authors have reported the antagonistic effect of indigenous microbiota on the survival of pathogenic microorganisms in biosolids and vermicompost [14,6,18]. In the present study, it was observed that the *Salmonella* decrease was greater in Class A biosolids or vermicompost; one possible reason for this was the high concentrations of heterotrophic plate count found in both.

Millner et al. [8] showed that *Salmonella* suppression is not due to a specific group of microorganisms; however, they reported that the presence of Gram negative bacteria, high levels of actinomycetes and mesophilic bacteria play an important role in *Salmonella* growth inhibition. This correlates with our results in which we found the presence of *Bacillus* spp, actinomycetes, and *Pseudomonas fluorescens* in high concentrations in the various substrates influencing *Salmonella* behavior (Data not shown). Although *Salmonella* reduction depends on the type and concentration of microorganisms, it does not depend on a single microbial species or group of organisms.

Pietronave et al. [13] studied the role of indigenous microbiota in the suppression of *Salmonella* in sterile and non-sterile compost under different moisture contents. They demonstrated that *Salmonella* grows rapidly in sterile compost in comparison to non-sterile

compost, where the inactivation rate of the bacterium was greater. Szczech and Smolinska [17] reported that vermicompost microbiota produced from animal manure significantly reduced populations of *Phytophthora nicotianae*, preventing infection in plants. Szczech [18] observed that *Fusarium oxysporum* is similarly eliminated and that the inhibitory effect against this fungus increases as the vermicompost application increases.

CONCLUSIONS

No *Salmonella enterica* subsp. *enterica* regrowth was observed in Class A biosolids or vermicompost individually or after addition to an agricultural soil at 30% moisture content at typical agronomic rates.

Salmonella was shown to survive in an agricultural soil and the same soil amended with Class A biosolids and vermicompost for at least 20 days. In contrast, the pathogen survived for less than 5 to 15 days in Class A biosolids and vermicompost, depending on the initial inoculum. Cautions should be taken when organic fertilizers are stored prior to land application to avoid pathogenic bacterial reinoculation by wild fauna.

The limited nature of the testing performed depends on the relative behavior of an ATCC culture compared to wild *Salmonella*, which is likely better adapted to the environment, hence it is highly recommended to perform further *Salmonella* regrowth experiments using an isolated wild strain.

ACKNOWLEDGMENTS

We profoundly thank QFB Célida Isabel Martínez Rodríguez for her technical support.

REFERENCES

- Burge, W.D., N.K. Enkiri, D. Hussong. *Salmonella* Regrowth in Compost as Influenced by Substrate (*Salmonella* Regrowth in Compost). *Microbial Ecology*, Vol. 14, No. 3, 1987, pp. 43–253.
- Castro-del Campo, N., I.L. Pepper, C.P. Gerba. Assessment of *Salmonella typhimurium* Growth in Class A Biosolids and Soil/Biosolid Mixtures. *Journal of Residual Science and Technology*, Vol. 4, No. 2, 2007, pp. 83–88.
- Cooker, E.G. 1988. *The Use of Sewage Sludge in Agriculture*. Capertown. IAWPCR/Pergaman Press Ltd.
- Estrada, I.B., A. Aller, F. Aller, X. Gómez, A. Morán. The Survival of *Escherichia coli*, faecal coliforms and Enterobacteriaceae in General in Soil Treated with Sludge from Wastewater Treatment Plants. *Bioresource Technology*, Vol. 93, No. 2, 2004, pp. 1991–1998.
- FDA. Food and Drug Administration. 2002. *Mejorando la seguridad y calidad de frutas y hortalizas frescas: Manual de formación para instructores*. University of Maryland, Symons Hall, Collage Park.
- Hussong, D., W.D. Burge, N.K. Enkiri. Occurrence, Growth, and Suppression of *Salmonellae* in Composted Sewage Sludge. *Applied and Environmental Microbiology*, Vol. 50, No. 4, 1985, pp. 887–893.
- Jurado, G.P., L.M. Luna, H.R. Barretero. Aprovechamiento de Biosólidos como Abonos Orgánicos en Pastizales Áridos y Semiáridos. *Técnica Pecuaria Mexicana*, Vol. 42, No. 3, 2004, pp. 379–395.
- Millner, P.D., K.E. Powers, N.K. Enkiri, W.D. Burge. Microbially Mediated Growth Suppression and Death of *Salmonella* in Composted Sewage Sludge. *Microbial Ecology*, Vol. 14, No. 3, 1987, pp. 225–265.
- Nicholson, F.A., S.J. Groves, B.J. Chambers. Pathogen Survival during Livestock Manure Storage and Following Land Application. *Bioresource Technology*, Vol. 96, No. 2, 2005, pp. 135–143.
- Paluszak, Z., A. Ligocka, B.B. Breza, H. Olszewska. The Survival of Selected Fecal Bacteria in Peat Soil Amended with Slurry. *Electronic Journal of Polish Agricultural University*, Vol. 6, No. 2, 2005, pp. 1–7.
- Pell, A. N. Manure and microbes: public and animal health problem?. *Journal of Dairy Science*, Vol. 80, No. 10, 1997, pp. 2673–2681.
- Pepper, I.L., K.L. Josephson, R.L. Bailey, M.D. Burr, C.P. Gerba. Survival of Indicator Organisms in Sonoran Desert Soil Amended with Sewage Sludge. *Journal of Environmental Science and Health*, Vol. 28, No. 6, 1993, pp. 1287–1302.
- Pietronave, S., L. Fracchia, M. Rinaldi, M.G. Martinotti. Influence of Biotic and Abiotic Factors on Human Pathogens in a Finished Compost. *Water Research*, Vol. 38, No. 8, 2004, pp. 1963–1970.
- Russ, C.F. and W.A. Yanko. Factors Affecting *Salmonellae* Repopulation in Composted Sludges. *Applied and Environmental Microbiology*, Vol. 41, No. 3, 1981, pp. 597–602.
- SEMARNAT. 2002. *Compendio de Estadísticas Ambientales*. Secretaría de Medio Ambiente y Recursos Naturales. México.
- Sidhu, J., R.A. Gibbs, I. Unkovich. The Role of Indigenous Microorganisms in Suppression of *Salmonella* Regrowth in Composted Biosolids. *Water Research*, Vol. 35, No. 4, 2001, pp. 913–920.
- Szczech, M. and U. Smolinska. Comparison of Suppressiveness of Vermicomposts Produced from Animal Manure and Sewage Sludge against *Phytophthora nicotianae* Breda de Haan var. *nicotianae*. *Journal of Phytopathology*, Vol. 149, No. 2, 2001, pp. 77–82.
- Szczech, M.M. Suppressiveness of Vermicompost against *Fusarium wilt* of Tomato. *Journal of Phytopathology*, Vol. 147, No. 3, 1999, pp. 155–161.
- Winfield, M.D. and E.A. Groisman. Role of Non-host Environments in the Lifestyles of *Salmonella* and *Escherichia coli*. *Applied and Environmental Microbiology*, Vol. 69, No. 7, 2003, pp. 3687–3694.
- Yeager, J.G. and R.L. Ward. Effects of Moisture Content on Long-term Survival and Regrowth of Bacteria in Wastewater Sludge. *Applied and Environmental Microbiology*, Vol. 41, No. 5, 1981, pp. 1117–1122.
- Zaleski, K.J., K.L. Josephson, C.P. Gerba, I.L. Pepper. Potential Regrowth and Recolonization of *Salmonellae* and Indicators in Biosolids and Biosolid-Amended Soil. *Applied and Environmental Microbiology*, Vol. 71, No. 7, 2005, pp. 3701–3708.

The Relationship Between Particle Size and Turbidity Fluctuations in Coagulation Process

WEN PO CHENG*, WEI YI CHEN, RUEY FANG YU and YING JU HSIEH

¹Department of Safety, Health and Environmental Engineering, National United 18 University, Miaoli, Taiwan

ABSTRACT: An on-line Nephelometric Turbidimeter Monitoring System (NTMS) was used in this study to measure water turbidity every second. The standard deviation (SD) of the measured turbidity was found proportional to the particle size; a greater turbidity SD indicated larger particle sizes. Also, a video camera (Watec Co Wat-202B) with image analysis (Matrox Inspector V2.2) was used to confirm whether NTMS is suitable for directly applying to particle size analysis. On the other hand, to understand the relationship between SD of the measured turbidity and particle size of the coagulated floc, the Poly Aluminum Chloride (PACl) prepared in laboratory was used as a coagulant in Jar Test to perform a solid-liquid separation study on a high turbidity (100 NTU) synthetic algae water (algae specie: *Chlorella sp.*). The experimental results indicate that for 100 NTU *Chlorella sp.* suspensions, the NTMS is simple and effective to find the floc size change in flocculation and selection the optimal flocculation conditions.

1. INTRODUCTION

JAR Test based on the residual turbidity in the treated water is generally used to evaluate the optimal conditions for particle treatment efficiency [1–6]. However, the final residual turbidity cannot show the variation of turbidity and floc formation during the coagulation process. This usually leads to over dosage of chemical coagulants, higher operation costs and increased chemical sludge. Thus, the average floc diameter measured using floc monitoring was studied to index the real coagulation efficiency. The current floc monitoring techniques, such as microscopy combined with photography or image analysis, and light scattering can be used as a qualitative tool in particle size and provides good data regarding particle shape and form [7–10]. But, the monitoring technique of microscopy, however, is time consuming requiring large sample sizes [11]. Recently, some research literatures provide a comprehensive understanding of the floc diameter, which is obtained by a Photometric Dispersion Analyzer (PDA) based on the turbidity fluctuation technique [12–16]. The theory of turbidity fluctuation technique is if a small volume of a colloidal suspension is observed microscopically, the particles was moved by a

Brownian diffusion in and out of the observed volume. Therefore, the total number of particles was viewed varies in a random manner. It can be shown that these variations follow the Poisson distribution. A very important consequence of the Poisson distribution is that the variance is equal to the mean; so that the standard deviation is the square root of the mean [11]. Therefore, in a Photometric Dispersion Analyzer (PDA) monitoring system, it can be assumed that the ration of the root mean square (V_{RMS}) of the turbidity fluctuating signal is roughly proportional to the particle size. However, the PDA is not a commonly used instrument in water treatment plants. For this reason, in the previous study, a Nephelometric turbidimeter monitoring system (NTMS) was used for on-line monitoring of turbidity fluctuations during the coagulation process [17]. The fluctuating turbidity data obtained from the NTMS were then analyzed to evaluate the floc size growth. Because the scattered light intensity produced from turbidity measurement depends on whether the incoming light is well illuminating a floc. When the suspension flocs become larger in sizes and fewer in numbers due to the flocculating mixing, the illuminated flocs become less uniform in particle distribution in the test solution. Hence, the turbidity values are fluctuating. Thus, the size of the flocs was proportional to the amplitude of turbidity fluctuations. The Standard Deviation (SD) of the turbidity data was found to be directly re-

* Author to whom correspondence should be addressed.
E-mail: cwp@nuu.edu.tw

lated to the size of the flocs.) Therefore, in this study, suspensions of *Chlorella sp.* algae cultivated in laboratory were used as the high turbidity sample (100 NTU) to test the turbidity fluctuations in Jar Test by NTMS for evaluating the floc size change in flocculation. Also, particle size analysis with images captured from cameras was used to confirm whether the SD data from NTMS technology is suitable be a factor for particle size analysis.

EXPERIMENTAL

1. Algae

Chiarella sp., a green algae existing commonly in Taiwan's lakes, is single celled with about 4.8 μm average cell diameter. Sources of the seeding algae came from Taiwan Provincial Fishery Research Institute Tong Kong Branch. The seeding algae were incubated aseptically in a one liter glass container for sometime until higher concentrations are reached. The suspension was transferred to a 5-liter cylindrical glass container, which had been sterilized at 121°C and 1.3–1.5 kg/cm² for 30 minutes and then cooled down to room temperature. The initial ratio of algae to cultivation solution was maintained at 4:6; the content was incubated with 1 L/min aseptic air under illumination sideways with fluorescence light at 3000–4000 Lux for 16 hr/day. The cultivated algal suspensions were diluted with super pure water until the turbidity was adjusted to 100 NTU and the initial pH to 9.0 prior to conducting the coagulation study.

2. Preparation of the Coagulant

The Poly Aluminum Chloride (PACl) synthesized used in the coagulation study was prepared in our labo-

ratory by adding 50 mL of 0.46 M NaOH to 50 mL of 0.2 M AlCl_3 solution at 0.05 mL/min with a peristaltic pump. At the completion of NaOH addition, the final solution was 100 mL containing 0.1 M $[\text{Al}^{3+}]$ ions and the synthesized PAC coagulant contained a Basicity (B) of 2.3 ($B = [\text{OH}^-]/[\text{Al}^{3+}]$).

3. The Relationship Between Particle Size and the SD of the Measured Turbidity Fluctuations

After drying and grinding the organic com cob, different size particles of the com cob were separated by screening them with a series of different mesh size sieves. The median value of the particle size range in every sieve number was taken as the representative average particle size for each sample. Five sets of different average com cob particle size test water were prepared. The sieve mesh range, particle size range and average particle size was presented in Table 1. For each size of 115, 137, 335, 460, 920 μm in particle diameter, 0.4 g of com cob particle was added into 1-L de-ionized water. Then, all the test water were stirred at a speed of 20 rpm. The turbidity measurement from a NTMS was done in every second for 10 minutes to yield 600 data. Thus, the Standard Deviation (SD) of the turbidity data for each particle size was found. Figure 1 shows the NTMS attachment. A hole was made in the wall of the test vessel to enable the probe of the Nephelometric turbidimeter to reach into the water. A Light-Emitting Diode (LED) on the probe of Nephelometric turbidimeter was used to illuminate the solution at 90° to the path of light entering the turbidimeter. The intensity of the scattered light, which was measured with the detector at 860 nm red light, was converted to turbidity value. The measured turbidity was recorded with a data acquisition unit (YOKOGAWA model FX-106-0-2) and then uploaded to a computer.

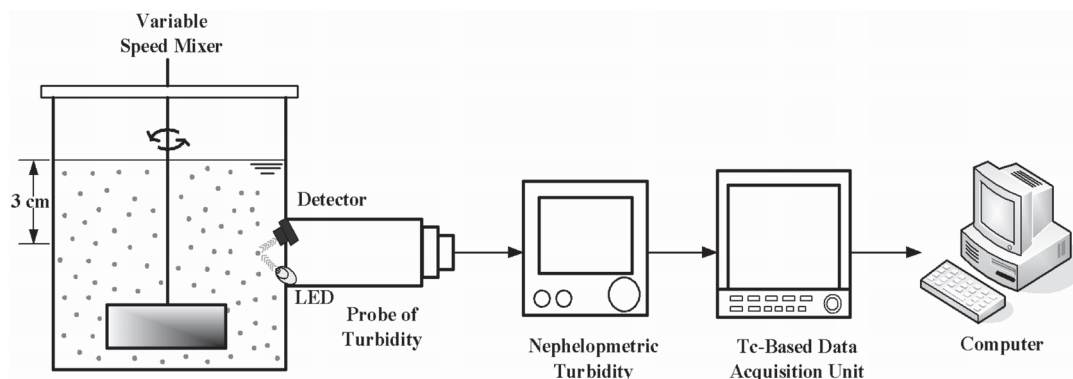


Figure 1. A schematic diagram of the Nephelometric Turbidimeter Monitoring System (NTMS) set-up.

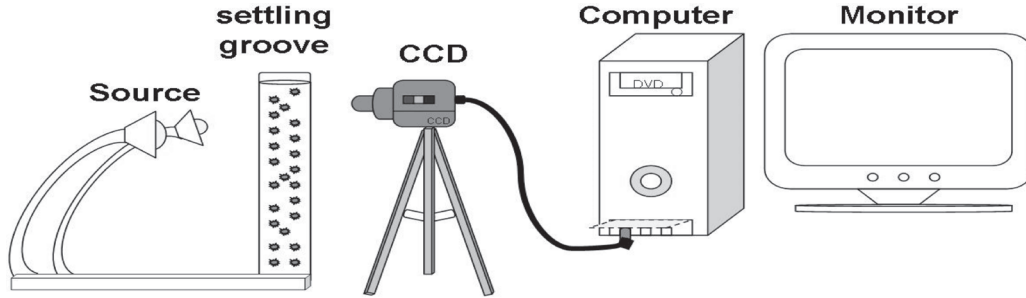


Figure 2. A schematic diagram of the particle size analysis with images captured (samples are taken using a pipette with an inner diameter of 5 mm and added to the settling groove under a microscope with a CCD camera to capture the digital floc images).

4. Particle Size Analysis with Images Captured from Cameras

In Figure 2, used a video camera (Watec Co Wat-202B) to record the different average particle size of com cob particle (115, 137, 335, 460, 920 μm) in a free settling test. Than the image analysis (Matrox Inspector V2.2) was used to measure the mean particle size confirming whether NTMS is suitable for directly applying to particle size analysis.

5. Jar Tests

Figure 1 also shows the schematic diagram of the setup for conducting the Jar Test. The prepared algal solution (1 L) was added to a covered dark opaque container with holes in the cover for adding coagulant. A Nephelometric turbidimeter was used to conduct continuous on-line monitoring of the suspension turbidity [17]. The turbidimeter probe (WTW model MIQ/C184) was placed 3 cm below the liquid surface. One liter of the prepared 10, 100 and 200 NTU synthetic algae sample were placed in the acrylic flask individually. After addition of chemicals, the content was rapidly mixed at 100 rpm for 1 minute followed by slow mixing at 20 rpm for 10 minutes, and followed by a settling period of 60 minutes. Instantaneous variations of the turbidity were monitored and shown on the computer monitor. The data were collected every second and processed in EXCEL to be displayed on the monitor for showing the turbidity variation curve.

RESULTS AND DISCUSSIONS

1. The Relationship Between Turbidity SD and Imaged Particle Size

During the coagulation process, the floc size is posi-

tively related with the SD of the measured turbidity [17–18]. For each size of 115, 137, 335, 460 and 920 μm in average particle diameters, 0.4 g of the com cob particle was added into 1 L of de-ionized water to prepare the turbidity standard solutions with various sizes of particles. Then, each solution was placed into the device shown in Figure 1 to monitor the fluctuations of the turbidity. While reading the turbidity, the solution was mixed at the speed of 20 rpm for 10 minutes. The turbidity data was collected in every second. For each solution, 600 turbidity data were collected and analyzed to find the turbidity SD of each standard solution. Figure 3 shows the turbidity SD is well linearly related to square root of the com cob particle diameter ($R_R^{1/2}$).

For each com cob particle solution, the solution was added drop by drop into the video recording device in Figure 2. After the video camera captured an image contained more than 3000 particles, software named Matrox Inspector V2.2 was used to calculate the average particle size of the com cob particle in the captured image. The data in Figure 4 shows that the particle di-

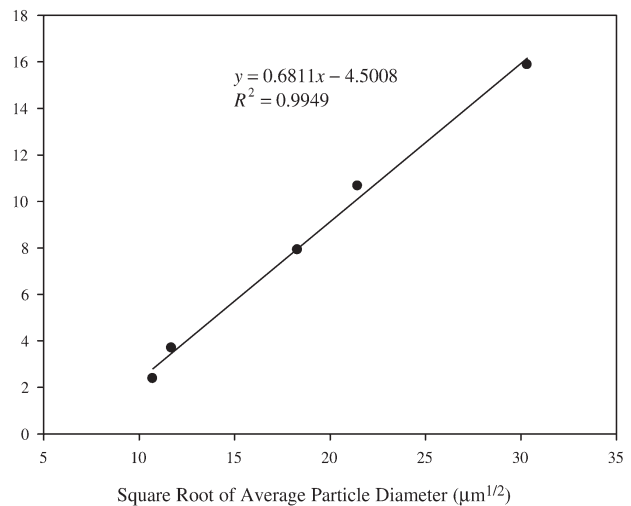


Figure 3. Linear relationship between turbidity SD and the square root of average particle diameter $R_R^{1/2}$ for com cob suspensions.

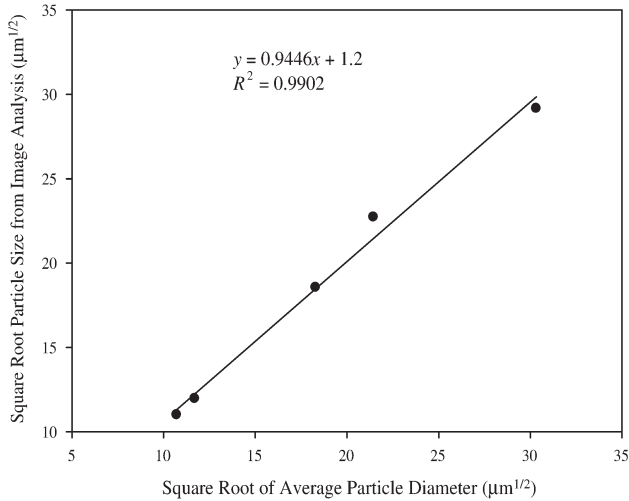


Figure 4. Linear relationship between square root of average particle diameter $R_p^{1/2}$ and the calculated diameter of the particle image $R_i^{1/2}$ for corn cob suspensions.

ameter used to prepare the standard solution has a good linear relationship with the particle diameter calculated from the video captured image. The interception of the trace line in Figure 4 is 1.2 and the slope of the line is close to 1, which means the image particle diameter (R_i) is very similar to the real particle diameter (R_R). Therefore, the method of using video camera device to obtain the particle size is feasible. Hence, considering the results of Figure 3 and Figure 4, a relationship between the turbidity SD and the particle size is found to be a linear equation, $R_I^{1/2} = 1.39SD + 7.44$. These results indicated that the values of turbidity SO have good relationship with real particle size and imaged particle size (R_I).

2. The Effect of Coagulant Dosage on Standard Deviation of the Turbidity Data

To understand the floc growth during the flocculation process, a study of the relationship between SD of the measured turbidity and particle size of the coagulated floc was conducted. In this study, the raw water containing *Chlorella sp.* alga at 100 NTU of turbidity was used. The coagulant was prepared from Polyaluminum Chloride, PACl. The Jar Test was conducted under the conditions at rapid mixing speed at 100 rpm for 1 minute, slow mixing at 20 rpm for 10 minutes, and settling for 1 hour. During the Jar Test, the turbidity measured by the device shown in Figure 1, was calculated. In Figure 5, under various PACl dosages, the fluctuation of the turbidity starts increasing at some coagulant dosages in the slow mixing stage. The increase of turbidity fluctuation indicates the floc is

Table 1. The Relationships Between Sieve Meshes and Particle Sizes, Which are Used in this Study.

Metals	Particle Size Range (μm)	Median Value of the Particle Size Range or Average Particle Size (μm)
120–140 mesh	105–125	115
100–120 mesh	125–149	137
40–60 mesh	250–420	335
35–40 mesh	420–500	460
18–20 mesh	840–1000	920

growing in size. Therefore, the turbidity data collected at the last 320 seconds during the slow mixing (the time from 341 sec to 660 sec in Figure 5) was used for calculating the turbidity SD to study the particle size changes at each coagulant dosage. The results of Figure 6 show that when the dosages are 16.2 and 21.6 mg/L (as Al), turbidity SD reaches to the maximum. The high turbidity SD represents the particle size is large. Therefore, in Figure 6 shows after 5 minutes settling, the residual turbidities in those solutions added 16.2 or 21.6 mg/L (as Al) PACl are significantly lower than the residual turbidities in the other dosages. This result indicates that under both 16.2 and 21.6 mg/L (as Al) PACl dosage additions, the particle size is relatively large and the particle itself can be rapidly settled. On the other hand, short of PACl dosage can not help the solution to form the large coagulation floc. Therefore, in Figure 6 for the low coagulant dosage solutions [0–5.4 mg/L (as Al)], the turbidity SD are significantly low. Hence, in the case of coagulant shortage in the solution, in Figure 5 also shows the residual turbidity after the settling is close to the initial concentration of 100 NTU. On the other hand, when the PACl dosage is higher than 21.6 mg/L (as Al), the turbidity SD decreases again was shown in Figure 6. This result indicates that even increasing the PACl dosage, the floc size in the over dosage solution may smaller than the floc size in the solutions added 16.2 or 21.6 mg/L (as Al) PACl. Therefore, as the results in Figure 6 the residual turbidities of the coagulation dosage 27.0 and 32.4 mg/L PACl are higher than those measured in the solutions added 16.2 or 21.6 mg/L PACl after 5 minutes settling. However, the experiment results in Figure 6 also indicate that the residual turbidities in the dosage rang from 16.2 to 32.4 mg/L (as Al) have very similar value after 10 minutes settling. According to this experiment results, proved the coagulation dosage of 27.0 and 32.4 mg/L have smaller floc size than dosage of 16.2 or 21.6 mg/L, therefore required longer time to settle. This experi-

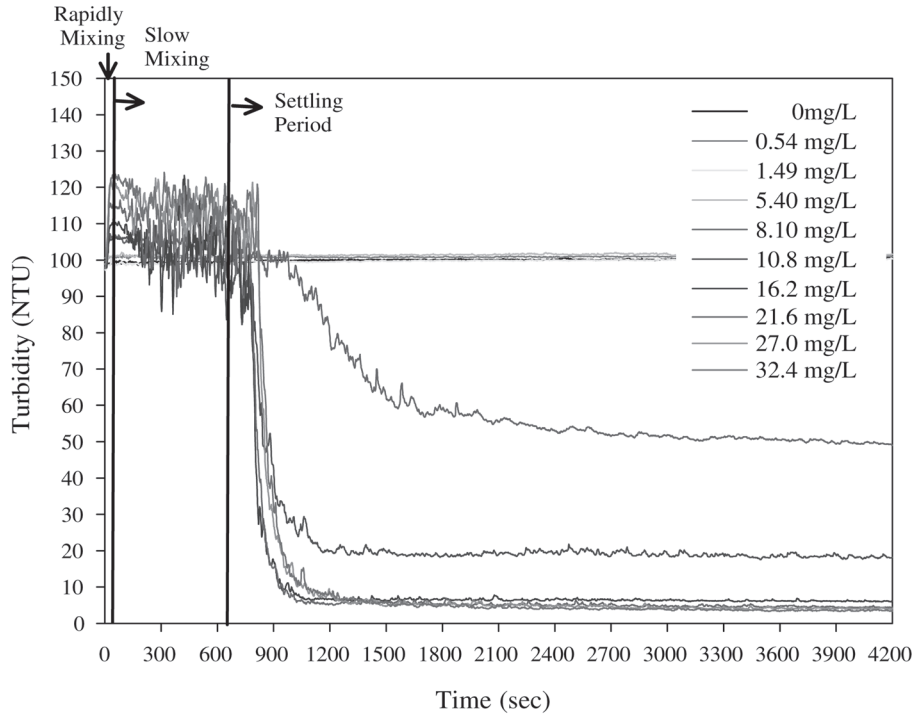


Figure 5. The changes of turbidity per second for samples coagulated using different PACI dosage with 60 second rapid mixing at 100 rpm and 60 sec slow mixing at 20 rpm, and followed by a settling period of 3600 sec. (The initial turbidity of algae solution is 100 NTU).

mental result indicates that in the process of determining optimum coagulation condition, other than measuring the final residual turbidity, a traditional method, turbidity SD is another alternative to rapidly and accurately determine the particle size during the coagulation process.

To confirm the relationship of the turbidity SD and the particle size of the coagulation floc, triplicate Jar Test experiments were conducted. The optimum dosage of 21.6 mg/L found in Figure 6 was used for the experiments. In each Jar Test experiment, turbidity data collected from rapid mixing and slow mixing processes were manipulated to obtain the turbidity SD of a certain time interval. In the rapid mixing stage, due to the initial PACI addition may cause an instant increase of the turbidity, the turbidity data at rapid mixing was only taken from the 16th to the 60th second to calculate the turbidity SD. At the 10 minutes slow mixing process, all turbidity data (600 data points) were grouped for every two minutes. The standard deviation (SD) for each group that consisted of 120 data points was plotted versus time. Therefore, using the turbidity SD at the rapid mixing stage as the initial turbidity SD, the change of the turbidity SD with the mixing time was plotted in Figure 7. The result of Figure 7 shows the average turbidity SD of the three experiments at different time

stages. According to the data of Figure 7, the average initial turbidity SD is 0.62, whose amount is relatively small. This result indicates that no coagulation particle was significantly formed during the rapid mixing process. After 2 minutes of flocculation process, the turbidity SD increases to an average of 3.7 but only increases a little in the later time. This result indicates that

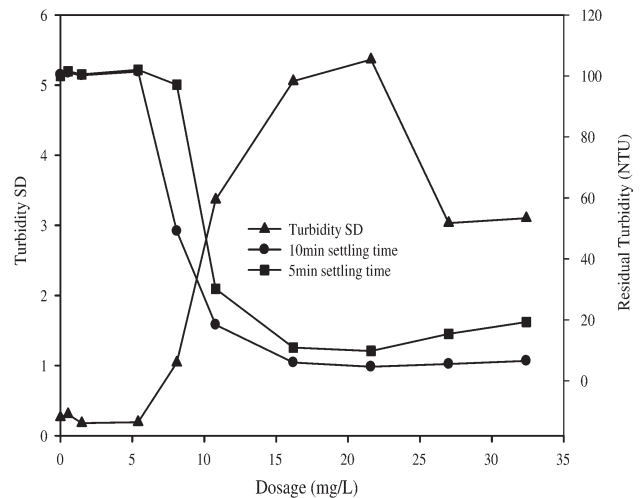


Figure 6. The relationship of turbidity SD and the residual turbidity (5 and 10 min settling time) at different PAC dosage (the turbidity data from the time 341 sec to 660 sec in Figure 5 was used for calculating the turbidity SD; the residual turbidity of 5 and 10 min settling time are the turbidity data of 960 sec and 1260 sec in Figure 5).

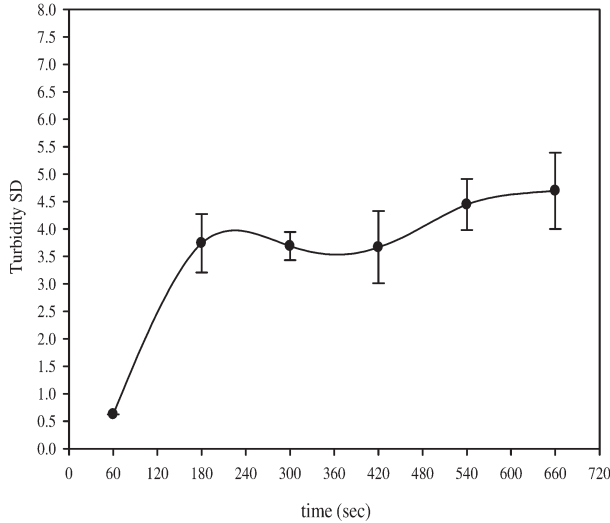


Figure 7. A plot of the SD of turbidity at various flocculation times (coagulation dosage 21.6 mg/L with triplicate Jar Test experiments).

the particle was formed right after starting the flocculation process (slow mixing). In order to confirm the particle size change during the coagulation process is really correlating with the turbidity SD, a drop of the coagulation solution sample was taken in ever two minutes in the flocculation or slow mixing process was proceed. The droplet sample was added into the device shown in Figure 2 to capture the image of the particles by a video camera. Then we use the captured image and the computer software to calculate the image particle diameter (R_I). According to the result of the previous discussion, the real particle diameter (R_R) can be expressed as the calculated particle size from the image. The data of Figure 8 shows the particle diameter (R_I) changes with the coagulation time insignificantly. Comparing both Figure 7 and Figure 8, one can find a similar result that is the coagulation floc was formed within 2 minutes during the coagulation process.

To confirm the reliability of the relationship between the turbidity SD and the particle size in the coagulation process, the turbidity SD in Figure 7 was plugged into the previous equation, $R_I^{1/2} = 1.39SD + 7.44$, to obtain the estimated coagulation particle diameter (R_D). In addition, the particle diameter (R_I) was calculated from a video capture image. The values of the ratio R_D/R_I in Figure 9 are in the range between 0.65 and 0.75. Although the ratio values are not equal to 1, the deviations of the values are limited in a small range. The reason causes this small deviation may be due to using the equation $R_I^{1/2} = 1.39SD + 7.44$ to obtain the floc diameter R_D . The equation was developed from the corn cob particle

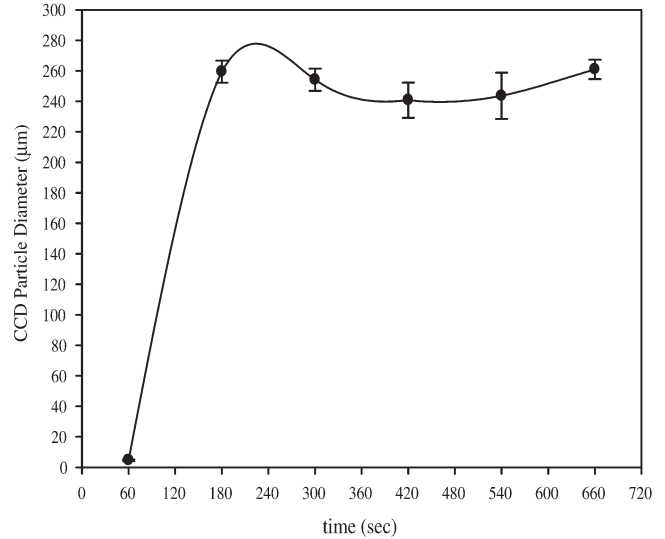


Figure 8. The variation of calculated particle size (R_I) from the captured image at the end of rapid mixing (data 0 sec) and various flocculation times.

density is different from the density of the *Chlorella sp.* alga in the test water. Probably due to this reason, the ratios of R_D/R_I was deviated from 1.

The result of limited ratio value in Figure 9 also indicates that using the turbidity SD to estimate the particle size R_D is feasible. In addition, because the turbidity SD is proportional to the square root of the particle size, the particle size is proportional to the square of the turbidity SD (i.e. SD^2). Then, the relationship can be expressed as $R_D/R_I = SD_1^2 / SD_0^2$. The values of R_1 and R_0 represent the particle size after coagulation for a certain time and the size before the coagulation, respectively. Similarly, SD_1^2 and SD_0^2 are the square of the turbidity SD after co-

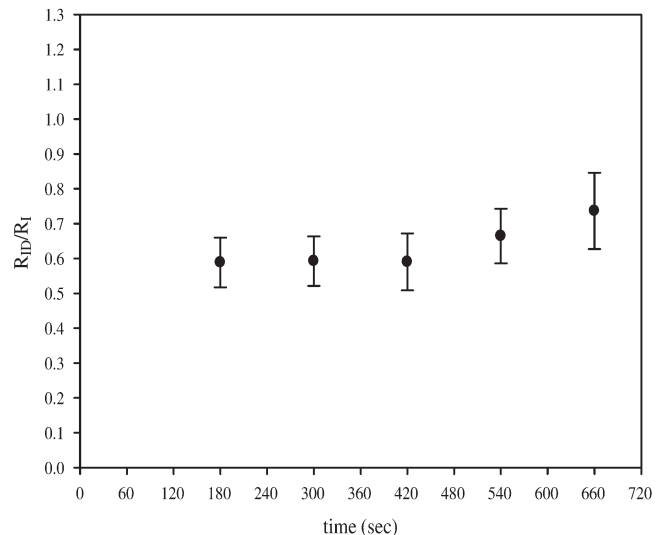


Figure 9. The ratio variation of the estimated particle size (R_D) to the image particle size (R_I) at various flocculation times.

agulation process and the square of the turbidity SD before the coagulation, respectively. According to the previous discussion, the particle size of the *Chlorella sp.* alga in test water is $4.8 \mu\text{m}$, determined from the video camera capture image. The initial turbidity SD is 0.62. These two values can be used as R_0 and SD_0 , respectively. Based on the data of Figure 7, the average turbidity SD can be found to be 4.05, which can be used for the value of SD_1 . Then, the value of R_1 is found to be $204.3 \mu\text{m}$. The ratio of the equation-estimated particle size to the real particle size calculated from a video captured image is 0.82, which is close to 1. Through the above two confirmation methods, using turbidity SD to estimate the particle size is a feasible method.

3. The Effect of Raw Water Turbidity (or total suspension solid) on standard deviation of the turbidity data

The raw water containing various initial turbidity levels of *Chlorella sp.* alga (i.e. 10, 100, and 200 NTU) are subject to flocculation. Jar Test was also conducted under the conditions at rapid mixing speed at 100 rpm for 1 minute, slow mixing at 20 rpm for 10 minutes. As mention previously (Figure 7), the standard deviation (SD) for each group that consisted of 120 data points in coagulation (45 data points for rapid mixing) was plotted versus time. Figure 10 shows that higher initial turbidity in raw water will lead to higher turbidity SD of the flocculated water but the pattern of the curves is remarkably similar. It means the kinetics of the coagulation process (floc formation almost without lag time)

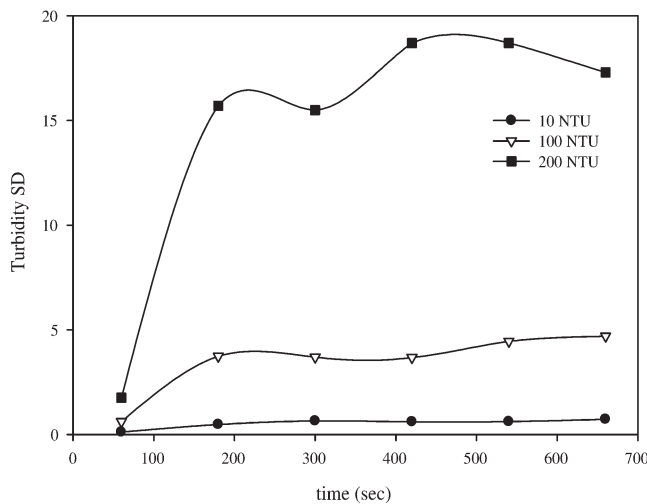


Figure 10. A plot of the turbidity SD at various flocculation times with difference concentration of *Chlorella sp.* alga. (coagulation dosage 21.6 mg/L).

are very similar in all results. These observations are similar to the results obtained by Gregory [11] using PDA to study floc formation. Apart from this, it seems likely from these results that the different turbidity SD values in Figure 10 are not only due to different floc sizes (the mean floc size of the 10, 100 and 200 NTU raw water are 225, 261 and 282 μm , respectively). Because the floc size is determined by a balance between growth and breakage in the flocculation process, under given shear conditions, floc size is not greatly affected by the number of alga particles (or initial turbidity values). Therefore, the phenomena of increasing particle concentrations give progressively larger turbidity SD values; it may be explained by the higher probability of impacts among the particles in the water with higher initial turbidity thus producing a larger number of flocculation flocs and causing the turbidity measurement unstable or turbidity fluctuation increase. In conclusion, the NTMS technique used here gives turbidity SD, which not only depends on the floc size but also cause by the particle concentration.

CONCLUSION

Through using an on-line Nephelometric Turbidimeter Monitoring System (NTMS) and a video camera (Watec Co Wat-202B) with image analysis (Matrox Inspector V2.2), several coagulation experiments were conducted. The results indicated that the square root of the particle size is proportional to the standard deviation (SD) of the measured turbidity from NTMS. By knowing this relationship of the turbidity SD and the particle size, the turbidity SD from NTMS can also be used to rapidly estimate the growing speed of the floc size during the coagulation process under a given turbidity value. The method developed in this study is very beneficial to determine the coagulation efficiency in a fast way. The method is different from the traditional method to determine the optimum coagulant dosage. The traditional method takes a long time to complete the experiments, because after the settling process, the final turbidity needed to be analyzed to determine the optimum coagulant dosage. Other than saving time for determining the coagulant dosage and increasing the accuracy of the coagulant dosage, the method developed by this study can rapidly know the growing effectiveness of the floc size during the coagulation process. The results found in this study may help the other coagulation study, such as the laboratory research in a full scale drinking water treatment plant. Es-

pecially, for the plant using automatic coagulant adding system, the application of this research could be further studied in the future.

ACKNOWLEDGMENT

We thank Mr. Shu-Yi Wu, Yu-Wei Huang and Sin-Ming Chen for assistance with laboratory work. The authors also acknowledge the financial support of National Science Council, Taiwan, R. O. C. for this work (NSC -95-2211-E-239-033).

REFERENCES

- Jiang, J.Q. and N.J.D. Graham, "Preliminary evaluation of the performance of new pre-polymerized inorganic coagulants for lowland surface water treatment", *Wat. Sci. Tech.*, Vol. 37, No.2, 1998, pp. 121-128.
- Rossini, M., J.G. Garrido and M. Galluzzo, "Optimization of the coagulation-flocculation treatment: influence of rapid mix parameters", *Water Res.*, Vol. 33, 1999, pp. 1817-1826.
- Franceschi, M., A. Girou, A.M. Carro-Diaz, M.T. Maurette and E. Puech-Coste, "Optimisation of the coagulation-flocculation process of raw water by optimal design method", *Water Res.*, Vol. 36, 2002, pp. 3561-3572.
- Byun, S., J. Oh, B.Y. Lee and S. Lee, "Improvement of coagulation efficiency using instantaneous flash mixer (IFM) for water treatment", *Colloid and Surface A.*, Vol. 268, 2005, pp.104-110.
- Cheng, W.P., F.H. Chi and R.F. Yu, "Evaluation the ability of polyaluminum silicate chloride coagulants for turbidity removal efficiency", *Separation Sci. Technol.*, Vol. 41, No.2, 2006, pp.297-308.
- Yu, J.F., D.S. Wang, M.Q. Yan, C.Q. Ye, M. Yang and X.P. Ge, "Optimized coagulation of high alkalinity, low temperature and particle water: pH adjustment and polyelectrolytes as coagulant aids", *Environmental Monitoring and Assessment*, Vol. 131, 2007, pp. 377-386.
- Mas, S. and C. Ghommidh, "On line size measurement of yeast aggregates using Image analysis", *Biotechnology and Bioengineering*, Vol. 76, No. 2, 2001, pp. 91-98.
- Huang, YX., Simultaneous measurement on particles in solution with size ranging from nm to sub-mm by microscope light scattering spectroscopy and image analyzing system. *Current Applied Physics*, 5, 549-552 (2005).
- Li, T., Z. Zhu, D. Wang, C. Yao and H. Tang, "Characterization of floc size, strength and structure under various coagulation mechanisms", *Powder Technology*, Vol. 168, 2006, 104-110.
- Mori, Y., K. Togashi and K. Nakamura, "Colloidal properties of synthetic hectorite clay dispersion measured by dynamic light scattering and small angle X-ray scattering" *Advanced Powder Technology*, Vol. 12, 2001, pp. 45-59.
- Gregory, J., "Monitoring particle aggregation processes", *Advances in Colloid and Interface Science*, Vol. 147-148, 2009, pp. 109-123.
- Gregory, J. and W. D. Nelson, "Monitoring of aggregates in flowing suspension", *Colloid and Surface A.*, Vol. 18, 1986, pp. 175-188.
- Huang, C.P. and G.S. Chen, "Use of the fiber-optical monitor in evaluating the state of flocculation", *Water Res.*, Vol. 30, 1996, pp. 2723-2727.
- Burgess, M.S. and J.S. Phipps, "Flocculation of PCC induced by polymer/microparticle systems: floc characteristics", *Nordic Pulp Paper Res. J.*, Vol. 15, 2000, pp. 572-578.
- Whittington, P.N. and N. George, "The use of laminar tube flow in the study of hydrodynamic and chemical influences on polymer flocculation of *Escherichia coli*", *Biotechnology and Bioengineering*, Vol. 40, No. 4, 1992, 451-458.
- Li, T, Z. Zhu, D. Wang, C. and Yao, H. Tang, "The strength and fractal dimension characteristics of alum-kaolin flocs", *International Journal of Mine Processing*, Vol. 82, 2007, pp. 23-29.
- Cheng, W.P., Y.P. Kao and R.F. Yu, "A novel method for on-line evaluation floc size in coagulation process", *Wat. Res.*, Vol. 42, 2008, pp. 2691-2697.
- Cheng, W.P., Y.P. Kao and R.F. Yu, "Comparison of three coagulants by on-line turbidity monitoring" *Water Management (In press)*.

Landfill Disposal of Alum Water Treatment Residues: Some Pertinent Geoengineering Properties

BRENDAN C. O'KELLY*

¹Department of Civil, Structural and Environmental Engineering, Museum Building, Trinity College Dublin, Dublin 2, Ireland

ABSTRACT: This paper presents the geoengineering properties of the alum water treatment residues derived from the production of potable water at three municipal works, including the effects of catchment geology; chemical additives; and thixotropic hardening phenomena, with reducing water content (increasing solids content) from the viscous slurry state to the semisolid state. The geoengineering behavior was akin to that of high-plasticity organic clays, with low values of bulk and dry density and high compressibility, although the consolidation rate was low (hydraulic conductivity of the order of 10^{-4} – 10^{-6} m/day). The data presented in this paper can be used to determine the level of dewatering necessary for more efficient landfill disposal, including the anticipated amounts and rates of settlement and the factor of safety against geotechnical instability of the residue slopes for the short- and long-term conditions. It is recommended that sludge and residues should be dewatered to achieve minimum shear strengths of 20 and 50 kPa for geotechnical stability at municipal landfills and dedicated monofills, respectively.

INTRODUCTION

WATER treatment residues (WTRs) are the gelatinous slurry by-products from the treatment processes used in the production of potable water at municipal works. The WTRs comprise sand, silt and clay particles, colloidal organic matter, and chemicals (coagulants, polyelectrolytes and conditioners) that have been added to the source water during the treatment processes. Chemical coagulation using ferric chloride, or more generally using aluminum sulfate (alum), causes the colloidal particles (i.e. less than 1 μm in size) that are suspended in the water entering the treatment plant to aggregate into flocs that settle out more readily under gravity. The residue is characterized as alum WTR or iron WTR depending on the coagulant type used. Polyelectrolytes are synthetic long-chained organic molecules that act as binding agents, thereby increasing the inherent shear strength of the newly formed flocs, and hence the viscosity of the slurry residue [1,2]. Conditioners including sulfuric acid, bentonite, calcium or sodium hydroxide, and sodium silicate may also be added, depending on the nature of the source water, in order to improve the polyelectrolyte performance.

Increasing quantities of WTRs are being produced worldwide annually due to the increasing demand for potable water and more stringent regulations: for example, the European Union Drinking Water Directive [3]. Currently, the principal disposal options are: (1) storage, often over an indefinite period, in sludge lagoons; (2) dewatering by mechanical and/or thermal means, followed by landfilling of the residue cake, either at dedicated monofills or co-disposal at municipal landfills; (3) incineration. However, more stringent regulation (for example by the US EPA [4] and the European Union [5,6]) has placed greater restrictions on these disposal options, principally to minimize environmental impacts. Landfill disposal of large volumes of soft residues may also lead to geotechnical problems, including slope instability and excessive differential settlement that may damage the landfill capping layer. Hence, the slurry residue must be adequately dewatered at the municipal works by mechanical and/or thermal means, or by allowing the slurry to dry naturally in drying beds.

In this paper, the amount of water within the pore space of the residue materials was quantified in terms of the water content (w), defined in the geotechnical literature as the mass of the pore water to the mass of the dry solids, expressed as a percentage. The water content is one of the most commonly determined parameters in

* Author to whom correspondence should be addressed.
E-mail: bokelly@ted.ie

characterizing geoen지니어ing behavior and is generally determined using the oven drying method, with the dry solids mass corresponding to the residual mass after oven drying the test specimen at $105 \pm 5^\circ\text{C}$ for a period of 24 h. Oven drying removes the free water in the pore space between the flocs; the internal water in the micro-channels within the flocs; and the pores within the constituent solid particles themselves [7]. Bound water in the form of water of hydration and adsorbed water held on the surface of the solid particles by electrical attraction are considered to be part of the solids in the residue materials and can not be removed by oven drying. The solids contents (*SC*), defined in the water-treatment literature as the mass of the dry solids fraction expressed as a percentage of the bulk wet mass, can be related to the water content by

$$SC = \frac{100}{1 + \left(\frac{w}{100}\right)} \quad (1)$$

Geoen지니어ing Properties of Alum WTRs from the Literature

Table 1 lists some typical geoen지니어ing data reported for alum WTRs in the literature [8–16]. Alum WTRs have very high Atterberg liquid and plastic limits; a relatively low specific gravity of solids; high total volatile solids (*TVS*); and are classified as high-plasticity organic clays. The wet residue, direct from the treatment works, has a low bulk density of 1.0–1.2 tonne/m³.

Figure 1 shows data for shear strength against water content for some alum and iron WTRs and also municipal sewage sludge. There is a significant variation in the shear strength value of these materials at a given water content, which is expected, due to the natural variability of the source waters and hence the mineralogy and organic content of the suspended solids. Different types

Table 1. Typical Geoen지니어ing Properties of Alum WTRs.

Parameter	Value
Liquid limit, %	100–550
Plastic limit, %	80–250
Specific gravity of solids	1.8–2.2
Total volatile solids, %	10–60
Bulk density, tonne/m ³	1.0–1.2
Dry density, tonne/m ³	0.12–0.36
Effective cohesion, kPa	0
Effective angle of shearing resistance, degree	28–44

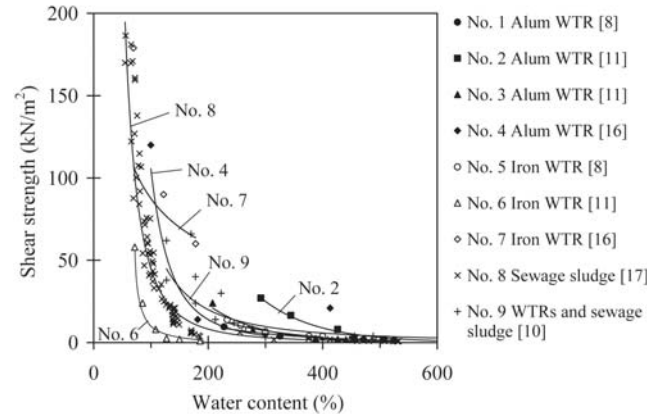


Figure 1. Shear strength against water content data for WTR and sewage sludge materials.

and levels of chemical treatment, and also biological treatment in the case of sewage sludge, had been applied in order to separate the residue by-products at the municipal works. In general, alum WTR tends to have slightly higher shear strength than iron WTR at a given water content, and both alum and iron WTRs tend to have higher shear strengths than sewage sludge.

Wet alum WTR is thixotropic, with Wang et al. [11] reporting strength gains (ratio of the shear strength measured after a specified curing period to the remolded shear strength, under constant external conditions and specimen composition) of 5.7–8.0 achieved after a ten-week curing period and for *SC* = 10–20%. The effective angle of shearing resistance (ϕ') values of 28–44° reported for alum WTRs are towards the upper end of the range normally associated with high-plasticity organic clays, although consistent with $\phi' = 32$ –37° reported for municipal sewage sludge (*TVS* = 70–50%) [17,18].

Alum WTR has a very low hydraulic conductivity, which reduces in value from the order of typically 10^{-4} to 10^{-6} m/day, with increasing effective stress from 2 to 540 kPa [12]. Note that the effective stress (σ'), which acts across the contacts between the solid particles, is defined as the difference between the applied stress (σ) and the excess pore water pressure in the saturated pore voids.

Volume Change Theory

Residues and sludge are soil-like materials and, as such, their settlement behavior in lagoons, monofills or dedicated deposition areas at municipal landfills can be assessed using soil mechanics theory [18], and a more comprehensive explanation of the following can be ob-

tained in undergraduate soil mechanics textbooks, including Craig [19].

The settlement due to a change in the state of effective stress comprises two components: primary consolidation (ΔH_c) and secondary compression (ΔH_s). Primary consolidation can be described by classical 1-D consolidation theory, whereby the change in the residue volume corresponds to the change in the volume of the pore water, assuming fully saturated conditions. The void ratio (e) is defined as the volume of the pore voids to the volume of the solids and, referring to Figure 2, the change in the void ratio (Δe) can be predicted by

$$\Delta e = C_c \log \frac{\sigma'_{vo} + \Delta \sigma'_v}{\sigma'_{vo}} \quad (2)$$

where

C_c = compression index (gradient of the void ratio against logarithm of effective stress curve)

σ'_{vo} = initial vertical effective stress

$\Delta \sigma'_v$ = increase in vertical effective stress (i.e. applied stress)

Wet alum WTR is highly compressible. For example, very high compression index values of $C_c = 5.3$ – 6.7 were reported for alum WTR that had been dewatered using a centrifuge and sand-drying method [11]. The primary consolidation settlement, which is due to the dissipation of the excess pore water pressure, can be estimated as

$$\Delta H_c = H_o \frac{\Delta e}{1 + e_o} = H_o \frac{C_c}{1 + e_o} \log \frac{\sigma'_{vo} + \Delta \sigma'_v}{\sigma'_{vo}} \quad (3)$$

where

e_o = initial void ratio

H_o = initial thickness of the saturated residue layer

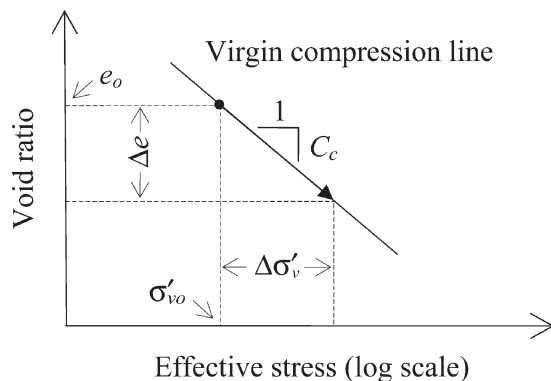


Figure 2. Theoretical consolidation plot. Note: e_o , initial void ratio; σ'_{vo} , initial vertical effective stress; Δe , change in void ratio due to a change in vertical effective stress, $\Delta \sigma'_v$; C_c , compression index.

Secondary compression (creep) settlement, which is due to the gradual rearrangement and compression of the solids (residue flocs) into a more stable configuration under the increased effective stress, is a time dependent process that can be expressed by

$$\Delta H_s = H_o C_{sec} \log \frac{t_1}{t_2} \quad (4)$$

where

C_{sec} = coefficient of secondary compression

t_1 = time period to achieve substantial completion of the primary consolidation phase

t_2 = time period that extends into the secondary compression phase ($t_2 > t_1$).

Objectives of this Study

The objectives of this paper are to study the geoengineering and hydraulic properties of alum WTRs derived from different catchments, and in particular to study the effects of several influencing factors: catchment geology; chemical additives; and thixotropic hardening phenomena. Geotechnical recommendations are made regarding the safe and efficient disposal of these residues in engineered landfills. In addition, pertinent data are presented that can be used to calculate the factor of safety against instability of the landfill slopes and the time-dependent settlement response.

TEST MATERIALS

Alum WTRs were sourced from three of the larger municipal water treatment plants in Ireland: the Ballymore Eustace and Leixlip works in County Kildare and the Clareville works in County Limerick, which produce about 91, 73 and 62 Mm³ of potable water per annum respectively, and taken together account for almost 30% of the potable water produced in the Republic of Ireland. The raw water entering these treatment plants is sourced from three different catchments, thereby providing a good overall representation of the alum WTRs produced in the country. The residues are coagulated at these municipal works using Chemifloc 4140[®] alum, supplied in its hydrated form [i.e. $Al_2(SO_4)_3 \cdot 14H_2O$], and Magnafloc LT25[®] polyelectrolyte, which are manufactured by Allied Colloids and Ciba Zietag. The combined dosages (given as mg/l source water) that had been added during

Table 2. Chemicals Added During the Treatment Processes.

Residue	Hydrated Alum	Polyelectrolyte		Dry H ₂ SO ₄
	mg/l	mg/l	Mean % Dry Residue Mass	mg/l
WTR 1	40–65	0.6–1.5	3.5	0
WTR 2a	60–100	0.8–2.0	4.8	0.5
WTR 2b	0	0	0	0
WTR 3	40–60	0.2–1.0	1.6	0

the different treatment processes are listed in Table 2, with the range of values reflecting the necessary adjustments to the dosage appropriate to the level of turbidity of the incoming source water. These dosages were broadly similar and are at the higher end of the ranges normally used in practice since the source waters were all medium high in turbidity. Also listed in Table 2 are the polyelectrolyte concentrations, expressed as a percentage dry solids mass of the residue by-product at the different works. These mean concentration values were calculated on the basis of the annual production of potable water, the mass of dry solids residue produced per annum, and the mean polyelectrolyte dosages as mg/l source water at the different works, assuming that all of the polyelectrolyte additives were retained in the residues.

Alum WTR 1 Sample

The alum residue from the Ballymore Eustace works (WTR 1) was derived from the treatment of medium color, medium-turbidity water sourced from the Dublin and Wicklow mountains (upland catchment of peat over granite bedrock) and which had been stored in Poulaphouca reservoir, County Wicklow, prior to its treatment. The slurry residue was dewatered using a recessed-plate filter press device under an applied stress of 1500 kPa, with about 1200 tonnes of the wet alum residue ($SC = 23\%$) produced at the treatment works in 2007. Samples of the pressed residue cake were obtained from the skip containers at the end of the dewatering process at the treatment works in November 2005.

Alum WTR 2a Sample

The alum residue from the Clareville works (WTR 2a) was derived from the treatment of high color, turbid water (typically 20–25 NTU) sourced from the lower

Shannon, Ireland's longest river, which drains the central lowland area of about 15700 km². The Shannon is a low gradient river, about 260 km in length with a mean annual discharge of 186 m³/s, that runs for much of its course through karstified limestone overlain by raised and riverine bogs, many of which have been harvested for peat over the years. Much of the turbidity and color in the water is likely to be attributed to the organic material associated with the peat.

The raw water is delivered upstream of the Ardnacrusha dam through an open channel to the Clareville treatment works. After the initial screening process, the turbid water passes through 8.0-m deep primary sedimentation (holding) tanks, before the coagulation process, where a high alum dosage of 60–100 mg/l raw water was added owing to its high turbidity. Sulfuric acid was also added to adjust the pH in order to improve the polyelectrolyte performance.

At the end of the treatment process, the slurry residue by-product was consolidated to about 700% water content under an applied stress of 800–1000 kPa using a belt-press device and the pressed material was then allowed to dry naturally in drying beds, with about 900 tonnes of the wet alum residue ($SC = 15\%$) produced at the treatment works in 2006. Residue samples were obtained from the drying beds for geotechnical laboratory testing in October 2006.

Residue WTR 2b Sample

Samples of the turbid water were withdrawn from the mid-height of the primary sedimentation tanks at the Clareville works using 22.5 liter drums in February 2008. These drum samples were allowed to evaporate and settle out over a period of about four weeks at ambient laboratory temperature of 20°C. The thickened slurry residue formed (WTR 2b) was poured from the drums into trays and the water content was allowed to reduce further by fan-assisted evaporation, again at ambient temperature, before the saturated slurry residue was mechanically dewatered using a consolidometer press. Although the solids in the drum samples were more than 40% volatile, the fact that the catchment source mainly comprised natural saturated peat meant that the bulk of these solids were already in a near stable condition. Hence, any biological activity that may have occurred during the course of settling and dewatering the drum samples in the laboratory would not have significantly altered the characteristics of the solids in residue WTR 2b.

One of the objectives of this study was to determine the effect of the chemical additives on the geoengineering and hydraulic properties, which was achieved by comparing the behaviors of alum WTR 2a and this non-chemically treated residue WTR 2b. These materials were practically identical in composition apart from the chemical additives in WTR 2a.

Alum WTR 3 Sample

The alum residue from the Leixlip works (WTR 3) was derived from the treatment of medium color, medium-turbidity water sourced from the river Liffey (upland catchment of limestone bedrock). The residue was dewatered using a recessed-plate filter press device under an applied stress of 1500 kPa, with about 1100 tonnes of the wet alum residue ($SC = 25\%$) produced at the treatment works in 2007. Samples of the pressed residue cake were obtained from the skip containers at the end of the dewatering process at the treatment works in November 2006.

PHYSIOCHEMICAL PROPERTIES

Table 3 lists the physiochemical properties that were determined using standard geotechnical-laboratory tests [20,21] and carried out on fresh residue specimens obtained directly from the treatment works.

The water content values were determined using the oven drying method and are an accurate measure of the combined amounts of free and internal water within the pore space of the residue materials [7]. The degree of oxidation of the volatile solids was not significant at the

oven drying temperature of $105 \pm 5^\circ\text{C}$ since the bulk of the organic material was already in a near stable condition and the polyelectrolyte additives only become unstable above about 150°C . The aluminum hydroxide precipitate degrades at higher temperatures of $180\text{--}600^\circ\text{C}$, with further calcination occurring above 1000°C .

The Atterberg liquid and plastic limits, defined as the water content values at the transitions from the liquid state to the plastic state and from the plastic state to the semisolid state respectively, were determined using the fall-cone penetrometer and Casagrande thread-rolling methods [20]. The plasticity index was calculated as the numeric difference between the liquid limit and plastic limit values. The residues had very high liquid limit (430–550%) and plasticity index (210–290) values. The adhesion limit, determined as the lowest water content at which the solids adhered to a clean dry spatula, was also very high; in excess of 240% water content. The bulk density (ρ) and the dry density (ρ_d) were calculated as the wet mass and the dry solids mass per unit volume respectively [20], with the dry density given by

$$\rho_d = \frac{100\rho}{100 + w} \quad (5)$$

where

w = water content (as %)

The dewatered residue samples from the treatment works had low bulk density and dry density values (1.06–1.10 and 0.18–0.26 tonne/m³, respectively) and a wide range of water contents, and hence void ratio values, due to inherent differences in their consolidation properties and also differences in the drainage conditions and confining pressures that had been applied by the recessed-plate filter press and belt press devices at the municipal works. WTR 2a was of slurry consistency (water content greater than the liquid limit value, where the liquid limit condition corresponds to undrained shear strengths of about 2 kPa). WTR 1 and WTR 3 were soft to firm in consistency due to the greater level of dewatering that had been achieved under the higher confining pressure of 1500 kPa applied by the recessed-plate filter press device. Nevertheless, their void ratio values of 5.7 and 6.3 were still very high.

X-ray diffraction analysis indicated that the crystalline fraction of the residues comprised quartz and manganoan calcite; both common bedrock minerals that are present as colloidal particles in the source waters. The chemical additives in the alum WTRs did not

Table 3. Properties of the Residue Materials Direct from the Treatment Works.

Parameter	WTR 1	WTR 2a	WTR 2b	WTR 3
Water content, %	340	570	–	300
Solids content, %	23	15	–	25
Bulk density, tonne/m ³	1.08	1.06	–	1.10
Dry density, tonne/m ³	0.25	0.18	–	0.26
Void ratio	6.3	11.3	–	5.7
Liquid limit, %	490	550	550	430
Plastic limit, %	240	260	280	220
Plasticity index	250	290	270	210
Total volatile solids, %	57	45	41	46
Specific gravity of solids	1.86	1.99	1.83	1.90
Adhesion limit, %	240	365	355	345
Linear shrinkage, %	47	45	38	48
Free swell, %	35	10	10	40
pH	8.6	7.1	7.9	7.2

WTR 1, WTR 2a and WTR 3 are alum water treatment residues; WTR 2b is a non-chemically treated residue.

feature in the analysis since the alum was present in its aluminum hydroxide form (disordered and without any definable crystalline structure), and the polyelectrolytes are organic molecules. Inductive-coupled plasma analysis was also carried out on six specimens of alum WTR 2a over the water content range of 120% to 1100%, which indicated that this residue comprised 24–28% aluminum by dry mass, in line with the range of $29.7 \pm 13.3\%$ reported for alum WTRs [22].

The total volatile solids (TVS) values of 41–57% were determined by heating dry powered residue specimens in a muffle furnace at a temperature of 440°C [21], which oxidizes both the polyelectrolytes and the organic solids. The polyelectrolytes, which are unstable above 150°C, typically comprised 3.3% dry solids mass (range 1.6–4.8% dry solids mass) for alum WTRs 1, 2a and 3 (Table 2). Nevertheless, the TVS value is a good reflection of the gravimetric organic content since the crystalline fraction remains stable at the ignition temperature of 440°C. For example, calcination to form lime occurs at a much higher temperature of about 850°C. The 4% higher TVS value measured for alum WTR 2a, compared to the non-chemically treated residue WTR 2b, is most likely due to the 4.8% polyelectrolyte by dry solids mass basis that had been added during the treatment processes at the municipal works and which was ultimately retained in alum WTR 2a. Some natural variations could also be expected in the composition of the suspended solids in the source water since residues WTR 2a and WTR 2b had been sampled in October and February, respectively. Organic matter in soil is generally responsible for high plasticity; low specific gravity of solids; high shrinkage; high compressibility; and low hydraulic conductivity [23]. Note that the organic fractions of WTR and sewage sludge materials mainly comprise colloidal-size particles (i.e. non fibrous), although the organic fraction of WTRs is usually in a near stable condition whereas sewage sludge is bioactive, with the organics usually at moderate to strong levels of biodegradation [17,18,24]. The specific gravity of solids values of 1.83–1.99, which were measured using the small picnometer method [20], were relatively low, although consistent with the high organic contents. Note that the specific gravity of solids for mineral soils is typically in the range 2.5–2.7.

Linear shrinkage was calculated as the percentage reduction in the length of a bar of the wet residue material, which had been prepared at the liquid limit condition using a mold 130 mm in length, and oven dried at a tem-

perature of $105 \pm 5^\circ\text{C}$ [20]. The linear shrinkage values of 38–48% were very high, indicating substantial reductions in volume would occur on drying the wet residue materials. The free swell values, defined as the maximum volumetric expansion that would occur on full re-saturation of the powered oven-dried residue materials, of 10–40% were also high, although consistent with the high plasticity index values. The pH of the residues was determined using an electrometric method [21] and, as expected, the pH was slightly alkaline due to the chemical conditioning of the water during the treatment processes.

The water content of the wet residue samples was reduced over time in the geotechnical laboratory by allowing thin layers of the wet material to dry naturally in trays at ambient temperature of 20°C.

COMPACTION PROPERTIES

Ordinary Proctor compaction tests using the one-liter compaction mold [25] were conducted on wet alum WTR samples that had been allowed to dry naturally over different periods, with regular remolding, thereby obtaining uniform materials with different water content values. The samples were regularly mixed during the drying process and any clumps were disaggregated to pass the 20 mm sieve size prior to the compaction tests. Sets of three cylindrical sub-specimens (38 mm in diameter and 76 mm high) were also prepared from the wet ordinary Proctor compacted specimens. The wet mass, bulk volume and water content values of these sub-specimens were measured after they had been allowed to slowly air-dry further, and shrink without cracking, at ambient laboratory temperature. The bulk density was calculated as the wet mass per unit volume, from which the dry density was calculated using Equation (5).

Figure 3(a) shows the density values achieved by ordinary Proctor compaction alone. Figure 3(b) shows the density values achieved by allowing the sub-specimens that had been prepared from the wet ordinary Proctor compacted specimens to reduce in water content by natural air drying. Note that the zero air voids curve included in Figure 3 corresponds to the fully saturated condition and therefore represents an upper bound for the dry density values. The zero air voids curve was determined from the measured specific gravity of solids values [19].

The bulk density and dry density values of 0.96–1.13 and 0.21–0.36 tonne/m³ respectively, achieved by ordi-

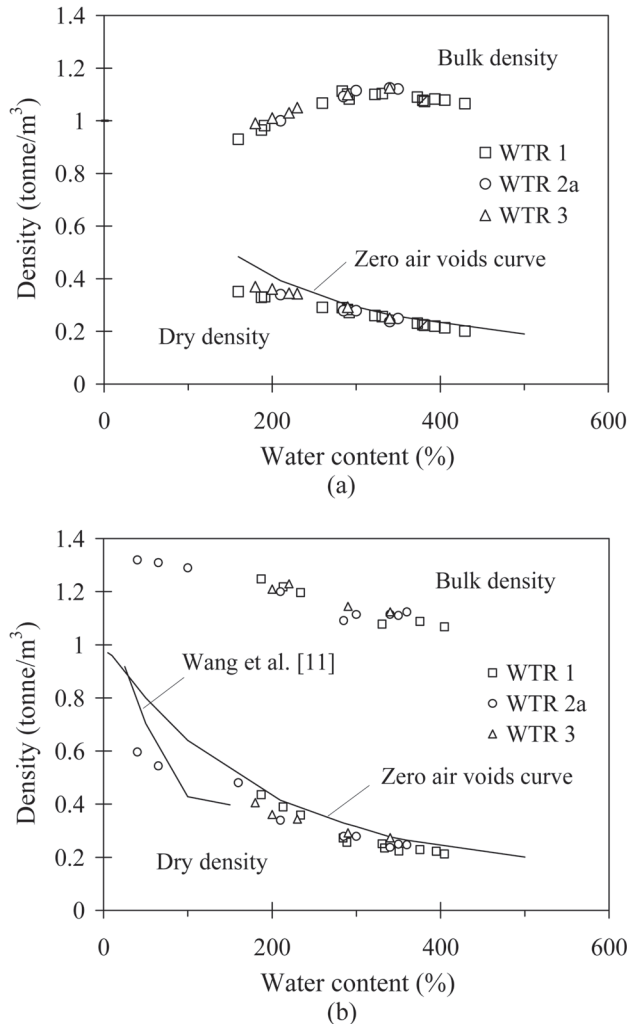


Figure 3. Ordinary Proctor compaction; (a) Compaction alone, (b) Compaction followed by air drying.

nary Proctor compaction [Figure 3(a)] were very low compared with mineral soils, although in line with the high water content of 200–400% and the low specific gravity of solids values. Furthermore, the dry density against water content curve in Figure 3(a) was relatively flat over the test range, which is a distinctive characteristic of these residue materials, with the dry density decreasing marginally in value with increasing water content, since the pore water constitutes an increasing proportion of the residue volume. The optimum water content to achieve the maximum dry density for ordinary Proctor compaction did not occur within the water content range tested and this trend in the dry density data is consistent with Wang et al. [11].

Figure 3(b) shows that below 200% water content, the bulk density and dry density values that had been achieved by allowing the compacted alum WTR material to air-dry naturally were consistently greater than

those achieved by ordinary Proctor compaction alone at the reduced water content value. Controlled drying and shrinkage without cracking of the wet sub-specimens had produced lower air voids contents ($A = 2.5\text{--}3\%$), compared with those achieved by ordinary Proctor compaction alone of the dried alum WTRs ($A = 3.5\text{--}5\%$). Note that the air voids content is defined as the ratio of the volume of the pore air voids to the bulk volume, given as a percentage. The residue materials were brittle below about 160% water content and crushed to a dust under the impact of the compaction rammer.

Hence, field compaction of these alum WTRs would be most efficiently carried out over the water content range of 200–240%, owing to the tendency for these residues to stick to machine plant above the adhesion limit value of 240% water content. *In situ* air drying and shrinkage of the compacted residues subsequently produce higher dry density values than achieved by compaction alone of material placed below 200% water content, thereby increasing the storage capacity of the residue monofill. Ordinary Proctor compactive effort was also found to be excessive for these alum WTRs, evident by some swelling of the compacted specimens at a constant water content, and it is suggested that a lighter field-compactive energy of about one-third ordinary Proctor compactive effort should be adequate in the case of residue monofills, following from recommendations by Loll [26] and O’Kelly [27]. Furthermore, residues for landfilling should not be dried beforehand below 160% water content since they would easily crush to a dust under the action of the compaction roller, raising additional environmental concerns.

SHEAR STRENGTH PROPERTIES

The undrained shear strength of the ordinary Proctor-compacted residue specimens was measured as a function of their water content using quick-undrained triaxial compression tests [28]. These data are pertinent to the placement and trafficability of the residues in monofills, and in determining the factor of safety against short-term geotechnical instability of the monofill slopes. The thixotropic hardening behavior was studied by carrying out laboratory vane and triaxial compression tests [28] on specimens of alum WTR 2a that had been allowed to cure, undisturbed and at a constant composition, over different periods.

The effective stress shear strength property values, which are used in determining the factor of safety against instability of the monofill slopes for the inter-

mediate and long-term conditions, were measured using isotropic consolidated-undrained triaxial compression tests, and with continuous measurement of the pore water pressure response [29].

Undrained Shear Strength

Quick-undrained triaxial compression tests were carried out on the partially saturated specimens (38 mm in diameter and 76 mm high) that had been prepared from the one-liter ordinary Proctor compacted specimens, which had air voids contents of 3.5–5%. Some of these triaxial specimens were allowed to air-dry slowly over different periods prior to shearing in order to simulate the strength gain that would occur due to air drying of the residue material used, for example, as daily cover on a municipal landfill. A cell confining pressure of 100 kPa was applied to the triaxial specimens, which were then sheared quickly at 2% axial strain/min in an undrained condition. Specimen failure was deemed to have occurred at a limiting 20% axial strain unless the measured shear stress value had reached a maximum at a lower strain value. Figure 4 shows data for shear stress against axial strain for pairs of WTR 2a and WTR 2b specimens that had been sheared at similar water contents.

Figure 5(a) shows the data for triaxial undrained shear strength against water content on a logarithm–logarithm plot. Figure 5(b) shows the water content values scaled in terms of the liquidity index [I_L , Equation (6)]. Overall, the shear strength values for the three alum WTRs were in good agreement and consistently greater than that measured for the non-chemically treated residue WTR 2b, with the shear strength approximately inversely related to the water content and the liquidity index on logarithm–logarithm and

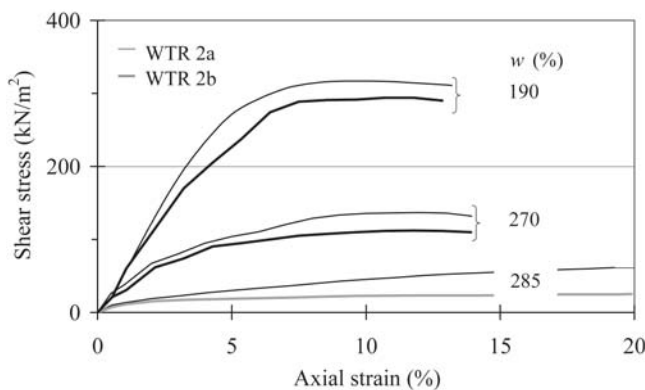


Figure 4. Shear stress against strain for WTR 2a and WTR 2b (chemically and non-chemically treated residues, respectively) under triaxial compression.

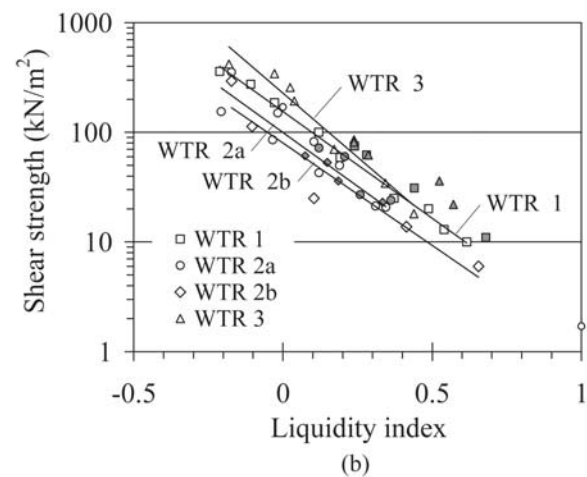
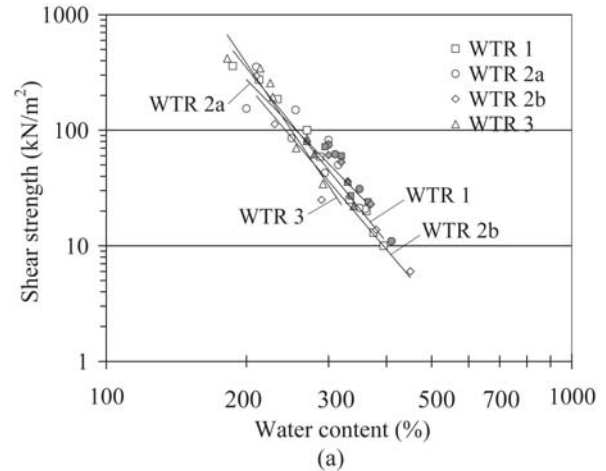


Figure 5. Undrained shear strength data: (a) Against water content, (b) Against liquidity index. Note: hollow and shaded symbols denote quick-undrained and consolidated-undrained triaxial compression tests, respectively.

logarithm–linear plots, respectively. Note that I_L values of unity and zero correspond to the Atterberg liquid limit and plastic limit conditions respectively, and $I_L < 0$ indicates that the material is in a semisolid state.

$$I_L = \frac{w - w_P}{w_L - w_P} \quad (6)$$

where

- w = water content
- w_L = liquid limit
- w_P = plastic limit

Thixotropy Effects

Laboratory Vane

Saturated alum WTR 2a material prepared at 365% and 520% water content ($I_L = 0.36$ and 0.90 , respec-

tively) was pressed into molds, 70 mm square in plan and 70 mm high, taking care to avoid trapping air voids, and hermetically sealed by wrapping in cling film. The vane shear strength of these specimens was measured [28] after standing periods of up to four weeks at ambient laboratory temperature of 20°C. The specimens were sheared quickly using a miniature cruciform vane, 25 mm in both width and length, which was rotated at 0.1 rev/min. Figures 6(a) and 6(b) show data for the increase in vane shear strength and the strength gain ratio against the standing period. For example, the vane shear strength measured for $I_L = 0.90$ (i.e. near the liquid limit condition) was found to increase from 3 kPa in the remolded state to about 7 kPa after a nine-day curing period, with a strength gain ratio of 3.3 achieved by the end of the four-week test period. The higher strength gain ratios of 5.7 to 8.0 that have been reported for alum WTRs by Wang et al. [11] correspond to a ten-week standing period and for higher liquidity index values of 1.6–2.0, which is in line with the expected trend of increasing thixotropic effects with increasing standing times and liquidity index values.

Triaxial Compression

Three physically-identical triaxial specimens A–C, each 38 mm in diameter and 76 mm high, were prepared from a saturated cake of alum WTR 2a that had been consolidated one-dimensionally from the slurry state under an applied vertical stress of 60 kPa to a water content near its plastic limit value ($I_L = 0.14$) using a large consolidometer press developed by O'Kelly [30,31]. The triaxial specimens A, B and C were allowed to cure, undisturbed and at a constant composition, for periods of 0, 5 and 12 days, respectively.

An isotropic cell confining pressure of 260 kPa was then applied to these triaxial specimens under undrained conditions, thereby mobilizing an effective isotropic confining pressure (σ'_c) of about 60 kPa, which had been approximately achieved under the applied vertical stress of 60 kPa and 1–D consolidation conditions in the consolidometer press. Next, the triaxial specimens were sheared in an undrained condition at $3.3 \times 10^{-5}\%$ axial strain/min, which was sufficiently slow to allow full equalization of the pore water pressures to occur throughout the specimens at failure.

Similar stress–strain behavior and shear strength values were measured for triaxial specimens A–C [Figure 6(c)], indicating negligible thixotropic strength gain over the curing period of up to 12 days, which was expected, since the specimen water content was near the

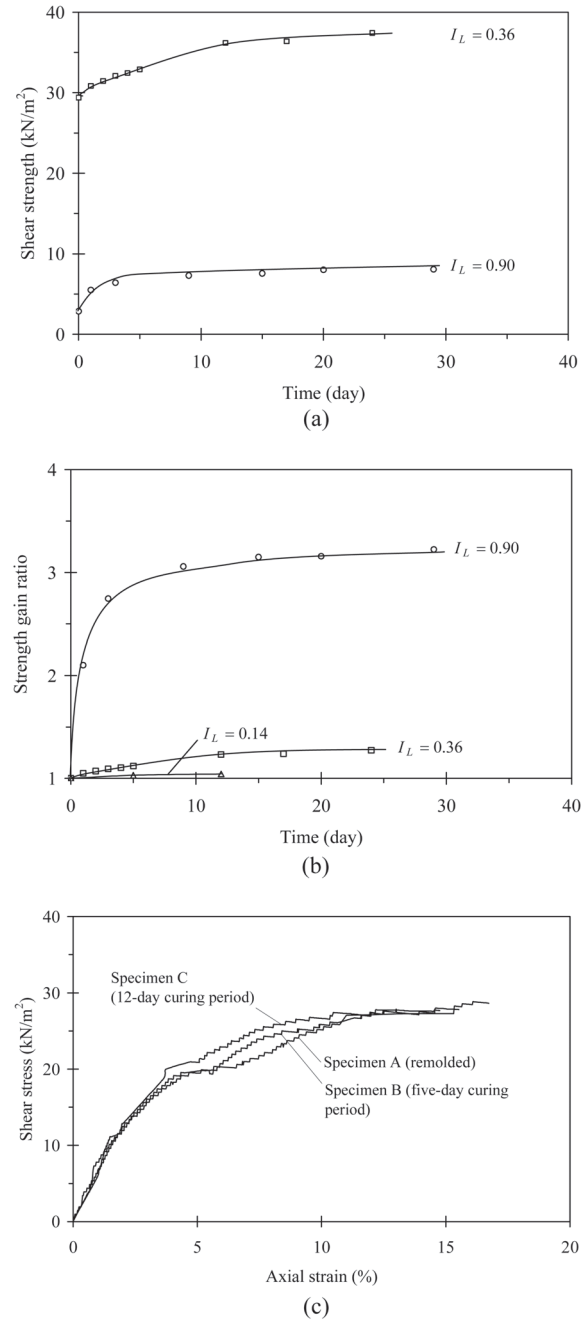


Figure 6. Thixotropic behavior of alum WTR 2a; (a) Laboratory vane, (b) Strength gain ratio, (c) Triaxial compression ($I_L = 0.14$).

plastic limit condition. Seed and Chan [32] reported that the effect of thixotropic hardening decreases with decreasing liquidity index and that the plastic limit represents a lower-bound water content value for thixotropic behavior.

Effective Stress Shear Strength Properties

A series of isotropic consolidated-undrained triaxial

compression tests [29], which included continuous measurement of the pore water pressure response, were carried out in order to study the effective stress shear strength properties. Four physically-identical triaxial specimens (38 mm in diameter and 76 mm high) were prepared for each residue material from saturated cakes that had been pressed from the slurry state in the consolidometer apparatus and allowed to equilibrate under an applied vertical stress of $\sigma_v = 30$ kPa. The sets of residue specimens were isotropically consolidated under effective cell-confining pressures of 30, 60, 120 and 150 kPa over a 24-hour period in the triaxial apparatus, with the specimens allowed to drain radially to filter-paper side drains and vertically to porous discs in contact with both specimen ends, against an applied specimen back pressure of 200 kPa over a 24-hour period. An effective cell-confining pressure of at least 30 kPa was applied to these specimens in order that they would be in a normally consolidated condition ($\sigma_c \geq \sigma_v$) during the triaxial shearing stage. The consolidated

specimens were sheared slowly in an undrained condition at strain rates of the order of $10^{-5}\%$ axial strain/min, determined from curve-fitting analysis of the data from the triaxial consolidation stage [29], and which were sufficiently slow to allow full equalization of the pore water pressures to occur throughout the specimens at failure. The standard corrections for the restraining effects of the filter-paper side drain and the enclosing rubber membrane on the barreling-type of specimen deformation response were applied to the measured data [29].

Figure 7 shows the s' - t' effective stress path plots; where $s' = (\sigma'_1 + \sigma'_3)/2$ and $t' = (\sigma'_1 - \sigma'_3)/2$ are the Massachusetts Institute of Technology stress path parameters; and σ'_1 and σ'_3 are the major and minor effective principal stresses, respectively. The failure lines of best fit in the s' - t' plots were drawn passing through the origin (i.e. effective cohesion of zero) and aligned with the stress points corresponding to specimen failure, which typically occurred between 2% and 10% axial strain. Note that the effective stress paths at failure for triaxial specimens A–C of alum WTR 2a, which had been sheared at similar strain rates but after different curing periods of 0, 5 and 12 days (thixotropy section), were also coincident with the alum WTR 2a failure line in Figure 7(b); further evidence that the effects of thixotropic hardening are not significant at low liquidity index values. Had thixotropy effects been significant, the effective stress paths at failure for specimens A–C would have located above the best-fit failure line for the uncured specimens. The ratio of the mobilized shear strength to the effective cell-confining pressure that had been applied during the triaxial consolidation stage had a mean value of 1.8. The effective angle of shearing resistance (ϕ') values of 39° to 44° , which were calculated from the gradient of the s' - t' failure lines in Figure 7 using Equation (7), are in line with the ϕ' values of 42° and 44° reported for two alum WTRs by Wang et al. [11].

$$\sin \phi' = \tan \alpha' \quad (7)$$

where

α' = gradient of the s' - t' failure line to horizontal s' axis

COMPRESSION PROPERTIES

The compression and consolidation properties were determined as a function of the state of effective stress by testing saturated residue specimens of different size,

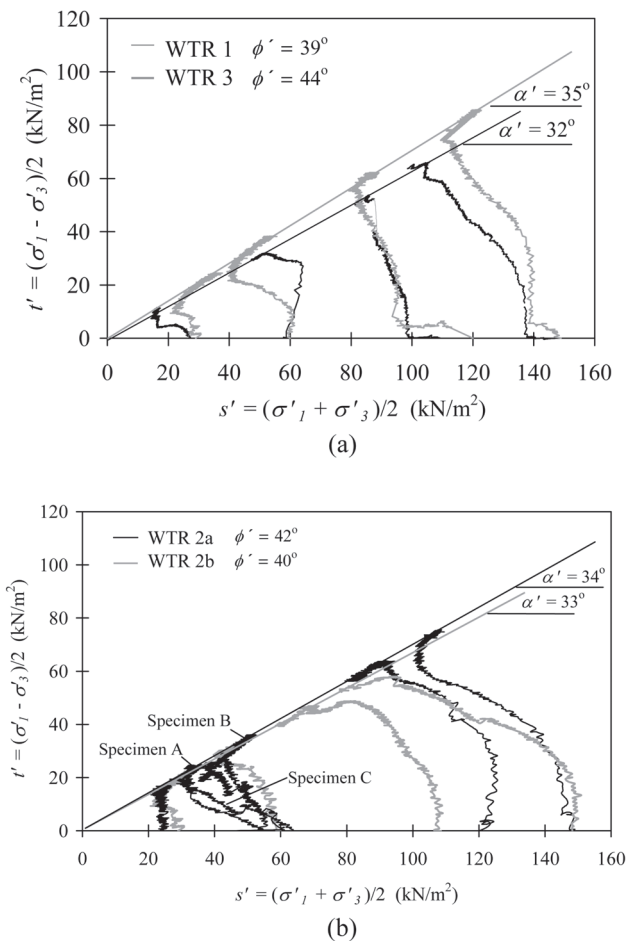


Figure 7. Effective stress path plots; (a) WTR 1 and WTR 3, (b) WTR 2a and WTR 2b.

aspect ratio and consistency under different loading and drainage conditions using the oedometer, consolidometer and triaxial apparatus [33]. Table 4 summarizes the initial dimensions and consistency of the specimens, drainage conditions and the applied stresses of between 3 and 800 kPa that covered the diverse levels of effective stress achieved in mechanically dewatering, storing and landfilling the residue materials: that is, low effective stress levels in lagoons, low to medium effective stress levels in landfills and the medium to very high stresses applied by mechanical dewatering devices at municipal works. The consolidometer and isotropic triaxial consolidation tests have already been outlined in the context of describing the measurement of the effective stress shear strength properties of the residue materials.

Oedometer Tests

Multiple-increment oedometer tests [33] were carried out on saturated materials that had been prepared by thoroughly mixing the dewatered alum residues from the municipal works with distilled water to form uniform slurry pastes, which were allowed to equilibrate in sealed containers over a two-day period prior to the compaction tests. The slurry paste was pressed into the 76-mm diameter confining ring of the oedometer apparatus, taking care to avoid trapping air

voids. The specimen was compressed one-dimensionally, with two-way vertical drainage to atmosphere, under an applied vertical stress that was doubled in moving from one load stage to the next, over the stress range 3–800 kPa. A displacement transducer in contact with the oedometer loading cap continuously measured the specimen deformation response. Each oedometer load stage was two days in duration in order to record sufficient data covering both the specimen consolidation and longer-term creep settlement responses under successive increments of applied stress.

Figure 8 shows the oedometer data, plotted in the conventional form of cumulative volumetric strain against the square root of elapsed time, for alum WTRs 1, 2a and 3. The slurry specimens were highly compressible, deforming at slow but steady rates, and by the end of the final load stage (800 kPa) had undergone very large volumetric strains of up to 62%. The primary consolidation component due to the dissipation of the excess pore water pressure was dominant during the early load stages, with primary compression ratio (defined as the proportion of the total strain for a particular load stage occurring due to primary consolidation) values of 0.75 to 0.90. However, secondary compression became increasingly significant at higher stress levels, with the primary compression ratio values for the alum residues reducing to 0.22–0.40 by the final load stage.

Table 4. Summary of the Consolidation Tests.

Test Method	Dimensions ^a mm	Consistency WTR 2a	Water Content		Applied Stress kN/m ²	Void Ratio		Duration Load Stage day	Drainage Conditions WTR 2b	Compression Index, C _c WTR 3
			Initial %	Final %		Initial	Final			
Oedometer										
WTR 1	76 × 29	Slurry	780	280	$\sigma_v = 3\text{--}800$ (MI)	14.5	6.2	2	Two-way vertical	3.2
WTR 2a	76 × 29	Slurry	700	190	$\sigma_v = 3\text{--}800$ (MI)	14.1	3.3	2	Two-way vertical	2.5
WTR 3	76 × 29	Slurry	690	310	$\sigma_v = 3\text{--}800$ (MI)	11.9	5.4	2	Two-way vertical	2.5
Consolidometer										
WTR 1	152 × 139	Slurry	625	475	$\sigma_v = 10\text{--}30$ (MI)	14.1	8.8	7	Two-way vertical	3.9
WTR 2a	152 × 139	Slurry	580	420	$\sigma_v = 10\text{--}30$ (MI)	10.9	8.4	7	Two-way vertical	3.1
WTR 2a	167 × 139	Very soft	500	330	$\sigma_v = 7.5\text{--}60$ (MI)	8.8	6.2	7	Two-way vertical	2.6
WTR 2b	152 × 167	Slurry	760	435	$\sigma_v = 10\text{--}30$ (MI)	15.4	8.1	7	Two-way vertical	5.5
WTR 3	152 × 93	Slurry	600	410	$\sigma_v = 10\text{--}30$ (MI)	11.1	7.8	7	Two-way vertical	3.1
Isotropic Triaxial										
WTR 1	38 × 76	Very soft	475	340	$\sigma'_c = 30\text{--}150$ (SI)	8.8	7.3	1	All around	2.3
WTR 2a	38 × 76	Very soft	420	350	$\sigma'_c = 30\text{--}150$ (SI)	8.4	7.9	1	All around	0.8
WTR 2b	38 × 76	Very soft	435	340	$\sigma'_c = 30\text{--}150$ (SI)	8.1	7.2	1	All around	1.1
WTR 3	38 × 76	Very soft	410	300	$\sigma'_c = 30\text{--}150$ (SI)	7.8	6.7	1	All around	1.4

MI, multiple increment; SI, single increment; σ_v , applied vertical stress; σ'_c , effective confining pressure.

^aSpecimen dimensions are given as diameter by height.

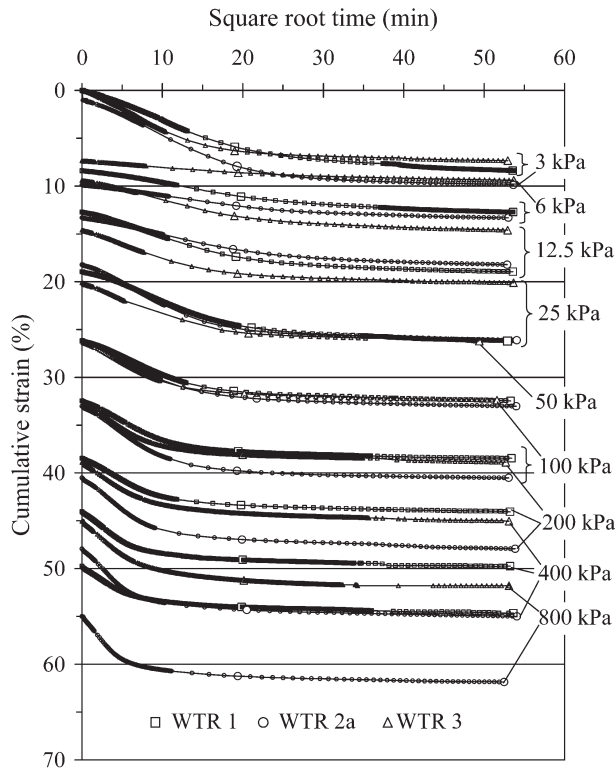


Figure 8. Oedometer data.

Consolidometer Tests

Specimens of very soft and slurry consistencies were compressed one-dimensionally under applied vertical stresses of 10–60 kPa, and with two-way vertical drainage to atmosphere, using a 152-mm diameter consolidometer press [30,31]. Each load stage was extended to seven days in duration, compared to the two days that had been used as standard for each oedometer load stage, because of the greater specimen drainage length in the consolidometer tests. Periodic measurements of the deformation response were recorded using a long-stroke dial gauge in contact with the specimen loading platen (Figure 9). Again, the slurry specimens were highly compressible, and by the end of the final load stage (30 kPa), had undergone large volumetric strains of up to 36%. Water content tests carried out on the pressed residue cakes confirmed that the water content distribution was uniform across the specimen thickness, indicating that full consolidation had been achieved throughout the specimens by the end of the final load stage.

Triaxial Consolidation Tests

Four triaxial specimens (38 mm in diameter and 76 mm high) were prepared for each residue material from

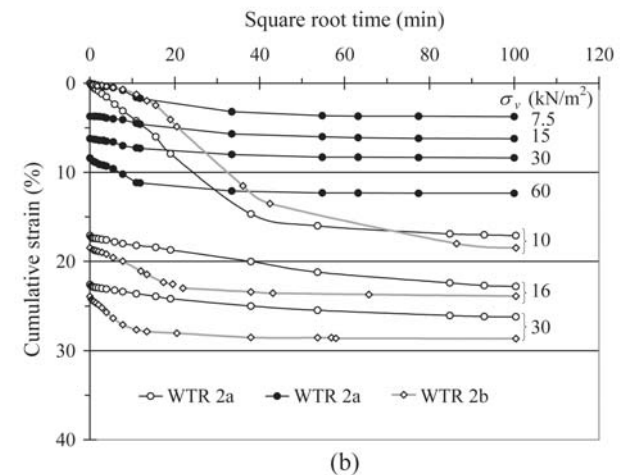
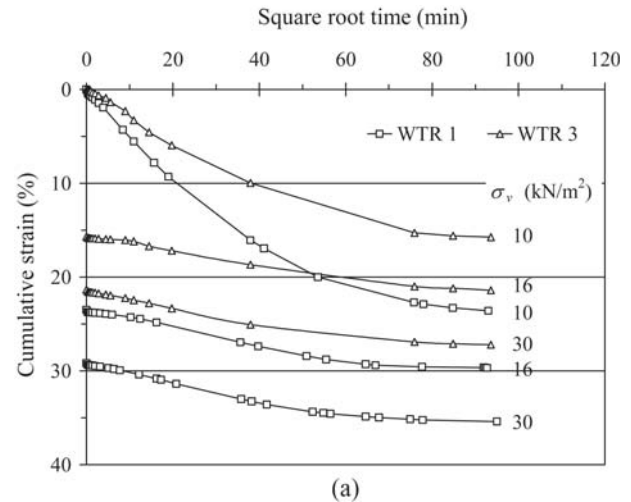


Figure 9. Consolidometer data; (a) WTR 1 and WTR 3, (b) WTR 2a and WTR 2b. Note: hollow symbols, slurry specimens; solid symbols, very soft specimen; σ_v , applied vertical stress.

the very soft cakes produced at the end of the consolidometer tests. The sets of residue specimens were allowed to drain radially to filter-paper side drains and vertically from both ends under isotropic effective confining pressures of 30, 60, 120 and 150 kPa, with continuous measurement of the volume of pore water that drained from the specimens over a 24 h period, against an applied back pressure of 200 kPa, in the triaxial apparatus [33]. The volumetric strain data are shown against the square root of elapsed time in Figure 10 and against the state of effective stress in Figure 11(a). The drained bulk modulus (B , as MN/m^2) response is shown in Figure 11(b), where B is defined as the ratio of the effective stress to the volumetric strain (decimal value). The very soft residue specimens were also highly compressible, and by the end of the consolidation stage at 150 kPa, had undergone large volumetric strains of up to 33%.

Compressibility Data

The stress–strain–time data from the oedometer, consolidometer and triaxial consolidation tests are summarized in the conventional form of void ratio against logarithm of effective stress in Figure 12.

The compression response was quantified in terms of the compression index (C_c) values, which are included in Table 4. Note that the level of compression depends on a range of factors, including: initial water content (void ratio); hydraulic conductivity; specimen thickness and drainage length; applied stress; and load-stage duration. The slurry residues were highly compressible, with values of $C_c = 3.2, 2.5$ and 2.5 given by the gradients of the oedometer void ratio against logarithm of effective stress curves [Figure 12(a)] for alum WTRs 1, 2a and 3, respectively. Note that for most inorganic clays, $C_c < 1.0$, and generally less than 0.5. The consolidometer data for the alum WTR slurries gave higher values of $C_c = 3.1–3.9$ (Table 4) due to greater amounts of secondary compression settlement having

occurred by the end of the longer-duration load stages (seven days compared to the two days used as standard for each oedometer load stage). Primary compression ratio [C_c^* , Equation (8)] values of 0.19, 0.17 and 0.20, which take into account the initial consistency (void ratio) of the specimens, were determined from the oedometer data for alum WTRs 1, 2a and 3 respectively.

$$C_c^* = \frac{C_c}{1 + e_o} \tag{8}$$

where

e_o = initial void ratio.

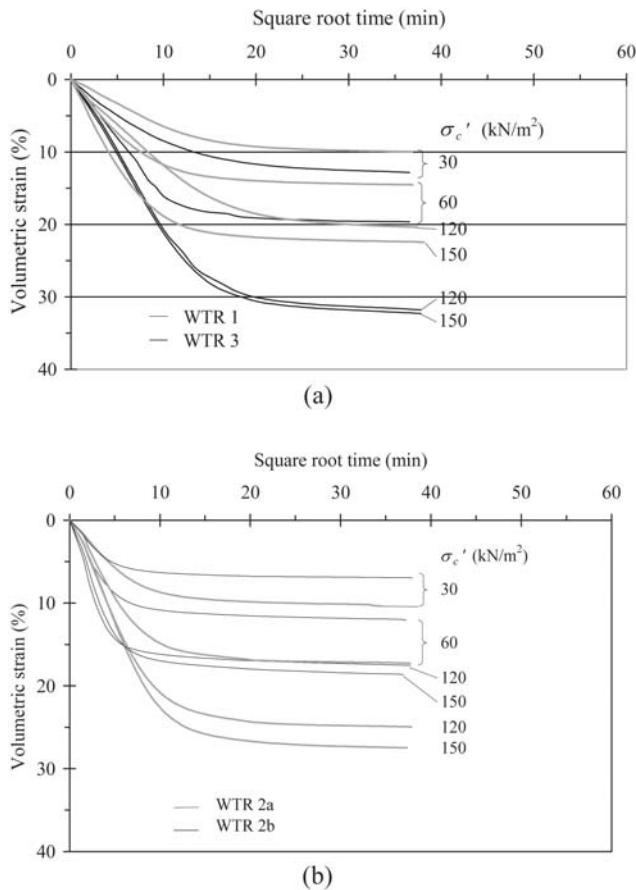


Figure 10. Triaxial consolidation data; (a) WTR 1 and WTR 3, (b) WTR 2a and WTR 2b. Note: σ'_c , effective confining pressure.

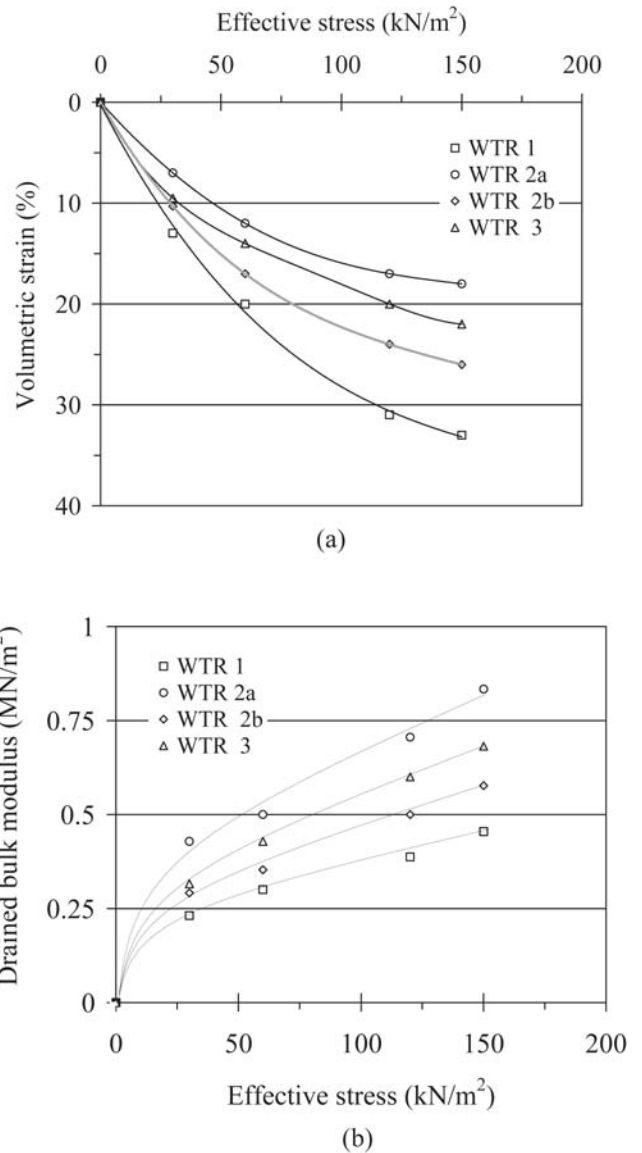


Figure 11. Dewaterability under isotropic confining pressure; (a) Volumetric strain, (b) Drained bulk modulus.

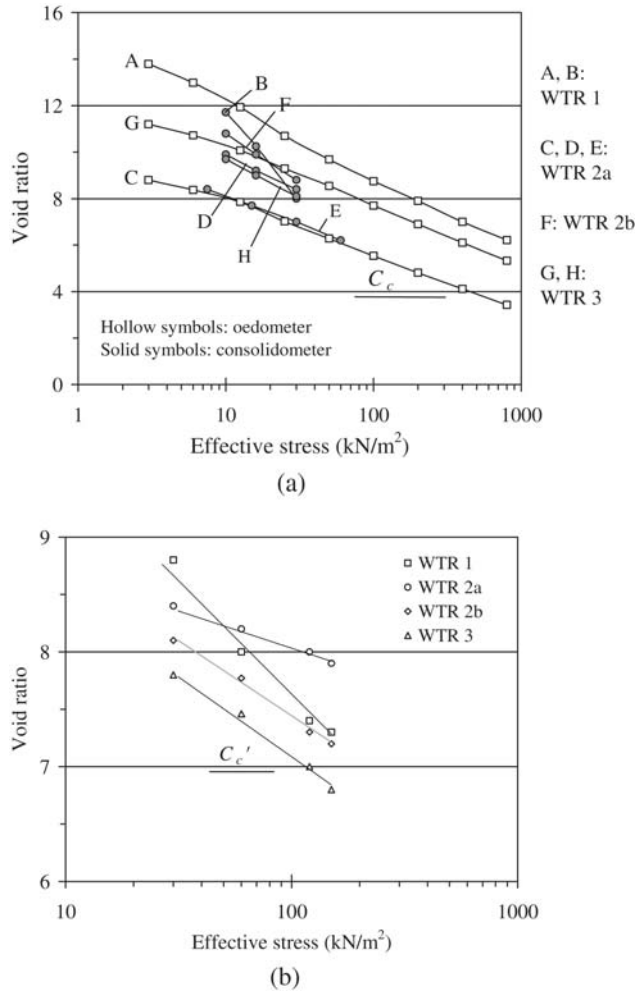


Figure 12. Void ratio against effective stress (primary consolidation settlement); (a) 1-D compression in oedometer and consolidometer apparatus, (b) Isotropic triaxial consolidation. Note: C_c , compression index.

Consolidation Rate

The rate of consolidation of the residue materials was very slow, typical of high-plasticity clays. Standard curve-fitting techniques [33] were applied to the oedometer and triaxial consolidation data presented in Figures 8 and 10 in order to determine the values of the coefficient of primary consolidation (c_v), which were in good agreement for the residue materials, increasing from $C_v = 0.1$ to 0.8 m²/year with increasing effective stress from 3 to 800 kPa (Figure 13).

Hydraulic Conductivity

The hydraulic conductivity [k , Equation (9)] was determined indirectly from the oedometer data presented in Figure 8 as

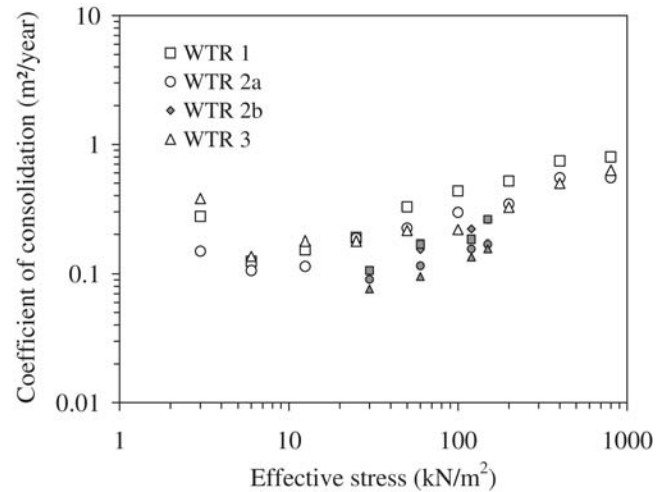


Figure 13. Coefficient of primary consolidation against effective stress. Note: hollow symbols, oedometer data; solid symbols, triaxial data.

$$k = m_v c_v \gamma_w \quad (9)$$

where

γ_w = density of the pore water (assumed 0.98 tonnes/m³)

m_v and c_v = coefficients of volume change and primary consolidation respectively, with m_v defined as the volumetric strain per unit increase in effective stress

The hydraulic conductivity values were very low and inversely related to the state of effective stress on a logarithm–logarithm plot [Figure 14(a)], with the hydraulic conductivity decreasing significantly from about 2×10^{-4} to 1×10^{-6} m/day with increasing effective stress (reductions in water content and void ratio) from 3 to 800 kPa. This is consistent with the experience of mechanically dewatering the wet alum WTRs at the treatment works. Wang and Tseng [12] also reported that the hydraulic conductivity of alum WTR reduced from the order of 10^{-4} to 10^{-6} m/day over the effective stress range of 2 to 540 kPa. Direct comparisons at the same levels of effective stress indicate that the hydraulic conductivity values of WTR 2a and WTR 3 are broadly similar and about one order of magnitude greater than that measured for WTR 1 [Figure 14(a)]. It is postulated that this difference in hydraulic conductivity values is partly due to the higher organic content of WTR 1 ($TVS = 57\%$) compared to either WTR 2a or WTR 3 ($TVS = 45\text{--}46\%$). The hydraulic conductivity data are also shown against the water content (w) in Figure 14(b) and against the void ratio (e) in Figure 14(c), since these parameters can be readily determined in practice using the

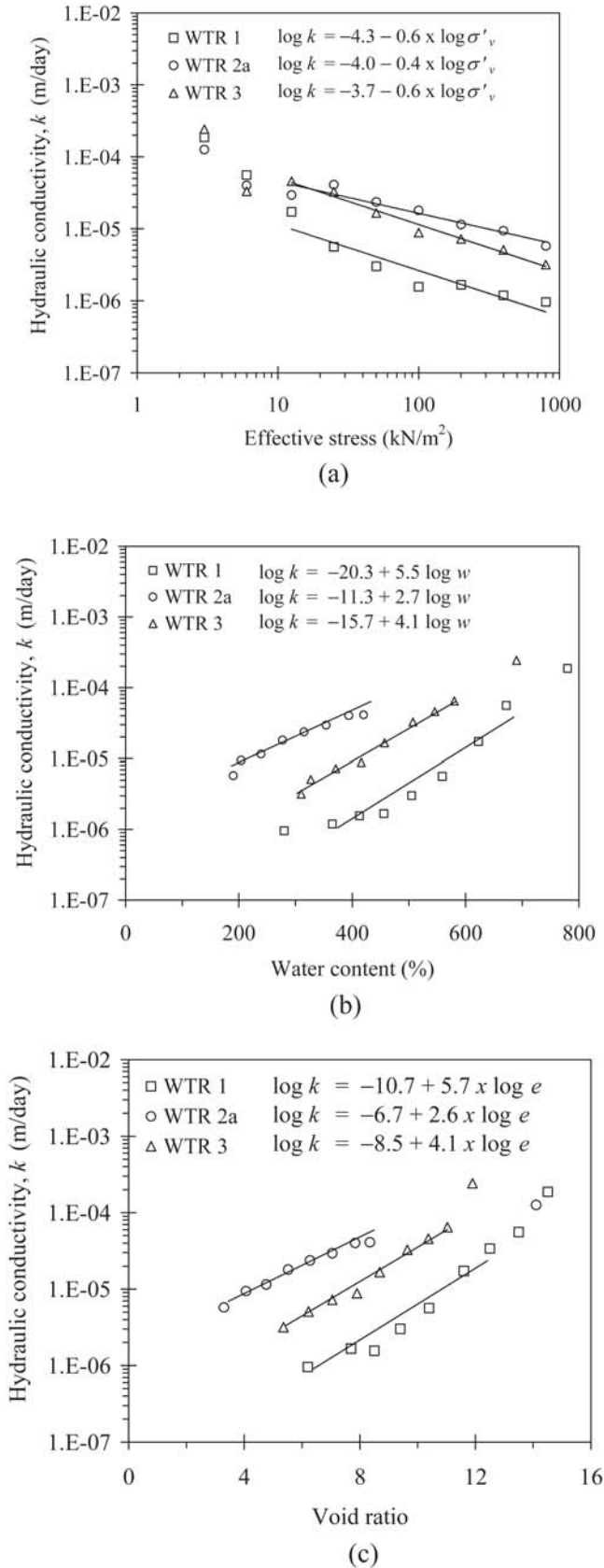


Figure 14. Hydraulic conductivity data; (a) Against effective stress σ'_v , (b) Against water content, w , (c) Against void ratio, e .

standard oven-drying method [20] and phase relationships respectively. For example, assuming fully saturated conditions, the void ratio is given by

$$e = wG_s \tag{10}$$

where

G_s = specific gravity of the solids

Secondary Compression Rate

The rate of secondary compression (creep) for the alum WTRs was quantified in terms of the coefficient of secondary compression C_{sec} , defined as the 1-D volumetric strain per ten-fold increase in elapsed time after the substantial completion of the primary consolidation phase (i.e. under constant effective stress). High values of $C_{sec} = 0.005-0.010$ were determined from the oedometer data, with a mean value of $C_{sec} = 0.006$ over the effective stress range 3–800 kPa (Figure 15). The C_{sec} values, and hence anticipated long-term settlements, were consistently greater for WTR 1 than for either WTR 2a or WTR 3, owing to its higher organic content [23]. Figure 15 also shows the data values of 0.15–0.18 determined for the secondary compression index [$C_{\alpha e}$, Equation (11)] and 0.03–0.05 determined for the ratio of $C_{\alpha e}/C_c$ [34], which are typical ranges for organic soils.

$$C_{\alpha e} = C_{sec}(1 + e_o) \tag{11}$$

EFFECTS OF CATCHMENT GEOLOGY AND CHEMICAL ADDITIVES ON THE ENGINEERING BEHAVIOR

Despite significant differences in catchment geol-

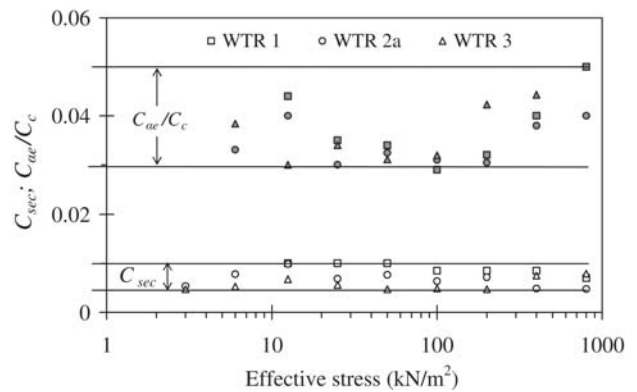


Figure 15. Secondary compression data. Note: C_c , compression index; C_{SEC} , coefficient of secondary compression; $C_{\alpha e}$, secondary compression index.

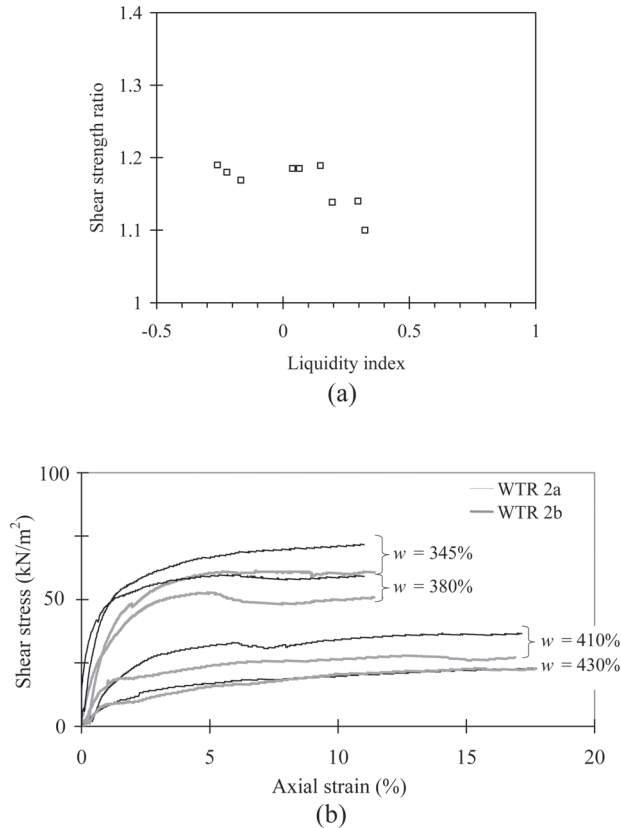


Figure 16. Effect of polyelectrolyte on the triaxial undrained shear strength; (a) Ratio of the undrained shear strength of alum WTR 2a to that of the non-chemically treated residue WTR 2b, (b) Shear stress against strain data for specimen pairs at similar water contents (w).

ogy, and allowing for minor differences in the chemical dosages and seasonal variations in the source waters (the test materials had been sampled at different times during the year), the three alum WTRs were found to have broadly similar geoenvironmental properties, most likely due to the fact that their behavior was dominated by the high organic content ($TVS = 41\text{--}57\%$).

At a given water content, the triaxial undrained shear strength of the alum WTRs was consistently greater than that measured for the non-chemically treated residue WTR 2b [Figure 5(b)], which can be explained by the action of the polyelectrolyte additive in aggregating and binding the constituent flocs to form floc clusters, thereby producing greater inter-particle contact and reducing the size of the pore voids and capillary channels (in combination with the deactivation of some pore water by the alum coagulant [12]). For example, Figure 16a shows the ratio of the triaxial undrained shear strength values measured for alum WTR 2a and the non-chemically treated residue WTR 2b. The shear strength of alum WTR 2a, which comprised 4.8% polyelectrolyte by dry solids mass, was between 1.1

and 1.2 times greater than that measured for the non-chemically treated residue WTR 2b. Stiffer responses and values of peak shear stress of up to 20% greater were also measured for alum WTR 2a, (compared with residue WTR 2b) from consolidated-undrained triaxial compression tests on specimen pairs at similar water contents [Figure 16(b)]. Hence, the effective angle of shearing resistance of alum WTR 2a was also slightly greater than that measured for residue WTR 2b ($\phi' = 42^\circ$ and 40° , respectively).

Although the chemical additives are necessary for the efficient operation of the treatment processes, they also have a downside in that the thickened alum WTRs are less compressible and potentially more difficult to consolidate. Hence, the larger bulk residue volume will settle over a longer period when placed in a lagoon or monofill. For example, Figure 12(b) shows that alum WTR 2a was less compressible than the non-chemically treated residue WTR 2b, with compression index values of $C_c = 3.1$ and 5.5 determined from the slurry consolidometer tests (Table 4). The hydraulic conductivity of alum WTR 2a is lower than that of the non-chemically treated residue WTR 2b, owing to the effect of the chemical additives, since the mineralogy; organic content; and test conditions are similar. This is consistent with the findings of Wang and Tseng [12] and O'Kelly [15] who reported that in the case of alum WTRs, relatively large amounts of additional pore water are trapped and absorbed by the aluminum hydroxide precipitates and polyelectrolyte molecules within the constituent flocs, which causes a reduction in hydraulic conductivity.

APPLICATION OF THE TEST DATA

Dewaterability of Slurry Residue at Treatment Works

The alum WTR slurry must be adequately dewatered at the treatment works in order to reduce its bulk volume, thereby lowering transportation and landfill-disposal costs, and to achieve an adequate shear strength for efficient handling, trafficability, and geotechnical stability of the landfill slopes. Dewatering is achieved by mechanical and/or thermal means, or by allowing the slurry residue to dry naturally in drying beds, depending on the size of the treatment works. The reduction in the residue volume, ΔV , achieved by mechanical dewatering systems can be estimated using Equation (12) and the void ratio–logarithm of effective stress data shown in Figure 12.

$$\Delta V = V_o \left(\frac{\Delta e}{1 + e_o} \right) = V_o \left(\frac{\sigma'}{B} \right) \quad (12)$$

where

V_o = initial volume

e_o = initial void ratio

Δe = reduction in void ratio under the effective stress

σ' = effective stress induced by the mechanical dewatering system

B = drained bulk modulus [Figure 11(b)]

Note that it is technically feasible to recover the alum from the slurry residue by chemical means and proprietary full-scale treatment systems are currently under development in practice. The aluminum hydroxide precipitate that forms during the coagulation process readily dissolves in highly acidic solutions [35] and the liquid alum can then be decanted and crystallized by evaporation. Alum recovery is most successfully carried out using sulfuric acid over the pH range of pH 2–3 and for retention periods of 10–20 min [36]. However, the effectiveness of these techniques has been varied to date, with the purity of the recovered alum and the overall economy of the recovery process remaining controversial issues. The data for alum WTR 2a and the non-chemically treated residue WTR 2b tested in this study indicated that the chemical additives had the effect of reducing the hydraulic conductivity of the slurry residue. Further studies are necessary in order to determine the extent to which these effects are reversible, since alum recovery may lead to greater levels of mechanical dewatering of the residue being achieved, and hence reduced landfill-disposal costs.

Acceptability of Residues for Landfilling Based on Shear Strength Criteria

In accordance with current guidelines [4–6], municipal landfill operators will usually not accept sludge or residues with a water content value greater than 300% ($SC = 25\%$), which has been set as an indirect measure of the shear strength necessary for efficient handling, trafficability and geotechnical stability. In municipal landfills, the wet residue material is usually placed in thin layers and mixed and scarified *in situ* with the solid waste, which has the effect of reducing the water content and increasing the shear strength of the residue fraction. Minimum shear strengths of 20 and 25 kPa have been recommended by Loll [26] and Siedlungsabfall [37], respectively, for the co-disposal of

sludge and residue materials at municipal landfills. An undrained shear strength of at least 20 kPa was achieved at 340% water content ($SC = 22\%$) for the three alum WTRs tested in this study [Figure 5(a)], although Figure 1 shows that for other municipal sludge and residue materials, the undrained shear strength achieved may be significantly less than 20 kPa [8,11,16] at the maximum 300% water content value set for municipal landfilling.

No universal relationship exists for soils between the water content and undrained shear strength, which is also dependent on a range of other factors, including: mineralogy; organic content; chemical dosages; and type of treatment used to separate the residue by-product. Hence, it would be more prudent for landfill operators to specify a minimum value of shear strength based on sound geotechnical considerations, rather than the current requirement for a maximum water content of 300% alone, in determining the acceptability of sludge and residue materials for landfilling. Note that in the case of residue monofills, higher shear strengths of at least 50 kPa are recommended for geotechnical stability.

Data for undrained shear strength against water content, such as that shown in Figure 5(a) for the alum WTRs tested in this study, can be used to select an appropriate mechanical dewatering system in order to achieve a specified minimum value of shear strength before the residue cake is transported for disposal offsite. For example, the recessed-plate filter press devices used at the Ballymore Eustace and Leixlip treatment works reduced the water content value of alum slurry residues WTR 1 and WTR 3 to 340% and 300% respectively (Table 3), thereby achieving adequate undrained shear strengths of about 25 and 31 kPa respectively, and satisfying geotechnical stability criteria for municipal landfilling. At the Clareville works, the water content value of alum WTR2a was reduced to about 700% using a belt-press device, and to about 570% by allowing the pressed residue to dry naturally in drying beds, although the remolded material was still of a slurry consistency and therefore unsuitable for municipal landfilling. Belt dryer devices that fully or partially dry the pressed residue cake at low temperatures; thermal treatments or soil-conditioning techniques can be investigated as alternative methods to dewater these residues sufficiently and expeditiously. The miniature vane apparatus [28] has been shown to provide a quick and accurate method of measuring the undrained shear strength (O'Kelly [27]; Loll [26]) in order to assess whether the residue material has been adequately

dewatered before leaving the treatment plant and again by the landfill operator before accepting the residue cake for disposal.

Settlement of Sludge Lagoons and Residue Monofills

The high values of compression index and coefficient of secondary compression measured for the alum WTRs indicate that residue lagoons and monofills will consolidate significantly and continue to settle by secondary compression (creep) over a long period. This time-dependent settlement response comprises the sum of the primary consolidation and secondary compression components, ΔH_c and ΔH_{sec} respectively, which can be quantified for 1-D settlement conditions using Equations (13)–(14). The time period necessary to achieve substantial completion of the primary consolidation component, t_1 , can be quantified using Equation (15).

$$\Delta H_c = H_o \frac{\Delta e}{1 + e_o} \quad (13a)$$

$$\Delta H_c = H_o \frac{C_c}{1 + e_o} \log \frac{\sigma'_{vo} + \Delta \sigma'_v}{\sigma'_{vo}} = H_o C_c^* \log \frac{\sigma'_{vo} + \Delta \sigma'_v}{\sigma'_{vo}} \quad (13b)$$

$$\Delta H_{sec} = H_o C_{sec} \log \frac{t_1}{t_2} \quad (14)$$

$$t_1 = \frac{T_v d^2}{c_v} \quad (15)$$

where

d = effective drainage length of the residue deposit (initially H_o in thickness)

e_o = initial void ratio

T_v = dimensionless time factor related to the average degree of consolidation

t_2 = time period that extends into the secondary compression phase ($t_2 > t_1$)

σ'_{vo} = initial vertical effective stress

Δe = reduction in the void ratio due to the increase in vertical effective stress, $\Delta \sigma'_v$ (i.e. applied stress increment)

The values of the compression index C_c [from Figure 12(a)]; coefficient of primary consolidation c_v [from Figure 13]; and coefficient of secondary compression C_{sec} [from Figure 15] that are used in these calculations must be consistent with the *insitu* effective stress; load-

ing and drainage conditions. A full explanation of the background to Equations (13)–(15) and their application in determining the magnitude and rate of settlement can be obtained in undergraduate soil mechanics textbooks, including Craig [19].

SUMMARY AND CONCLUSIONS

Despite significant differences in catchment geology, and allowing for minor differences in the chemical dosages and seasonal variations in the source waters, the three alum water treatment residues (WTRs) tested in this study were found to have similar geotechnical and hydraulic properties, akin to high-plasticity non-fibrous organic clays. These viscous slurry residues were highly compressible, although the consolidation rate was low (hydraulic conductivity of the order of 10^{-4} – 10^{-6} m/day), and underwent thixotropic hardening in an undisturbed condition. For mechanically-dewatered residue, the ratio of the triaxial shear strength to the effective confining pressure was about 1.8.

Ordinary Proctor compaction produced low values of bulk density and dry density of 0.96–1.13 and 0.21–0.36 tonne/m³ respectively, over the water content range 200–400%, although field compaction would be most efficiently carried out over the water content range 200–240% using a compactive energy of about one-third that of ordinary Proctor compactive effort. It is also recommended that landfill operators specify minimum shear strengths of 20 and 50 kPa for residue disposal at municipal landfills and dedicated monofills respectively, in order to satisfy geotechnical stability criteria. Significant settlements of residue lagoons and monofills can be expected to occur over a long period, owing to the low consolidation and high creep rates.

The triaxial undrained shear strength of the alum WTRs was found to be 10–20% greater than that measured for non-chemically treated residue of similar mineralogy and organic content, which can be largely explained by the action of the polyelectrolyte additive in aggregating and binding the constituent flocs to form floc clusters. Although the chemical additives are necessary for the efficient operation of the municipal treatment processes, they also have a downside in that the thickened alum residue was potentially more difficult to consolidate; hence the larger bulk volume would settle to a greater extent, although over a longer period, when placed in a lagoon or monofill.

ACKNOWLEDGMENTS

The author would like to thank Martin Carney, Michael Quille, Stephen Conlon, Brian Devaney, Patrick Fogarty, Mbakure Johnson, and Emma Quinn for carrying out the tests on the residue materials at the geotechnical laboratories, Trinity College Dublin; Paul Johnston for his helpful comments during the preparation of this paper; and Michael Quille for his assistance in producing the tables and figures contained in this paper.

REFERENCES

- Chih Chao, W.; H. Chihpin and D. J. Lee, "Effects of polymer dosage on alum sludge dewatering characteristics and physical properties", *J. Colloids and Surfaces A: Physicochemical and Engineering Aspects*, Vol. 122, No. 1–3, 1997, pp. 89–96.
- Turchiuli, C. and C. Fargues, "Influence of structural properties of alum and ferric flocs on sludge dewaterability", *J. Chemical Engineering*, Vol. 103, No. 1–3, 2004, pp. 123–131.
- Council of the European Union. 1998. Council Directive 1998/83/EC of 3rd November 1998 on the Quality of Water Intended for Human Consumption, In *Official Journal of the European Communities*, L330, pp. 32–54.
- US Environmental Protection Agency. 1996. *Technology Transfer Handbook: Management of Water Treatment Plant Residuals*, EPA 625-R-95-008, Cincinnati, OH: Environmental Protection Agency.
- Council of the European Union. 1999. Council Directive 1999/31/EC of 26th April 1999 on the Landfill of Waste, In *Official Journal of the European Communities*, L182, pp. 1–19.
- Council of the European Union. 2006. Council Directive 2006/12/EC of the Council of 5th April 2006 on Waste, In *Official Journal of the European Communities*, L114, pp. 1–13.
- O'Kelly, B. C., "Accurate determination of moisture content of organic soils using the oven drying method", *J. Drying Technology*, Vol. 22, No. 7, 2004, pp. 1767–1776.
- Novak, J. T. and D. C. Calkins, "Sludge dewatering and its physical properties", *J. American Water Works Association*, Vol. 67, No. 1, 1975, pp. 42–45.
- Raghu, D. and H-N.Hsieh, "Material properties of water treatment plant sludges", *J. Civil Engineering for Practicing and Design Engineers*, Vol. 5, No. 11–12, 1986, pp. 927–941.
- Geuzens, P. and W. Dieltjens. 1991. "Mechanical strength determination of cohesive sludges—a Belgian research project on sludge consistency", In *Recent Developments in Sewage Sludge Processing*. Eds. Colin, F.; P. J. Newman and Y. J. Puolanne, London: Elsevier, pp. 14–23.
- Wang, M. C.; J. Q. Hull; M. Jao; B. A. Dempsey and D. A. Cornwell, "Engineering behavior of water treatment sludge", *ASCE J. Environmental Engineering*, Vol. 118, No. 6, 1992, pp. 848–864.
- Wang, M. C. and W. Tseng, "Permeability behavior of a water treatment sludge", *ASCE J. Geotechnical Engineering*, Vol. 119, No. 10, 1993, pp. 1672–1677.
- Lim, S.; W. Jeon; J. Lee; K. Lee and N. Kim, "Engineering properties of water/wastewater-treatment sludge modified by hydrated lime, fly ash and loess", *J. Water Research*, Vol. 36, No. 17, 2002, pp. 4177–4184.
- Roque, A. J. and M. Carvalho. 2006. "Possibility of using the drinking water sludge as geotechnical material", In *Proceedings of the 5th International Congress on Environmental Geotechnics*, Cardiff, UK, Vol. 2, pp. 1535–1542.
- O'Kelly, B. C., "Geotechnical properties of a municipal water treatment sludge incorporating a coagulant", *Canadian Geotechnical J.*, Vol. 45, No. 5, 2008, pp. 715–725.
- Wichmann, K. and A. Riehl, "Mechanical properties of waterwork sludges—shear strength", *J. Water Science and Technology*, Vol. 36, No. 11, 1997, pp. 43–50.
- O'Kelly, B. C., "Mechanical properties of dewatered sewage sludge", *J. Waste Management*, Vol. 25, No. 1, 2005, pp. 47–52.
- O'Kelly, B. C., "Geotechnical properties of municipal sewage sludge", *J. Geotechnical and Geological Engineering*, Vol. 24, No. 4, 2006, pp. 833–850.
- Craig, R. F. 2004. *Craig's Soil Mechanics*, 7th edn., Taylor & Francis.
- British Standards Institution. 1990. *Methods of Test for Soils for Civil Engineering Purposes. Part 2: Classification Tests*, BS1377–2, London, British Standards Institution.
- British Standards Institution. 1990. *Methods of Test for Soils for Civil Engineering Purposes. Part 3: Chemical and Electro-Chemical Tests*, BS1377–3, London, British Standards Institution.
- Babatunde, A. O. and Y. Q. Zhao, "Constructive approaches toward water treatment works sludge management: An international review of beneficial reuses", *J. Environmental Science and Technology*, Vol. 37, No. 2, 2007, pp. 129–164.
- Mitchell, J. K. and K. Soga. 2005. *Fundamentals of Soil Behavior*, 3rd edn., New Jersey: Wiley and Sons.
- O'Kelly, B. C., "Effect of biodegradation on the consolidation properties of a dewatered municipal sewage sludge", *J. Waste Management*, Vol. 28, No. 8, 2008, pp. 1395–1405.
- British Standards Institution. 1990. *Methods of Test for Soils for Civil Engineering Purposes. Part 4: Compaction-Related Tests*, BS1377–4, London, British Standards Institution.
- Loll, U. 1991. "Measurement of laboratory vane shear strength as community standard or reference method for testing the suitability of dewatered sludges for use as landfill", In *Treatment and Use of Sewage Sludge and Liquid Agricultural Wastes*. Ed. L'Hermite P., London: Elsevier, pp. 310–315.
- O'Kelly, B. C., "Geotechnical aspects of sewage sludge monofills", *J. Municipal Engineer, Proceedings of the Institution of Civil Engineers*, Vol. 157, No. 3, 2004, pp. 193–197.
- British Standards Institution. 1990. *Methods of Test for Soils for Civil Engineering Purposes. Part 7: Shear Strength Tests (Total Stress)*, BS1377–7, London, British Standards Institution.
- British Standards Institution. 1990. *Methods of Test for Soils for Civil Engineering Purposes. Part 8: Shear Strength Tests (Effective Stress)*, BS1377–8, London, British Standards Institution.
- O'Kelly, B.C. 2008. "Development of a large consolidometer-permeameter apparatus for testing soft soils", In *Proceedings of the ASCE GeoCongress on the Challenge of Sustainability in the Geoenvironment*, New Orleans, Louisiana, Geotechnical Special Publication 179, pp. 60–67.
- O'Kelly, B. C., "Development of a large consolidometer apparatus for testing peat and other highly organic soils", *J. SUO—Mires and Peat*, Vol. 60, No. 1–2, 2009, pp. 23–36.
- Seed H. B. and C. K. Chan, "Structure and strength characteristics of compacted clay", *ASCE J. Soil Mechanics and Foundations Division*, Vol. 85, No. SM5, 1959, pp. 87–109.
- British Standards Institution. 1990. *Methods of Test for Soils for Civil Engineering Purposes. Part 5: Compressibility, Permeability and Durability Tests*, BS1377–5, London, British Standards Institution.
- Mesri, G.; M. Shahien and T. W. Feng. 1995. "Compressibility parameters during primary consolidation", In *Proceedings of the International Symposium on Compression and Consolidation of Clayey Soils*, Hiroshima, Vol. 2, pp. 1021–1037.
- Xu, G. R.; Z. C. Yan; Y. C. Wang and N. Wang, "Recycle of alum recovered from water treatment sludge in chemically enhanced primary treatment", *J. Hazardous Materials*, Vol. 161, No. 2–3, 2009, pp. 663–669.
- Abodo, M. S. E.; K. T. Ewida and Y. M. Youssef, "Recovery of alum from waste sludge produced from water treatment plants", *J. Environmental Science Health*, Vol. 28, No. 6, 1993, pp. 1205–1216.
- Siedlungsabfall, T. A. 1993. *Dritte Allgemeine Verwaltungsvorschrift zum Abfallgesetz*, Munich: Bundesanzeiger.

Neuropsychiatric Effects of Lead and Arsenic: Were these associated with “A Touch of Evil”?

ROD O’CONNOR^{1,*}, THOMAS G. BURNS² and P. “BRENT” DUNCAN³

¹Chemical Consulting Services, 1300 Angelina Court, College Station, TX 77840

²Department of Neuropsychology, Children’s Healthcare of Atlanta, 1001 Johnson Ferry Road NE, Atlanta, GA 30342

³Department of Biology, Forensic Sciences, University of North Texas, P.O. Box 305220, Denton, TX 76203

ABSTRACT: Adverse health effects from ingestion and/or inhalation of arsenic-and-lead-contaminated materials have been recognized for many years, including a variety of neurological effects. Severe neuropsychiatric disorders, including hallucinations, impaired judgment and memory, mania, psychosis resembling paranoid schizophrenia, and criminal behavior have been associated with lead and arsenic exposure. The question is posed as to whether or not such exposures might account for some of the bizarre incidents reported in two *Dateline NBC* episodes dealing with a small town in northeast Texas. Evidence suggests that health effect studies and medical monitoring programs in areas polluted by lead and arsenic should include neuropsychiatric testing.

THE STORY BEHIND “A TOUCH OF EVIL”

ON March 8, 2002 and on April 23, 2004 the program *Dateline NBC* aired extensive stories titled “A Touch of Evil”, dealing with bizarre episodes in Gilmer, a small town in northeast Texas. As the announcer phrased it, “There are tales of strange and ghoulish acts.” Transcripts of the television programs can be obtained from BurrellsLuce at <http://tapesandtranscripts.burrellsluce.com>.

The story began with the disappearance in 1992 of a teenage girl, and evolved into tales of ritual murder, cannibalism, child abuse and satanic cult practices. The most horrific stories came from young children, but many of the details were also reported by adults. After numerous arrests, questions were raised as to which, if any, of the startling allegations had any basis in fact, and most of the criminal charges were subsequently dropped for lack of sufficient evidence. Many of the most horrendous stories and confessions were eventually recanted. Newspaper accounts ranged from local papers [1] to the big city dailies [2], and even to the *New York Times* [3]. Extensive details were reported in “The Strange Case of the Gilmer (Texas) Cannibal Cult” [4] and “When Satan Came to Texas” [5], and were even reviewed by The United States Court of Appeals [6,7].

The complete truth of the Gilmer, Texas episodes will probably never be known. However, at the very least, there is clear evidence of extremely strange behavior among both children and adults in the community with respect to the chronicled events in the 1990s. Were these events a singular aberration in an otherwise normal community, or is there evidence that something about this town warrants further investigation?

THE GILMER, TEXAS COMMUNITY

There are six communities in northeast Texas in the population range of 4,000–6,000 as of the 2000 census. They are in six different counties, but all of them are impacted to some extent by the emissions from coal-burning power plants in that area of the state. Comparisons for the year 2000 are given in Table 1, showing that Gilmer, in Upshur County, is about average in demographics as reflected in the 2000 U.S. Census Bureau data. There is nothing obviously unique about Gilmer in the patterns of age, sex, race, median income or poverty level.

There is, however, something unique in the crime statistics comparisons for these communities, as compiled by the Texas Department of Public Safety at www.txdps.state.tx.us/crimereports/citindex.htm/. The category “Total Crimes” includes all reports of murder, rape, robbery, aggravated assault, burglary, larceny, and auto theft. As shown in Table 2, Gilmer had a sig-

* Author to whom correspondence should be addressed.
E-mail: docroc34@hotmail.com

Table 1. Year 2000 Demographics.

County	City	Population	Median Age	%Male	%White	%Afro	%Other	Median Income	%Below Poverty
Camp	Pittsburg	4,347	32.4	46.7	54.5	28.0	17.5	28,398	23.8
Cherokee	Rusk	5,085	37.8	60.7	62.7	30.0	7.3	33,952	16.2
Gregg	White Oak	5,624	34.1	48.5	94.6	1.9	3.5	50,781	9.9
Smith	Whitehouse	5,346	31.8	47.9	93.1	2.5	4.4	49,393	6.7
Upshur	Gilmer	4,799	39.5	45.5	75.9	20.2	3.9	39,688	15.9
Wood	Mineola	4,550	39.8	46.7	77.2	13.4	9.4	37,528	16.2

Median income is family income in 1990 dollars.

Below Poverty represents the "families below poverty level".

nificantly higher total crime rate than the other comparison communities, both as an average and as a range, for the years 1990–2007. Except for the two years 1991–92 in which Gilmer was second to Pittsburg, Gilmer had the highest total crime rates among the six comparison communities (i.e., for 89% of the 18 years). Moreover, for the period 1990–2007 the total crime rate for Gilmer averaged 6,715 per 100,000 people (range 5,052–9,798) compared to a statewide average for all communities of only 5,644 per 100,000 (range 4,600–7,827).

ENVIRONMENTAL FACTORS

Neuropsychiatric reactions to the environmental toxins lead and arsenic are many and varied [8,9,10], with symptoms that include impaired visual memory, agitation, confusion, delirium, dementia, emotional lability, frontal lobe dysfunction, hallucinations, impaired judgment and memory, mania, and psychosis resembling paranoid schizophrenia, and that are often reflected by increased criminal activity. Consideration of the reported "suspected neurotoxic" emissions in or near the six comparison communities (Table 3) fails to reveal why Gilmer had the bizarre episodes reported in the Dateline NBC stories, or why its total crime rate has consistently been so high.

Examination of the sources and specific chemical nature of neurotoxic emissions in the late 1900s, some of which were not included in TRI reports, in and near the comparison communities does reveal a possible explanation. In the other comparison communities, most of the "suspected neurotoxic" emissions were organic solvents or (in Pittsburg) hydrogen fluoride, none of which have been associated with the types of bizarre episodes and crime rates characteristic of Gilmer. There were some minor amounts of lead and arsenic emitted by the power plant in Pittsburg, and a small amount of arsenic emitted by a wood treatment plant in Mineola. However, in Gilmer, there were four identifiable sources of the environmental neurotoxins lead and arsenic known to be linked to the specific types of events noted. Within a small area of the town (Figure 1), and near schools and residences, were an arsenic acid production plant, a wood treatment facility known to burn CCA-treated wood waste, a pottery plant disposing of lead-containing wastes, and a hot dip galvanizing plant emitting lead into the air.

Many of the health effects of arsenic and lead are well established and widely recognized [e.g., 11,12]. Accordingly, public health studies and medical monitoring programs for communities impacted by arsenic and/or lead typically focus on cancers, learning disabilities, peripheral neuropathies and cardiovascular dis-

Table 2. "Total Crime" Statistics for Comparison Communities 1990–2007 (as number of offenses per 100,000 persons).

County	City	Distance from Gilmer	Year 2000 Population	Crime Rate Average	Crime Rate Range
Camp	Pittsburg	19 mi.	4,793	4,978	3,683–6,330
Cherokee	Rusk	78 mi.	4,666	2,786	1,375–4,164
Gregg	White Oak	19 mi.	5,624	2,216	1,290–2,924
Smith	Whitehouse	45 mi.	5,867	2,153	1,059–4,419
Upshur	Gilmer		5,820	6,715	5,052–9,798
Wood	Mineola	38 mi.	5,290	2,932	1,887–5,406*

*Through 2002, the last year for which reliable data were available. For the entire state of Texas, the 1990–2007 average was 5,644, with a range of 4,600–7,827.

Table 3. Suspected Neurotoxic Air Pollutants.

County	Amount (pounds)	Principal Emissions Locations	Comparison Community	Distance from Emissions Location
Camp	194,450	Pittsburg	Pittsburg	0
Cherokee	28,048	Jacksonville	Rusk	14 mi.
Gregg	3,539,655	Longview	White Oak	8 mi.
Smith	388,994	Tyler	Whitehouse	10 mi.
Upshur	106,017	Gilmer	Gilmer	0
Wood	6,605	Mineola	Mineola	0

(from EPA TRI data for 2002, at www.scorecard.org)

eases. There is, however, significant information suggesting that such studies and such monitoring should include neuropsychiatric disorders, especially in light of reports on the combined effects of arsenic and lead [13,14,15,16].

Neuropsychiatric effects of lead are well established, although the influence of sociodemographic factors cannot be disregarded [17,18].

A “second-order effect” may be significant in areas

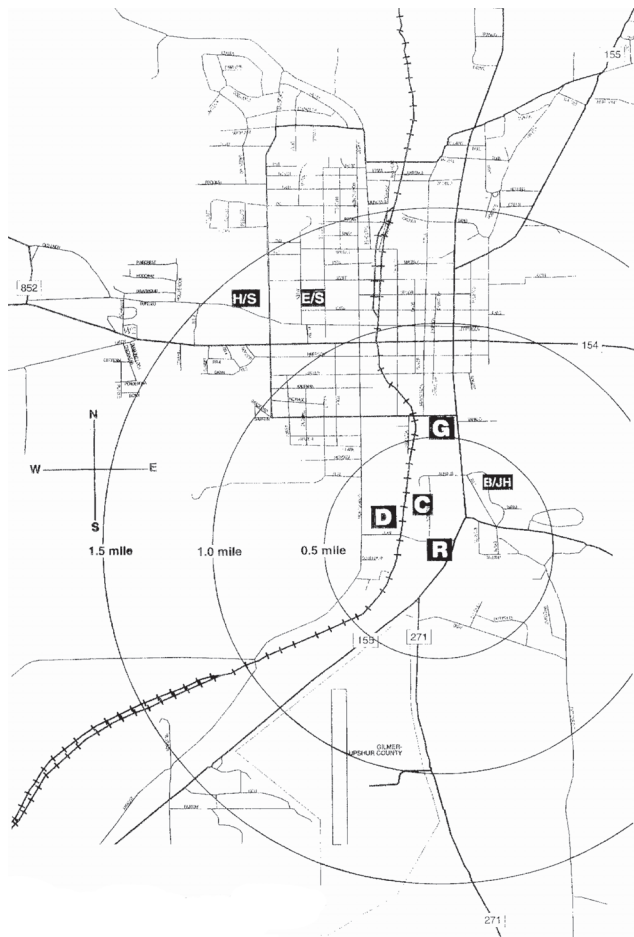


Figure 1. Gilmer, Texas. Key: D = wood treatment (CCA) plant, C = arsenic acid plant, G = pottery plant, R = hot dip galvanizing plant, H/S = high school, E/S = elementary school, B/JH = junior high school (formerly African-American school area).

of long term lead exposure, since children from homes in which the parents have suffered from lead exposure may have been maltreated in such a way as to affect their behavior, which was then further influenced by their own exposures to lead.

Neuropsychiatric effects of lead are often first noted in small children by parents and teachers as major behavioral problems. For example, Marlow and Bliss [19] reported in 1993 that concentrations of lead in hair samples of preschool children “was significantly related to increased scores on the teacher and parent rated behavior scales”. Teachers’ and parents’ reports of antisocial behavior and delinquency at 7 and 11 years of ages were correlated with bone lead levels by Needleman and colleagues [20] in 1996. Similar results, using parental responses, were reported in 2003 by LeClair and Quig [21] suggesting that “. . . lead exposure is significantly associated with anxiety-related behavioral symptomatology, both before and after controlling for the effects of social and family status, subject age, and subject sex.”

The exposure to lead *in utero* or during early childhood is of particular significance in terms of neuropsychological effects observed in later “post-childhood” years [22,23]. In 2001 Dietrich and colleagues [24] reported that both prenatal and postnatal exposure to lead were associated with antisocial acts and juvenile delinquency. Needleman, et al [25] found that elevated body lead burdens in youths aged 12–28 were associated with adjudicated delinquency, and a 2008 study by Wright and colleagues [26] of 250 individuals aged 19 to 24 years demonstrated an association between developmental lead exposure and early adulthood criminal behavior. Opler and colleagues [27,28] studied archived serum samples from live births between 1959 and 1966 in comparison with later adult cases of schizophrenia, concluding that early environmental exposures to lead appear to be associated with adult-onset psychiatric disorders.

Nevin [29,30,31] has suggested that widespread ex-

posures to lead, particularly preschool lead exposures, result in irreversible brain alterations associated with increased adult criminal activity. Although some authors [32] have disagreed with Nevin's analysis, their problem may be largely with Nevin's focus on lead-based paint and leaded gasoline as the principal sources of lead exposure, whereas careful analysis [33] has demonstrated that other sources, such as smelter operations, are probably more important factors. Questions remain, but extensive studies confirm a relationship between lead exposure and criminal behavior [34,35,36].

Much less is known about the neuropsychiatric effects of arsenic, and studies are complicated by numerous antagonistic, additive, and synergistic effects of neurotoxic pollutants in most areas studied [37]. Beckett and colleagues [38] reported in 1985 on a case of delirium apparently associated with occupational exposure to arsenic, and two similar cases were reported in 1989 by Morton and Caron [39]. It was not, however, until after the 1994 report by Burns, Cantor and Holden to the National Academy of Neuropsychology [40] that attention began to be focused on neuropsychiatric effects of long-term low level exposures to arsenic.

In 2003, Ratnaik [41] discussed chronic exposures to arsenic as including "changes in behavior, confusion, and memory loss". In that same year, Rodriguez and colleagues [42] reported that arsenic exposure can result in "hallucinations, disorientation, and agitation". Fujino and colleagues [43] suggested in 2004 that mental health of persons in an arsenic-affected village in Inner Mongolia was significantly worse than that of those in a comparison arsenic-free village. To what extent, if any, the neuropsychiatric effects of arsenic may be reflected in criminal tendencies has not yet been determined, but clues are available from the crime rates of

two Texas communities having arsenic as a major contaminant from arsenic acid plants operating until the mid 1990s (Table 4). During the period 1999–2007, the Total Crime rate in Commerce, Texas where an arsenic acid plant operated for many years [44] averaged 5,652 reports per 100,000 people, and that of Bryan, Texas where a similar plant operated for about 60 years [45] averaged 6,737 per 100,000. Both rates are lower than that of Gilmer, where lead appears to have been a major factor, but both were significantly higher than the average (4,956 per 100,000) for all Texas reporting communities during that period.

There are many other factors involved in neuropsychiatric disorders, and several elements in addition to lead and arsenic, including manganese and cadmium, have been identified with aberrant behavior. The complex analyses of multiple impacts of environmental chemicals on mental health have been addressed by Anderson [9] and by Masters and colleagues [46]. It is certain that lead is rarely the sole culprit in cases of neurotoxic metal pollution [47,48,49].

SOURCES OF ARSENIC AND LEAD IN GILMER

CCA Wood Treatment

The wood treatment plant in Gilmer occasionally burned CCA-treated wastes at ground level in the open, and regularly burned such wastes in its on-site boiler plant (beginning in 1978). An air model [50] prepared for the plant estimated ambient air levels of arsenic to range from 196 to 236 ng/m³ during typical boiler operation using CCA-sawdust as fuel (Figure 2). Actual air monitoring of full-time employees on site [51] revealed air arsenic levels from < 300 to 2,100 ng/m³. For com-

Table 4. Crime Rates in Three Arsenic-Impacted Communities.

"Total Crime" per 100,000 Persons				
Year	Gilmer	Bryan	Commerce	Texas
1999	5,487	6,883	6,636	5,032
2000	5,292	7,315	5,696	4,955
2001	6,927	6,017	6,515	5,152
2002	5,707	6,484	6,829	5,197
2003	6,037	6,973	6,164	5,144
2004	9,493	7,285	5,129	5,032
2005	9,798	7,170	4,982	4,857
2006	7,830	6,378	4,022	4,600
2007	6,974	6,132	4,891	4,631
Average	7,061	6,737	5,652	4,956
Range	5,292–9,798	6,017–7,315	4,022–6,829	4,600–5,197



Figure 2. CCA wood waste smoke contained arsenic.

parison, the ATSDR [11] reports that urban areas generally have arsenic levels in the range of 20–30 ng/m³, and the National Institutes of Safety and Health (NIOSH) [52] has recommended a maximum 15-minute workplace exposure limit of 2,000 ng/m³.

Arsenical Production

The arsenic acid plant in Gilmer (started in 1985) was a probable additional source of arsenic emissions, but no monitoring or air modeling data were available. By comparison, arsenic acid plants in Commerce [44] and Bryan, Texas [45] clearly demonstrate the potential for arsenic exposures around such facilities.

Hot Dip Galvanizing

The galvanizing plant in Gilmer used a molten mixture that at various times contained up to 13% lead, by weight. Fumes from the hot mixture (Figure 3) escaped



Figure 3. Hot dip galvanizing fumes contained lead.

from the plant and deposited residues near the plant (at high levels 1964–83, and at reduced levels thereafter). The lead/zinc ratio in sampled house dusts averaged 9.4% lead, consistent with fume compositions.

Pottery Wastes

The pottery plant in Gilmer (started in 1952) was a source of lead emissions [53]. Lead was used as a fluxing agent for glazes on dinnerware and pottery until the late 1990s, by which time it was generally phased out. Air emissions containing lead were associated with spray glazing operations, and with dusts from outdoor disposal of wastes.

ENVIRONMENTAL SAMPLING IN GILMER

Materials and Methods

Sampling was performed in June 1998, July 2000, November 2000, and July 2001 by Kara and Justin Sabrsula and by personnel from Aqua-Tech Laboratories, Bryan, Texas on house dusts, soils, and paint chips (from homes identified as having old, peeling paint), following methods of the U.S. Environmental Protection Agency [54,55]. Sampling personnel wore hooded Ty-Vac suits, gloves, goggles, and dust masks. Suits and other gear were placed in trash bags after leaving each residence to avoid any possibility of cross-contamination. Paint samples were collected from areas believed to have the oldest paint at the home. Topsoil samples were collected from track-in areas near homes. House dusts were collected from HVAC filters and rarely dusted locations such as the tops of ceiling fans or beneath large furniture, using separate brushes for each sample.

Samples were delivered to Aqua-tech Laboratories where they were prepared and digested according to Method SW846 3050B, then analyzed for arsenic, lead, and zinc by ICP (inductively coupled plasma spectrometry) according to Method SW846 6010B. All parameters followed standard protocol.

RESULTS AND DISCUSSION

Surface soil samples (Table 5) contained low levels of arsenic, consistent with the rapid loss of air-deposited arsenicals due to dissolution in rainwater and removal by biological processes. Soil lead concentrations were moderate in areas one mile or less from the emis-

Table 5. Surface Soil Contaminants (ppm).

n	Distance*	Arsenic	Lead	Zinc
7	< 0.5 mi.	< 0.4–1.0	5.4–143	37–259
6	0.5–1.0 mi.	<0.4–1.3	6.5–26	17–172
1	1.0–1.5 mi.	1.0	39	27
4	1.5–2.0 mi.	< 0.4–0.7	14–30	85–139

*From principal emission source midpoint.

sion sources, consistent with the lower rainwater solubility of many lead compounds, and low at further distances. Soil zinc levels were moderate, and similar to background zinc levels, consistent with the rainwater solubility of zinc compounds typical of galvanizing plant emissions [56].

By contrast, house dust samples (Table 6) contained high levels of arsenic, lead, and zinc, consistent with airborne deposition, rather than track-in of surface soils. Peak concentrations of contaminants were highest near the emission sources, and dropped off to essentially background levels at distances of 1.5 miles or greater.

Arsenic concentrations greater than 20 ppm exceed the Texas residential health-based policy level [57], as applied in the Commerce, Texas cleanup program [44]. Lead levels in soil or dust greater than 80 ppm (revised from the previous 150 ppm) exceed the recent California Human Health Screening Level [58].

CONCLUSIONS

This study clearly demonstrates that exposures to lead and arsenic are consistent with the types of aberrant behavior in Gilmer, Texas reported in the *Dateline NBC* stories of “A Touch of Evil”, and with the pattern of total crimes in the community. While genetic and socioeconomic factors were undoubtedly contributors, it is more likely than not that the neuropsychiatric effects of arsenic and lead exposure, especially in the vicinity of public schools, were significant in this area.

Both the Gilmer study and the peer-reviewed literature suggest that neuropsychiatric testing is warranted in health studies and in medical monitoring programs for areas impacted by lead, and especially when other neurotoxic species such as arsenic are present in levels exceeding normal backgrounds.

ACKNOWLEDGEMENTS

The authors wish to thank Ms. Janet Phelps of the

Table 6. House Dust Contaminants (ppm).

n*	Distance**	Arsenic	Lead	Zinc
21	< 0.5 mi.	8.4–211	39–364	340–5780
22	0.5–1.0 mi.	2.6–55	38–336	328–3780
10	1.0–1.5 mi.	1.0–46	24–153	353–5150
5	1.5–2.0 mi.	< 0.4–5.0	6.0–55	106–2200

*Excluding homes found with lead-based paint.

**From principal emission source midpoint.

Bryan/College Station, TX Eagle and Mr. Justin Sabrsula, Department of Business Administration, University of North Carolina, for their assistance in developing background information for this paper. Appreciation is also expressed to Ms. Lori Kirk, Statistician, Uniform Crime Reporting, Texas Department of Public Safety for her assistance with crime data, and to Dr. Barry S. Levy for his comments and suggestions.

DISCLAIMER

One of the authors (O'Connor) has served as an expert in litigation involving arsenic and lead exposures. Parts of this work, specifically sampling, analyses and data tabulation costs, were funded by The Carlile Law Firm, Marshall, Texas, having no direction or control over the content of this article, which is the sole responsibility of the authors. The authors state that they have no competing financial interests.

REFERENCES

- Loe, V. 1995. Satanic Cult Scare Takes Massive Toll in Texas Town. *Buffalo, Texas News*. December 3, 1995. Available at www.tmarchives.org/dbdoc.htm?...Satanic.
- Bragg, R. 1994. Strange twist to town's nightmare: Trusted cop is charged in murder case laden with horror. *The Houston Chronicle*. January 27, 1994. Available at www.tmarchives.org/dbdoc.htm?...Strange.
- Verhovek, S.H. 1994. Ritual Killer? Or an Officer Wronged? *The New York Times*. April 2, 1994. Available at <http://www.nytimes.com/1994/04/02/us/ritual-killer-or-an-officer-wronged.html>.
- Anon. 1997. The Strange Case of the Gilmer (Texas) Cannibal Cult: A Summary of Events in Gilmer, Texas. Available at <http://earthops.org/cult/gilmer-tx.html>.
- Wade, R.M. 1999. When Satan Came to Texas: A Study in Satanic Panic Witch Craze. *Skeptical*. 7 (4), 40–44. Available for \$5.95 U.S. at amazon.com.
- Eugene Kerr, et al vs. Roland Scott Lyford, et al. Cause No. 97-41553 in The United States Court of Appeals for the Fifth Circuit. April 14, 1999 Available at <http://cases.justica.com/us-court-of-appeals/F3/171/330/557711>.
- James York Brown vs. Roland Scott Lyford, et al. Cause No. 99-41297 in The United States Court of Appeals for the Fifth Circuit. February 20, 2001 Available at <http://laws.findlaw.com/5th/9941297.html>.
- Hartman, D.E. 1995. Neuropsychological Toxicology: *Identification*

- and Assessment of Human Neurotoxic Syndromes. Plenum Press, New York.
9. Anderson, G.S., 2007. *Biological Influences on Criminal Behavior*. CRC Press, Boca Raton, FL.
 10. Doctor, S.V. 2008. *Neuropsychiatric aspects of poisons and toxins*. The American Psychiatric Publishing Textbook of Neuropsychiatry and Behavioral Neurosciences. Fifth Edition, American Psychiatric Publishing, Inc., Washington, DC.
 11. ATSDR. 2007. *Toxicological Profile for Arsenic*. U.S. Department of Health and Human Services, Public Health Services, Agency for Toxic Substances and Disease Registry, Atlanta, GA.
 12. ATSDR. 2007. *Toxicological Profile for Lead*. U.S. Department of Health and Human Services, Public Health Services, Agency for Toxic Substances and Disease Registry, Atlanta, GA.
 13. ATSDR. 2004. *Interaction Profile for: Arsenic, Cadmium, Chromium, and Lead*. U.S. Department of Health and Human Services, Public Health Services, Agency for Toxic Substances and Disease Registry, Atlanta, GA.
 14. Mejia, J.J., F. Diaz-Barriga, J. Calderon, C. Rios, and M.E. Jimenez-Capdeville. 1997. Effects of lead-arsenic combined exposure on central monoaminergic systems. *Neurotoxicol. Teratol.* 19: 489–497.
 15. Calderon, J., M.E. Navarro, M.E. Jimenez-Capdeville, M.A. Santos-Diaz, A. Golden, L. Rodriguez-Leyva, V. Borja-Aburto, and F. Diaz-Barriga. 2001. Exposure to arsenic and lead and neuropsychological development in Mexican children. *Environ. Research, Section A*. 85: 69–76.
 16. de Burbure, C., J. Buchet, A. Leroyer, C. Nisse, J. Haguenoer, A. Mutti, Z. Smerhovsky, M. Cikrt, M. Trzcinka-Ochocka, G. Razniewska, M. Jakubowski, and A. Bernard. 2006. Renal and neurologic effects of cadmium, lead, mercury, and arsenic in children: Evidence of early effects and multiple interactions at environmental exposure levels. *Environ. Health Perspect.* 114: 584–590.
 17. McMichael, A.J., P.A. Baghurst, G.V. Vimpani, E.F. Robertson, N.R. Wigg, and S. Tong. 1992. Sociodemographic factors modifying the effect of environmental lead on neuropsychological development in early childhood. *Neurotoxicol. Teratol.* 14: 321–327.
 18. Hebben, N. 2001. Low lead levels and neuropsychological assessment: Let us not be misled. *Arch. Clin. Neuropsych.* 16: 353–357.
 19. Marlowe, M. and L.B. Bliss. 1993. Hair element concentration and young children's classroom and home behavior. *J. Orthomol. Med.* 8: 79–88.
 20. Needleman, H.L., J.A. Riess, M.J. Tobin, G.E. Biesecker, and J.B. Greenhouse. 1996. Bone lead levels and delinquent behavior. *JAMA* 275: 363–369.
 21. LeClair, J.A. and D.W. Quig. 2003. Hair lead and cadmium levels and specific depressive and anxiety-related symptomology in children. *J. Orthomol. Med.* 18: 97–107.
 22. Stokes, L., R. Letz, F. Gerr, M. Kolczak, F.E. McNeill, D.R. Chettle, and W.E. Kaye. 1998. Neurotoxicity in young adults 20 years after childhood exposure to lead: the Bunker Hill experience. *Occup. Environ. Med.* 55: 507–516.
 23. Ris, M.D., K.N. Dietrich, P.A. Succop, O.G. Berger, and R.L. Bornschein. 2004. Early exposure to lead and neuropsychological outcome in adolescence. *J. Int. Neuropsych. Soc.* 10: 261–270.
 24. Dietrich, K.N., M.D. Ris, P.A. Succop, O.G. Berger, and R.L. Bornschein. 2001. Early exposure to lead and juvenile delinquency. *Neurotoxicol. Teratol.* 23: 511–581.
 25. Needleman, H.L., C. McFarland, R.B. Ness, S.E. Feinberg, and M.J. Tobin. 2002. Bone lead levels in adjudicated delinquents: A case control study. *Neurotoxicol. Teratol.* 24: 711–717.
 26. Wright, J.P., K.N. Dietrich, M.D. Ris, R.W. Hornung, S.W. Wessel, B.P. Lanphear, M. Ho, and M.N. Rae. 2008. Association of prenatal and childhood blood lead concentrations with criminal arrests in early adulthood. *PLoS Med.* 5: 0732–0740.
 27. Opler, M.G.A., A.S. Brown, J. Graziano, M. Desai, C. Schaefer, P. Factor-Litvak, and E.S. Susser. 2004. Prenatal lead exposure, δ -aminolevulinic acid, and schizophrenia. *Environ. Health Perspect.* 112: 548–552.
 28. Opler, M.G.A., S.L. Buka, J. Groeger, I. McKeague, C. Wei, P. Factor-Litvak, M. Bresnahan, J. Graziano, J.M. Goldstein, L.J. Seidman, A.S. Brown, and E.S. Susser. 2008. Prenatal exposure to lead, δ -aminolevulinic acid, and schizophrenia: Further evidence. *Environ. Health Perspect.* 116: 1586–1590.
 29. Nevin, R. 2000. How lead exposure relates to temporal changes in IQ, violent crime, and unwed pregnancy. *Environ. Res. Section A*. 83: 1–22.
 30. Nevin, R. 2007. Understanding international crime trends: The legacy of preschool lead exposure. *Environ. Res.* 104: 315–336.
 31. Carpenter, D.O. and R. Nevin. 2009. Environmental causes of violence. *Physiol. Behav.* doi: 10.1016/j.physbeh.2009.09.001.
 32. McCall, P.L. and K.C. Land. 2004. Trends in environmental lead exposure and troubled youth, 1960–1995: an age-period-cohort-characteristic analysis. *Soc. Sci. Res.* 33:339–359.
 33. O'Connor, R. and P.B. Duncan. 2008. Lead-based paint residuals: Culprit or cop-out? *J. Residuals Sci. Tech.* 5: 161–170.
 34. Stretsky, P.B. and M.J. Lynch. 2001. The relationship between lead exposure and homicide. *Arch. Pediatr. Adolesc. Med.* 155: 579–582.
 35. Hornung, R.W., B.P. Lanphear, and K.N. Dietrich. 2009. Age of greatest susceptibility to childhood lead exposure: A new statistical approach. *Environ. Health Perspect.* 117: 1309–1312.
 36. Narag, R.E., J. Pizarro, and C. Gibbs. 2009. Lead exposure and its implications for criminology theory. *Crim. Justice Behav.* 36: 954–973.
 37. Burns, T.G. 1995. *Neurotoxicological Effects of Long-Term Exposure to Arsenic*. (Doctoral dissertation). Available from UMI Dissertation Services, Ann Arbor, MI. (UMI Number: 9534536).
 38. Beckett, W.S., J.L. Moore, J.P. Keogh, and M.L. Bleeker. 1985. Acute encephalopathy due to occupational exposure to arsenic. *Brit. J. Ind. Med.* 43: 66–67.
 39. Morton, W.E. and G.A. Caron. 1989. Encephalopathy: An uncommon manifestation of workplace arsenic poisoning? *Amer. J. Ind. Med.* 15: 1–5.
 40. Burns, T.G., D.S. Cantor, and G. Holder. 1995. Neurofunctional correlates of long-term arsenic exposure in humans. [Abstract from the 14th Annual Meeting of the National Academy of Neuropsychology]. *Arch. Clin. Neuropsych.* 10: 303–304.
 41. Ratnaike, R.N. 2003. Acute and chronic arsenic poisoning. *Postgrad. Med.* 79: 391–396.
 42. Rodriguez, V.M., M.E. Jimenez-Capdeville, and M. Giordano. 2003. The effects of arsenic on the nervous system. *Toxicol. Lett.* 145: 1–18.
 43. Fujino, Y., X. Guo, J. Liu, L. You, M. Miyatake, and T. Yoshimura. 2004. Mental health burden amongst inhabitants of an arsenic-affected area in Inner Mongolia, China. *Soc. Sci. Med.* 59: 1969–1973.
 44. TNRCC. 1998. Notice of Intent to Delete Hi-Yield from the Texas Superfund Registry. Texas Register. 23 TexReg 7136–7137.
 45. Seale, A. 1992. Arsenic and Old Lakes. *Insite*. February 1992: 11–14. Available at: www.allysite.com/arsenic_files/arsenic.pdf
 46. Masters, R.D., B. Hone, and A. Doshi. 1998. Environmental pollution, neurotoxicity, and criminal violence. In Rise, J. (Ed.). *Environmental Toxicology*. Gordon and Breach. Amsterdam.
 47. Lynch, A.J., N.R. McQuaker, and D.F. Brown. 1980. ACP/AES analysis and the composition of airborne and soil materials in the vicinity of a lead/zinc smelter complex. *JAPCA*, 30: 257–260.
 48. Hartwell, T.D., R.W. Handy, B.S. Harris, S.R. Williams, and S.H. Gehlbach. 1983. Heavy metal exposure in populations living around zinc and copper smelters. *Arch. Environ. Health.* 38: 284–295.
 49. Pilgrim, W. and R.N. Hughes. 1994. Lead, cadmium, arsenic and zinc in the ecosystem surrounding a lead smelter. *Environ. Monit. Assess.* 32: 1–20.
 50. Trozzo, D. 1988. Ambient Concentrations Resulting from CCA Sawdust Firing in a Wellons Boiler. Private Communication from Keystone Environmental Resources, Inc., Monroeville, PA.
 51. Juba, M.H. 1986. Wolman Licensee-PEL Monitoring Program. Private Communication from Koppers Company, Inc., Monroeville, PA.

52. NIOSH Pocket Guide to Chemical Hazards. 2005. Available at www.cdc.gov/niosh/npg.
53. CERMA-Pittsburgh. 2007. Clay Ceramic Area Source NESHAP. Available at www.cerma.org/pdf/EPA_NESHAP_Update.ppt.
54. USEPA. 1994. Chip, Wipe, and Sweep Sampling. SOP#: 2011. Available at www.dem.ri.gov/pubs/sops/wmsr2011.pdf.
55. USEPA. 2000. Standard Operating Procedures. Soil Sampling. Available at earth1.epa.gov/region09/toxic/nea/.../EPA-ERT-SOIL-SOP-2012.pdf.
56. Dufresne, A., G. Perrault, C. Roy, J. Lauzon, D. Michaud, and M. Baril. 1988. Characterization of ambient air contaminants from hot-dip galvanizing plants. *Ann. Occup. Hyg.* 32: 179–189.
57. Baldwin, L. and H. McCreary. 1998. Study of State Soil Arsenic Regulations. Available at www.aehs.com/surveys/arsenic.pdf.
58. OEHHA. 2009. Revised California Human Health Screening Level for Lead (Review Draft). Available at oehha.ca.gov/risk/pdf/LeadCHHSL51809.pdf.

Elemental Concentrations of Atmospheric Aerosols and the Soil Samples on the Selected Playgrounds in Istanbul

GOKSEL DEMIR^{1,*}, SELDA YIGIT¹, HUSEYIN OZDEMIR¹, GULSUM BORUCU¹ and ARSLAN SARAL²

¹*Bahcesehir University Faculty of Engineering, Department of Environmental Engineering,
34349 Besiktas-Istanbul, Turkey*

²*Yildiz Technical University, Faculty of Civil Engineering, Department of Environmental Engineering,
34210 Davutpaşa-Istanbul, Turkey*

ABSTRACT: Considering the most of their time is in playgrounds, children are under a significant health risk in urban areas due to the exposure of high air pollution. In this study, 3 different playgrounds are chosen according to their locations; one is in the city where there is highly traffic jam, the other is on the coast line of Istanbul Bosphorus, and the last one is near a high way. In these playgrounds, concentrations of particulate matter (PM) fractions (PM_{2.5} and PM₁₀) were determined in the specified periods. The elemental composition of PM were determined by measuring the concentrations of Al, K, Na, Mg, Ca, Pb, Cu, Cr, Cd, Zn, Co, Ni, and V using inductively coupled plasma-optical emission spectrometer. The correlation matrices are also developed in order to determine the relation between trace metal concentrations. The elemental concentrations and PM results showed variations between the selected playgrounds.

INTRODUCTION

THE major environmental problem of urban cities is air pollution due to its direct health effects. The main sources of air pollution in urban areas are traffic, industry and fossil fuel burning for heating purposes. Particulate matter (PM) constitutes significant part of air pollution in cities. Since major sources of PM are anthropogenic sources as traffic, natural sources as resuspension from soil and secondary formation in the atmosphere [17].

The atmospheric particles are composed of a complex mixture of different elements and compounds. These are mainly constituted of sulfates, nitrates, ammonium, organic compounds, marine salts, soil elements and heavy metals [1]. Especially the presence of heavy metals in particulate matter has a significant importance on human health. Since some heavy metals are toxic even at extremely low concentrations and they are potential cofactors, initiators or promoters in many diseases as cardiovascular diseases and cancer [6,11]. Because of higher minute ventilation and higher levels of physical activity of children, they have increased exposure to air pollutants than adults. Considering that the

considerable amount of their time is in playgrounds children are under a significant risk of health especially in urban areas with a high air pollution.

In addition children are also under a risk of soil pollution, which is mainly caused by deposition of PM in playgrounds. The metal toxicity risk of children are increasing when they faced with the soil pollution in playgrounds. Children are sensible to metal toxicity mainly for two reasons; firstly the unattained children in the playground may ingest soil and dust by bringing their fingers in the mouth and sucking foreign objects; secondly their digestive system has more absorption capacity than adults and so their hemoglobin is more susceptible to toxic metals [11].

They inhale and ingest big amount of dust that contains many chemical materials in the playgrounds. These chemicals include metals such as Al, K, Na, Mg, and Ca as well as the toxic trace metals such as Pb, Cu, Cr, Cd, Zn, Co, Ni, and V.

This study aims to identify the aerosol originated trace metal concentrations and its deposition on soil with respect to chosen playgrounds in Istanbul. The correlation matrices are also developed in order to determine the relation between trace metal concentrations and to obtain information about the sources of these elements.

* Author to whom correspondence should be addressed.
E-mail: goksel.demir@bahcesehir.edu.tr

METHODOLOGY

Study Area and Sampling Site

Istanbul is the most populated city of Turkey and the fourth in Europe with nearly 4.5% annual population growth rate and approximately 12 million inhabitants [14]. Air pollution is one of the significant environmental problems of Istanbul mainly because of traffic emissions. However, some regions of Istanbul have been continuously exposed to high pollution levels during the heating season (November–March), so this phenomena is another reason of air pollution [4].

Istanbul is located in the north-west Marmara Region of Turkey. It encloses the southern Bosphorus, which places the city on two continents; Europe and Asia. The city boundaries cover a surface area of 1,831 km², while the Province of Istanbul, covers 6,220 square km².

In this study, 3 different types of playgrounds are chosen; in the city where there is a high traffic jam (PG 1), near Istanbul Bosphorus (PG 2), where there is a sea effect and near high way in Istanbul (PG 3). In these playgrounds, which have different locations, PM fractions are measured in the specified periods as given in details in the methods.

Table 1. Approximate Numbers of Vehicles that Passes Through Near Chosen Playgrounds [18].

	Weekdays	Weekend
PG 1	184,890	72,645
PG 2	152,406	59,940
PG 3	422,994	158,150

Sampling

Sampling period of the study was between march and april in 2009. The PM fractions were collected by a low volume sampler “Zambelli ISO PLUS 6000”, operating at a flow rate of 1 m³/hr. Sampling time was considered as 24 hours and samples were collected every 6 days of the week. PTFE (Polytetrafluoroethylene) filters were used to collect the PM, which have 2 µm pore size and 47 mm diameter. Sampling device only collects one fraction at a time thus PM_{2,5} and PM₁₀ were collected on two sequential days in the week. Sampling height was approximately 2 m as stated in “EPA 40 CFR PART 50” standards.

Before sampling, filters were pre-conditioned by placing them into a desiccator at room temperature in open plastic petri dishes for 24 hours to obtain a constant humidity. After conditioning process, filters were



Figure 1. Sampling sites.

weighted using a microbalance. The procedure that is performed after sampling is the same.

Chemical Analysis

The concentrations of Al, Na, K, Ca, Mg, Pb, Cu, Cr, Co, Zn, Ni, Cd and V associated with PM_{2.5} and PM₁₀ were determined by Inductively Coupled Plasma-Optical Emission Spectrometer (ICP-OES, Perkin Elmer Inc.).

Before ICP analysis, acid digestion process was applied to PM collected filters in order to analyze the samples in the solution phase. To derive this process optimum amount of acid and the digestion procedure was determined as follows; 5 ml concentrated H₂SO₄ and 5 ml HClO₄. This acid mixture was added to teflon vessels which have filters in it. Then the filters were closed and placed into the microwave device. Temperature of the microwave was increased slowly to 210°C during the 20 minutes digestion time. After cooling the digestion vessels, the content was transferred to the measuring flask and it was diluted to 50 ml with deionized water.

RESULTS AND DISCUSSION

Both results of air samples and soil samples should be considered in order to determine the effect of aerosol originated heavy metal concentrations on the deposition to the soil samples of chosen playgrounds.

Results of Air Samples

Air samples were collected as PM₁₀ and PM_{2.5} size fractions. The trace metal analysis were performed on

these samples and the results are given in Table 2, 3, and 4 with respect to the chosen playgrounds.

The results showed that the concentrations of the selected trace metals were generally higher in PM₁₀ measurements. It is recognized that these elements are mostly produced because of vehicles mechanical wearing process that produces coarse particles [13]. However, in a typical urban atmosphere, concentrations of Pb, Ni and V are determined by motor vehicle emissions, those of Al, Na, K, Ca, Mg and Co are determined by resuspended soil and concentrations of Cd, Cr, Cu and Zn are determined by industrial activities [16].

Yatkin et al. (2007) were investigated elemental composition and sources of particulate matter in the ambient air of Izmir where is the other metropolitan city of Turkey. The metal concentrations were determined in their study from PM₁₀ and PM_{2.5} samples.

Since the heavy metal toxicity of children are caused by the soil and dust in playgrounds, the PM₁₀ and PM_{2.5} results were given in this study to give an idea about aerosol originated heavy metal concentrations on soil of playgrounds.

Result of Soil Samples

The chemical composition of soil, particularly its metal content, is environmentally important, because depending on their concentrations, levels of toxic elements can reduce soil fertility, can increase input to food chain, which leads to accumulate toxic metals in foodstuffs, and in ultimately can endanger human health [19]. In cities, the chemical composition of soil is affected from the deposition of atmospheric particles; but the composition of atmospheric aerosol is also affected from the composition of surface soil, because re-

Table 2. Heavy Metal Concentrations of PG1 Between 01–18.03.2009.

Results of PM _{2.5} Measurements														
Date	PM _{2.5} g/m ³	Al ng/m ³	Na ng/m ³	K ng/m ³	Ca ng/m ³	Mg ng/m ³	Pb ng/m ³	Cu ng/m ³	Cr ng/m ³	Co ng/m ³	Zn ng/m ³	Ni ng/m ³	Cd ng/m ³	V ng/m ³
02.03.09	37.50	166.15	761.19	394.67	723.15	147.18	33.54	106.78	36.97	19.80	53.66	30.85	12.23	30.64
08.03.09	34.80	401.84	923.37	305.63	808.80	198.16	38.34	68.08	20.41	12.69	50.66	17.97	11.00	23.86
14.03.09	30.43	121.80	1560.74	413.67	934.27	134.60	33.97	91.21	21.46	13.81	95.99	20.04	11.24	17.13
Results of PM ₁₀ Measurements														
Date	PM ₁₀ g/m ³	Al ng/m ³	Na ng/m ³	K ng/m ³	Ca ng/m ³	Mg ng/m ³	Pb ng/m ³	Cu ng/m ³	Cr ng/m ³	Co ng/m ³	Zn ng/m ³	Ni ng/m ³	Cd ng/m ³	V ng/m ³
03.03.09	48.20	395.94	2817.98	691.89	2016.45	290.35	74.22	109.63	29.85	18.03	83.31	23.55	12.17	11.46
07.03.09	181.00	5743.34	1662.98	1789.10	9813.19	1860.34	38.88	110.81	35.42	15.75	99.92	23.51	11.78	30.14
18.03.09	27.80	308.49	1390.89	302.12	1392.19	182.42	67.59	88.38	25.89	15.20	106.43	19.18	13.32	18.22

Table 3. Heavy Metal Concentrations of PG2 Between 20.03.2009–06.04.2009.

Results of PM _{2.5} Measurements														
Date	PM _{2.5} g/m ³	Al ng/m ³	Na ng/m ³	K ng/m ³	Ca ng/m ³	Mg ng/m ³	Pb ng/m ³	Cu ng/m ³	Cr ng/m ³	Co ng/m ³	Zn ng/m ³	Ni ng/m ³	Cd ng/m ³	V ng/m ³
23.03.09	26.00	108.51	930.29	269.45	497.18	97.40	67.27	73.69	22.86	14.35	54.01	21.24	14.70	22.67
30.03.09	69.56	712.8	1107.4	887.4	1328.2	235.6	54.9	46.3	4.5	0.7	114.8	30.6	1.15	67.1
03.04.09	21.60	199.08	1624.90	442.25	1057.75	91.48	11.37	105.01	6.99	–	35.60	17.03	–	–
Results of PM ₁₀ Measurements														
Date	PM ₁₀ g/m ³	Al ng/m ³	Na ng/m ³	K ng/m ³	Ca ng/m ³	Mg ng/m ³	Pb ng/m ³	Cu ng/m ³	Cr ng/m ³	Co ng/m ³	Zn ng/m ³	Ni ng/m ³	Cd ng/m ³	V ng/m ³
26.03.09	34.60	467.78	1797.15	382.68	1677.12	257.35	30.60	97.59	22.70	12.74	69.29	19.49	10.74	12.69
28.03.09	78.30	2258.7	3034.8	830.0	2393.4	389.7	332.8	116.8	15.6	0.089	219.3	22.7	20.2	32.1
05.04.09	30.26	974.47	4453.07	340.62	3466.46	351.50	115.98	120.47	0.29	–	131.35	4.25	–	–

suspended soil particles is an important component of aerosol mass, particularly in the coarse fraction [16]. In order to determine the concentrations of the trace metals in the soil of chosen playgrounds, three samples were analyzed for each playground and the average results of the analysis were illustrated in Table 5. The effect of coastal region were observed in PG 2 as an increase in Na, K, Ca and Mg concentrations.

Concentrations of some heavy metals that exist in soil were given as range of values, applicable and maximum values in Table 6. In general, the results of the study are not exceeding the maximum values which are given in the Table 6, but the differences in the heavy metal concentrations of playgrounds becomes important in this case. Since the concentrations of heavy metals are increasing depending on traffic intensity of the chosen monitoring site. As depicted in Table 1, the traffic intensity of the PG 3 is higher than the others, accordingly the heavy metal concentrations is higher.

Sezgin et al. (2003) were investigated the heavy

metal concentrations of street dust in Istanbul and they concluded the study with these average concentrations as 211.8 mg/kg for Pb, 208.49 mg/kg for Cu, 397.90 mg/kg for Mn, 520.81 mg/kg for Zn, 1.91 mg/kg for Cd and 31.52 mg/kg for Ni. The results of this study has an importance to evaluate the heavy metal deposition caused by vehicle emissions in Istanbul. The results of the study that was performed by Sezgin et al. (2003) are higher than results of this study. Since the samples of their study were collected directly from street so the heavy metal deposition were higher.

Some of the studies which were performed in dust or soil samples have approximately same values of this study and also some of them have definitely different results. Ruiz-Cortes et al. (2005) was found concentration values of some selected metals in soils of playgrounds as 40.5 mg/kg for Cr, 56.8 mg/kg for Cu, 21.6 mg/kg for Ni, 146 mg/kg for Pb and 121 mg/kg for Zn. Another study was performed in background soil in Madrid by the De Miguel et al. (1998) and the results

Table 4. Heavy metal concentrations of PG3 (Okmeydanu) between 07.04.2009–2304.2009.

Results of PM _{2.5} Measurements														
Date	PM _{2.5} g/m ³	Al ng/m ³	Na ng/m ³	K ng/m ³	Ca ng/m ³	Mg ng/m ³	Pb ng/m ³	Cu ng/m ³	Cr ng/m ³	Co ng/m ³	Zn ng/m ³	Ni ng/m ³	Cd ng/m ³	V ng/m ³
08.04.09	56.20	267.5	319	402.4	222.7	59.4	44.6	31.4	2.4	0.8	83.1	2.4	–	7.9
17.04.09	43.3	530.74	3074.46	1270.13	1066.23	189	13.01	218.22	16.15	–	100.52	19.9	–	–
20.04.09	47.5	2244.8	3010.81	389.58	1310.12	133.3	11.07	120.63	2.34	–	85.64	10.18	–	4.95
Results of PM ₁₀ Measurements														
Date	PM ₁₀ g/m ³	Al ng/m ³	Na ng/m ³	K ng/m ³	Ca ng/m ³	Mg ng/m ³	Pb ng/m ³	Cu ng/m ³	Cr ng/m ³	Co ng/m ³	Zn ng/m ³	Ni ng/m ³	Cd ng/m ³	V ng/m ³
09.04.09	129.58	2644.9	1242.5	1713.6	5535.2	788.8	18.21	125.8	12.4	8.9	125.1	10.8	1	17.4
14.04.09	69.2	1722	7851.26	2297.88	14677.8	1127.11	6.1	175.4	7.22	–	322.09	13.53	–	–
19.04.09	92.2	2284.59	8108.85	884.69	6033.2	648.52	19.09	263.84	20.31	–	234.32	30.12	–	42.33

Table 5. Heavy Metal Concentrations on the Soil Samples of Chosen Playgrounds in Istanbul (mg/kg).

Location	Date	Al	Na	K	Ca	Mg	Pb	Cu	Cr	Co	Zn	Ni	Cd	V
Beşiktaş Barbaros Avenue (PG1)	01–18 March 2009	45583	7230	12097	8119	1641	33	31	54	10	98	20	–	51
Kabataş coast (PG2)	19 March–6 April 2009	40085	26425	22918	16620	4608	148	67	55	16	201	18	–	61
Abide-i Hürriyet (PG3)	07–23 April 2009	21710	16910	21927	8915	1380	270	26	65	30	283	27	–	65

were determined as 6.42 mg/kg for Co, 74.7 mg/kg for Cr, 71.7 mg/kg for Cu, 14.1 mg/kg for Ni, 161 mg/kg for Pb and 210 mg/kg for Zn. A similar study was implemented in playgrounds in Hong Kong by Sai Leung et al. (2007), but the results of their study was highly different. They are reported as 1883 mg/kg for Zn, 143 mg/kg for Cu, 7 mg/kg for Cd, 263 mg/kg for Cr and 77.3 mg/kg for Pb. This similarities and differences of results points the dependency on the sources, meteorology and air pollution load.

Correlation Between Metals

Calculation of correlations among elements in a given size fraction is a alternative tool, which can be used to define the possible groups and/or behaviors of elements [5]. Correlation matrices were calculated to determine the relation between the trace metal concentrations. The correlation matrices of the trace elements in PM_{2.5} and PM₁₀ size fractions at three different playgrounds are given in Tables 7, 8, 9. The significant correlations are depicted using bold fonts.

In the correlation results of first playground, the differences between PM_{2.5} and PM₁₀ samples were pointed out. According to the results, Pb which is mainly emitted to the atmosphere as micron sized particles by motor vehicles, has no significant correlation values both in PM_{2.5} and PM₁₀ analysis. However, heavy metals; Ni, Cd, Cu, Cr, and Co have significant correlation val-

ues and these values are higher in fine particles than coarse particles.

For the second playground (PG 2), which is on the coast of Bosphorus, Na has no high correlation value in PM_{2.5} samples. However, in PM₁₀ analysis it has significant correlation with Ca, Mg, and Cu. The correlation between Na and Mg indicates a certain part of PM was originated from marine salt [17]. These trace metals were transported as water droplets from sea and these aerosols have a particle size greater than 10 microns. There was no relationship between Pb, Zn, Cd, and V in PM_{2.5} different from PM₁₀. This may indicate that Pb is mainly existed in the coarse fraction of a source which is mainly motor vehicles.

In the results of PG 3, correlations of Pb is different from the results of the other playgrounds. Since Pb has high correlation with Co in both coarse and fine particle sizes. Also, it is significantly correlated with Cd and Al elements in PM₁₀ analysis. This may show that the sources of these trace metals for PG 3 sampling site were the same.

Although the measurement parameters and the sampling were same, the correlation values between trace metals considerably vary among three playgrounds. This situation was related with the variability of pollution sources, meteorology and the locations of sampling sites.

CONCLUSION

The results of the trace metals which are analyzed on PM₁₀ and PM_{2.5} samples were given in this study to give an idea about aerosol originated heavy metal concentrations on soil of playgrounds. Since the heavy metal toxicity of children are mostly caused by the soil and dust in playgrounds.

According to the results obtained from soil samples of playgrounds in three representative locations, the average metal concentrations were 35792.6 mg/kg for Al, 16855.0 mg/kg for Na, 11218.0 mg/kg for Ca, 2543.0

Table 6. Heavy Metal Concentrations that Exist in Soil, mg/kg Dry Soil [8].

Metals	Range	Acceptable Value	Maximum Value
Pb	0.1–20	100	100
Cd	0.1–1	3	3
Cr	10–50	100	100
Cu	5–20	50	100
Ni	10–50	50	50
Zn	10–50	300	300
Co	1–10	50	–
V	10–100	50	–

Table 7. The Correlation Matrices of the Trace Metal Concentrations at PG 1 ($PM_{2.5}$ and PM_{10}).

$PM_{2.5}$	Al	Na	K	Ca	Mg	Pb	Cu	Cr	Co	Zn	Ni	Cd	V
Al													
Na	-0.460												
K	-1.000	0.476											
Ca	-0.254	0.975	0.271										
Mg	0.999	-0.496	-1.000	-0.292									
Pb	0.974	-0.247	-0.970	-0.027	0.964								
Cu	-0.848	-0.081	0.838	-0.298	-0.826	-0.946							
Cr	-0.419	-0.613	0.403	-0.772	-0.382	-0.614	0.837						
Co	-0.499	-0.539	0.484	-0.712	-0.464	-0.683	0.883	0.996					
Zn	-0.667	0.968	0.680	0.890	-0.697	-0.481	0.171	-0.397	-0.312				
Ni	-0.502	-0.537	0.487	-0.709	-0.467	-0.685	0.884	0.996	1.000	-0.309			
Cd	-0.532	-0.507	0.517	-0.684	-0.498	-0.710	0.900	0.992	0.999	-0.276	0.999		
V	0.145	-0.945	-0.163	-0.994	0.185	-0.083	0.402	0.837	0.785	-0.834	0.783	0.761	
PM_{10}	Al	Na	K	Ca	Mg	Pb	Cu	Cr	Co	Zn	Ni	Cd	V
Al													
Na	-0.323												
K	0.971	-0.087											
Ca	0.999	-0.273	0.982										
Mg	0.999	-0.282	0.980	1.000									
Pb	-0.982	0.497	-0.908	-0.970	-0.973								
Cu	0.552	0.611	0.735	0.595	0.587	-0.383							
Cr	0.916	0.083	0.985	0.936	0.933	-0.823	0.614						
Co	-0.320	1.000	-0.084	-0.269	-0.278	0.494	0.614	0.087					
Zn	0.231	-0.995	-0.008	0.180	0.188	-0.412	-0.684	-0.178	-0.996				
Ni	0.505	0.653	0.697	0.550	0.542	-0.332	0.999	0.809	0.656	-0.723			
Cd	-0.706	-0.442	-0.855	-0.742	-0.736	0.558	-0.980	-0.931	-0.446	0.526	-0.968		
V	0.929	-0.651	0.813	0.908	0.912	-0.982	0.203	0.703	-0.648	0.575	0.150	-0.393	

Table 8. The Correlation Matrices of the Trace Metal Concentrations at PG 2 ($PM_{2.5}$ and PM_{10}).

$PM_{2.5}$	Al	Na	K	Ca	Mg	Pb	Cu	Cr	Co	Zn	Ni	Cd	V
Al													
Na	-0.136												
K	0.991	-0.001											
Ca	0.835	0.432	0.901										
Mg	0.985	-0.307	0.952	0.726									
Pb	0.171	-0.999	0.037	-0.400	0.341								
Cu	-0.764	0.743	-0.670	-0.282	-0.865	-0.767							
Cr	-0.709	-0.602	-0.798	-0.980	-0.575	0.573	0.087						
Co	-0.581	-0.728	-0.685	-0.933	-0.430	0.703	-0.082	0.986					
Zn	0.935	-0.479	0.878	0.585	0.982	0.510	-0.943	-0.412	-0.254				
Ni	0.902	-0.551	0.835	0.514	0.963	0.580	-0.968	-0.334	-0.172	0.996			
Cd	-0.559	-0.746	-0.665	-0.923	-0.405	0.722	-0.109	0.981	1.000	-0.227	-0.145		
V	0.888	-0.576	0.818	0.488	0.955	0.605	-0.975	-0.305	-0.141	0.993	1.000	-0.114	
PM_{10}	Al	Na	K	Ca	Mg	Pb	Cu	Cr	Co	Zn	Ni	Cd	V
Al													
Na	0.236												
K	0.937	-0.117											
Ca	0.163	0.997	-0.191										
Mg	0.885	0.662	0.667	0.604									
Pb	1.000	0.236	0.938	0.162	0.884								
Cu	0.607	0.916	0.292	0.883	0.907	0.606							
Cr	-0.069	-0.986	0.282	-0.996	-0.527	-0.069	-0.835						
Co	-0.714	-0.849	-0.426	-0.807	-0.958	-0.714	-0.990	0.748					
Zn	0.989	0.376	0.877	0.305	0.943	0.989	0.716	-0.214	-0.809				
Ni	0.398	-0.797	0.692	-0.841	-0.076	0.398	-0.488	0.888	0.358	0.260			
Cd	0.669	-0.564	0.886	-0.625	0.245	0.669	-0.185	0.695	0.043	0.553	0.948		
V	0.777	-0.428	0.947	-0.495	0.394	0.777	-0.030	0.574	-0.114	0.677	0.887	0.988	

Table 9. The Correlation Matrices of the Trace Metal Concentrations at PG 3 ($PM_{2.5}$ and PM_{10}).

$PM_{2.5}$	Al	Na	K	Ca	Mg	Pb	Cu	Cr	Co	Zn	Ni	Cd	V
Al													
Na	0.586												
K	-0.402	0.507											
Ca	0.759	0.972	0.291										
Mg	0.202	0.912	0.816	0.791									
Pb	-0.643	-0.997	-0.443	-0.987	-0.880								
Cu	0.097	0.863	0.873	0.722	0.994	-0.825							
Cr	-0.394	0.514	1.000	0.300	0.821	-0.451	0.877						
Co	-0.602	-1.000	-0.489	-0.977	-0.904	0.999	-0.853	-0.497					
Zn	-0.262	0.628	0.989	0.429	0.892	-0.571	0.935	0.990	-0.612				
Ni	0.059	0.843	0.890	0.695	0.990	-0.803	0.999	0.895	-0.832	0.948			
Cd	ND	ND	ND	ND	ND	ND	ND	ND	ND	ND	ND		
V	0.022	-0.797	-0.924	-0.634	-0.975	0.752	-0.993	-0.928	0.785	-0.971	-0.997	ND	
PM_{10}	Al	Na	K	Ca	Mg	Pb	Cu	Cr	Co	Zn	Ni	Cd	V
Al													
Na	-0.776												
K	-0.523	-0.132											
Ca	-0.940	0.513	0.783										
Mg	-0.773	0.200	0.945	0.944									
Pb	0.835	-0.995	0.033	-0.596	-0.296								
Cu	-0.234	0.795	-0.706	-0.112	-0.435	-0.731							
Cr	0.505	0.152	-1.000	-0.770	-0.938	-0.054	0.720						
Co	0.796	-0.999	0.099	-0.541	-0.233	0.998	-0.775	-0.120					
Zn	-0.982	0.880	0.353	0.859	0.641	-0.923	0.413	-0.334	-0.896				
Ni	-0.005	0.635	-0.850	-0.337	-0.630	-0.555	0.973	0.860	-0.609	0.192			
Cd	0.796	-0.999	0.099	-0.541	-0.233	0.998	-0.775	-0.120	1.000	-0.896	-0.609		
V	0.520	0.135	-1.000	-0.781	-0.944	-0.036	0.708	1.000	-0.102	-0.351	0.851	-0.102	

mg/kg for Mg, 41.3 mg/kg for Cu, 58.0 mg/kg for Co, 194.0 mg/kg for Zn, 21.67 mg/kg for Ni, and 59.0 mg/kg for V. The highest concentration values were observed for the toxic trace metals as Pb (270 mg/kg), Cr (65 mg/kg), Zn (283 mg/kg), Co (30 mg/kg), Ni (27 mg/kg), and V (65 mg/kg) in the playground near highway (PG 3). Comparison of measured concentrations of elements in the selected locations in the city has demonstrated that concentrations of average trace elements of the soil have been modified by the deposition of anthropogenic particles.

In order to define the possible groups and behaviors of elements, correlations were calculated among trace metals in $PM_{2.5}$ and PM_{10} size fractions. Variations in the correlation values between trace metals of three playgrounds was related with the variability of pollution sources, meteorology, and the locations of sampling sites.

In urban environment, all breathing system of children are affected by the outdoor air pollution (especially PM pollution). This particulate matter pollution causes serious health effects such as asthma, coughing, difficult or painful breathing, chronic bronchitis, decreased lung functions etc. [15].

Playgrounds are common places for children to perform outdoor activities. The scientists argue that soil ingestion because of hand to mouth activity represents a significant direct exposure pathway to lead [9]. As known, the heavy metal pollution on soil primarily caused by the PM deposition. For this reason, in this study the elemental concentrations of both atmospheric aerosols and the soil samples on playgrounds were measured. According to data collected, it is clear that the playgrounds should be located far away from the traffic and so air pollution sources.

The results which determined in this study could be a significant suggestion for the future studies that should concentrate on how much far away the playgrounds located from the main roads and highways.

ACKNOWLEDGEMENTS

This study was supported by TUBITAK (The Scientific and Technological Research Council of Turkey). Project number is 108Y173. The authors would like to acknowledge the financial support from Tubitak.

REFERENCES

- Dallarosa, J., Teixeira, E.C., Meira, L., Wiegand, F., Study of the chemical elements and polycyclic aromatic hydrocarbons in atmospheric particles of PM₁₀ and PM_{2.5} in the urban and rural areas of South Brazil, *Atmospheric Research* 89, 2008, 76–92.
- De Miguel, E., Jimenez de Grado, J., Llamas, J.F., Martin-Dorado, A., Mazadiego, L.F., The overlooked contribution of compost application of the trace element load in the urban soil of Madrid (Spain), *Science of the Total Environment* 215, 1998, 113–122.
- Gao, Y., Nelson, E.D., Field, M.P., Ding, Q., Li, H., Sherrell, R.M., Gliotti, C.L., Van Ry, D.A., Glenn, T.R. and Eisenreich, S.J., Characterization of atmospheric trace elements on PM_{2.5} particulate matter over the New York- New Jersey harbour estuary, *Atmospheric Environment* 36, 2002, 1077–1086.
- Gulsoy, G., Tayanc, M., Erturk, F., Chemical analysis of the major ions in the precipitation of Istanbul, Turkey, *Environmental Pollution* 105, 1999, 273–280.
- Karaca, F., Alagha, O., Erturk, F., Y?lmaz, Y. Z. and ?zkara, T., Seasonal Variation of source contributions to atmospheric fine and coarse particles at suburban area in Istanbul, Turkey, *Environmental Engineering Science* 25 (5), 2008, 767–781.
- Nriagu, J. O., A silent epidemic of environmental metal poisoning?, *Environmental Pollution* 50, 1988, 139–161.
- ?zcan, H.K., Sezgin, N., Demir, G., Nemlio?lu, S. and Bayat, C., Evaluation of heavy metal pollution on street dust of Istanbul E-5 highway, *Journal of Y?ld?z Technical University*, 2003, 97–105.
- ?zcan, H.K., Nemlio?lu, S., Sezgin, N., Demir, G., and Bayat, C., Heavy metal concentrations of atmospheric ambient deposition dust in Istanbul-Bosphorus Bridge Tollhouses, *Journal of Residuals Science and Technology* 4 (1), 2007, 55–59.
- Ren, H.M., Wang, J.D., Zhang, X.L., Assessment of soil lead exposure in children in Shenyang, China, *Environmental Pollution* 144, 2006, 327–335.
- Ruiz-Cortes, E., Reinoso, R., Diaz-Barrientos, E., Madrid, L., Concentrations of potentially toxic metals in urban soils of Seville: relationship with different land uses, *Environmental Geochemistry and Health* 27, 2005, 465–474.
- Sai Leung, N. G., Chan, L.S., Lam, K.C. and Chan, W.K., Heavy metal contents and magnetic properties of playground dust in Hong Kong, *Environmental Monitoring and Assessment* 89, 2003, 221–232.
- Sastre, J., Sahuquillo, A., Vidal, M., Rauret, G., Determination of Cd, Cu, Pb and Zn in environmental samples: microwave-assisted total digestion versus aqua regia and nitric acid extraction, *Analytica Chimica Acta* 462, 2002, 59–72.
- Sezgin, N., ?zcan, H.K., Demir, G., Nemlio?lu, S. and Bayat, C., Determination of heavy metal concentrations in street dust in Istanbul E-5 highway, *Environmental International* 29, 2003, 979–985.
- SIS, The Republic of Turkey, Prime ministry State Institute of Statistics, 2003. Available from: <http://www.die.gov.tr/ENGLISH/index.html>.
- The United States Environmental Protection Agency (USEPA), 1997 Technology Transfer Network OAR Policy and Guidance Website. <http://www.epa.gov/oar/particlepollution/health.html>
- Yatin, M., Tuncel, S., Aras, N.K., Olmez, I., Aygun, S., Tuncel, G., Atmospheric trace elements in Ankara, Turkey: I. factors affecting chemical composition of fine particles, *Atmospheric Environment* 34, 2000, 1305–1318.
- Yatkin, S. and Bayram, A., Elemental composition and sources of particulate matter in the ambient air of a metropolitan city, *Atmospheric Research* 85, 2007, 126–139.
- Municipality of Istanbul Metropolis, Transportation and Traffic Department, 2008.
- Guvenc, N., Alagha, O., Tuncel, G., Investigation of soil multi-element composition in Antalya, Turkey, *Environment International* 29, 2003, 631–640.

GUIDE TO AUTHORS

1. Manuscripts shall be sent electronically to the Editor-in-Chief, Dr. P. Brent Duncan at pduncan@unt.edu using Microsoft Word in an IBM/PC format. If electronic submission is not possible, three paper copies of double-spaced manuscripts may be sent to Dr. P. Brent Duncan, (Editor of the *Journal of Residuals Science & Technology*, University of North Texas, Biology Building, Rm 210, 1510 Chestnut St., Denton, TX 76203-5017) (Tel: 940-565-4350). Manuscripts should normally be limited to the space equivalent of 6,000 words. The editor may waive this requirement in special occasions. As a guideline, each page of a double-spaced manuscript contains about 300 words. Include on the title page the names, affiliations, and addresses of all the authors, and identify one author as the corresponding author. Because communication between the editor and the authors will be electronic, the email address of the corresponding author is required. Papers under review, accepted for publication, or published elsewhere in journals are normally not accepted for publication in the *Journal of Residuals Science & Technology*. Papers published as proceedings of conferences are welcomed.
2. Article titles should be brief, followed by the author's name(s), affiliation, address, country, and postal code (zip) of author(s). Indicate to whom correspondence and proofs should be sent, including telephone and fax numbers and e-mail address.
3. Include a 100-word or less abstract and at least six keywords.
4. If electronic art files are not supplied, submit three copies of camera-ready drawings and glossy photographs. Drawings should be uniformly sized, if possible, planned for 50% reduction. Art that is sent electronically should be saved in either a .tif or .JPEG files for superior reproduction. All illustrations of any kind must be numbered and mentioned in the text. Captions for illustrations should all be typed on a separate sheet(s) and should be understandable without reference to the text.
5. DEStech uses a numbered reference system consisting of two elements: a numbered list of all references and (in the text itself) numbers in brackets that correspond to the list. At the end of your article, please supply a numbered list of all references (books, journals, web sites etc.). References on the list should be in the form given below. In the text write the number in brackets corresponding to the reference on the list. Place the number in brackets inside the final period of the sentence cited by the reference. Here is an example [2].

Journal: 1. Halpin, J. C., "article title", *J. Cellular Plastics*, Vol. 3, No. 2, 1997, pp. 432–435.

Book: 2. Kececioglu, D. B. and F.-B. Sun. 2002. *Burn-In Testing: Its Quantification and Optimization*, Lancaster, PA: DEStech Publications, Inc.

6. Tables. Number consecutively and insert closest to where first mentioned in text or type on a numbered, separate page. Please use Arabic numerals and supply a heading. Column headings should be explanatory and carry units. (See example at right.)

Table 5. Comparison of state-of-the-art matrix resins with VPSP/BMI copolymers.

Resin System	Core Temp. (DSC peak)	Char Yield,	
		T _E	%
Epoxy (MY720)	235	250	30
Bismaleimide (H795)	282	>400	48
VPSP/Bismaleimide copolymer			
C379: H795 = 1.9	245	>400	50
C379: H795 = 1.4	285	>400	53

7. Units & Abbreviations. Metric units are preferred. English units or other equivalents should appear in parentheses if necessary.
8. Symbols. A list of symbols used and their meanings should be included.
9. Page proofs. Authors will receive page proofs by E-mail. Proof pages will be in a .PDF file, which can be read by Acrobat Reader. Corrections on proof pages should be limited to the correction of errors. Authors should print out pages that require corrections and mark the corrections on the printed pages. Pages with corrections should be returned by FAX (717-509-6100) or mail to the publisher (DEStech Publications, Inc., 439 North Duke Street, Lancaster, PA 17602, USA). If authors cannot handle proofs in a .PDF file format, please notify the Editor, Dr. P. Brent Duncan at pduncan@unt.edu.
10. Index terms. With proof pages authors will receive a form for listing key words that will appear in the index. Please fill out this form with index terms and return it.
11. Copyright Information. All original journal articles are copyrighted in the name of DEStech Publications, Inc. All original articles accepted for publication must be accompanied by a signed copyright transfer agreement available from the journal editor. Previously copyrighted material used in an article can be published with the *written* permission of the copyright holder (see #14 below).
12. Headings. Your article should be structured with unnumbered headings. Normally two headings are used as follows:
Main Subhead: DESIGN OF A MICROWAVE INSTALLATION Secondary Subhead: Principle of the Design Method
If further subordination is required, please limit to no more than one (*Third Subhead*).
13. Equations. Number equations with Arabic numbers enclosed in parentheses at the right-hand margin. Type superscripts and subscripts clearly above or below the baseline, or mark them with a caret. Be sure that all symbols, letters, and numbers are distinguishable (e.g., "oh" or zero, one or lowercase "el," "vee" or Greek nu).
14. Permissions. The author of a paper is responsible for obtaining releases for the use of copyrighted figures, tables, or excerpts longer than 200 words used in his/her paper. Copyright releases are permissions to reprint previously copyrighted material. Releases must be obtained from the copyright holder, which is usually a publisher. Forms for copyright release will be sent by the editor to authors on request.

General: The *Journal of Residuals Science & Technology* and DEStech Publications, Inc. are not responsible for the views expressed by individual contributors in articles published in the journal.